Master's thesis

NTNU
Norwegian University of Science and Technology
Faculty of Natural Sciences
Department of Chemistry

Pauline Verula Braaten

Study of snow, supraglacial debris and particulate matter released from the glacier systems of Austre Brøggerbreen and Vestre Brøggerbreen at Ny-Ålesund, Svalbard

Master's thesis in Sustainable Chemical and Biochemical Engineering
Supervisor: Øyvind Mikkelsen
June 2023

NTNU
Norwegian University of Science and Technology

Pauline Verula Braaten

Study of snow, supraglacial debris and particulate matter released from the glacier systems of Austre Brøggerbreen and Vestre Brøggerbreen at Ny-Ålesund, Svalbard

Master's thesis in Sustainable Chemical and Biochemical Engineering
Supervisor: Øyvind Mikkelsen
June 2023

Norwegian University of Science and Technology
Faculty of Natural Sciences
Department of Chemistry

NTNU
Norwegian University of
Science and Technology

Abstract

As a result of climate change, the Arctic has experienced increased temperatures [1, 2]. One of the most drastic trends was seen at Austre Brøggerbreen in the Ny-Ålesund area [3].

Different particulate matter, such as cryoconite, supraglacial debris, flow sediment and snow, collected from the two glacier systems, Austre Brøggerbreen and Vestre Brøggerbreen, in the Ny-Ålesund area were determined in order to increase the knowledge about the chemical compositions of particulate matter released from glacier systems on Svalbard. Most of the samples were collected directly from the surface of the glaciers.

Samples were analysed for element component analysis using inductively coupled plasma mass spectrometry (ICP-MS). Water and snow samples were analysed by high temperature combustion with Non-Dispersive Infrared detection (NDIR) for Total Carbon (TC), Total Inorganic Carbon (TIC) and Total Organic Carbon (TOC). Sediment samples were analysed by high temperature combustion with Non-Dispersive Infrared detection (NDIR) for Total Carbon (TC), Total Nitrogen (TN). Freeze-dried material were decomposed by microwave assisted digestion. Decomposition by use of HNO_3 were included.

Differences in the chemical and physical properties of different sample materials collected within the same glacier system and between the two glacier systems have been observed. A variation of factors may be responsible for the differences in chemical and physical properties. The major elemental composition in cryoconite, supraglacial debris, supraglacial debris collected from snow, flow sediment and snow differed. Fe, Al, Mg, Ca, and Na concentrations were dominating in the cryoconite, supraglacial debris. The snow samples were dominated by Ca, Na, and Mg concentrations. The supraglacial debris and cryoconite samples showed a statistical significantly differences of Pb and Zn concentrations between the glacier systems, with similarities as presented in previous studies.

The supraglacial debris and cryoconite samples contained a higher level of inorganic material, with low TC and TN content. Although within the range of previously published research. The TC and TN content did show a statistically significant difference between the two glacier systems of Austre Brøggerbreen and Vestre Brøggerbreen. The highest TC and TN content were determined in samples from the glacier system of Vestre Brøggerbreen. There were not observed statistical significant differences in the TC (%) and TN (%) concentrations between cryoconite and supraglacial debris samples collected on Austre Brøggerbreen. Statistical significant differences in the TC (%) and TN (%) concentrations were observed between cryoconite and supraglacial debris samples collected on Vestre Brøggerbreen. $SUVA_{254}$ values of snow samples and meltwater were in the range of hydrophilic substances, and no values did indicate any levels of hydrophobic and aromatic substances. The $SUVA_{254}$ did not show any statistical differences between the two glacier systems.

Long term environmental monitoring of the different glacial systems and more collected data is required in order to discuss the connection between different glacial particulate matter, such as cryoconite and supraclacial debris, the cryoconite age and their abilities of accumulation of elements, particulate matter from different cryoconite holes and depth, sampling location, size of glacier and glacier type, element speciation, to analyse trace elements, environmental contamination and their impact on the environment, as the global climate is in change.

Sammendrag

Som et resultat av klimaendringer har Arktis opplev økte temperaturer [1, 2]. En av de mest drastiske trendene har blitt observert på Austre Brøggerbreen i Ny-Ålesundsområdet [3].

Ulike partikulære materiale som kryokonitt, supraglasiale materiale, strømningssediment, og snø samlet inn fra de to bresystemene Austre Brøggerbreen og Vestre Brøggerbreen, i Ny-Ålesundsområdet ble undersøkt for å øke kunnskapen om de kjemiske sammensetningene av materiale frigjort fra bresystemene på Svalbard. De fleste prøvene ble samlet inn direkte fra overflaten av isbreene.

Prøver ble analysert for elementkomponentanalyse ved bruk av induktivt koblet plasma masse spektrometri (ICP-MS). Vann- og snøprøver ble analysert ved høytemperaturforbrenning med ikke-dispersiv infrarød deteksjon (NDIR) for totalt karbon (TC), totalt uorganisk karbon (TIC) og totalt organisk karbon (TOC). Sedimentprøver ble analysert ved høytemperatur-forbrenning med ikke-dispersiv infrarød deteksjon (NDIR) for totalt karbon (TC) og totalt nitrogen (TN). Frysetørket materiale ble dekomponert ved mikrobølgeassistert dekomponering. Dekomponering ved bruk av HNO_3 ble inkludert.

Det ble funnet forskjeller i de kjemiske og fysiske egenskapene til ulike prøvematerialer samlet inn fra samme bresystem og mellom de to bresystemene. En variasjon av ulike faktorer kan være årsaken til forskjellene i kjemiske og fysiske egenskaper. Det ble funnet forskjeller i de elementære sammensetningene i kryokonitt, supraglasiale materiale, supraglasiale materiale samlet fra snø, og elvesediment. Fe-, Al-, Mg-, Ca- og Na-konsentrasjoner var dominerende i kryokonitten og supraglasiale materiale. Konsentrasjoner av Ca, Na, og Mg dominerte i snøprøvene. Supraglasiale materiale og kryokonittprøver viste en statistisk signifikant forskjell i Pb- og Zn-konsentrasjoner mellom bresystemene, med likheter som presentert i tidligere studier.

Supraglasiale materiale og kryokonittprøver inneholdt et høyere nivå av uorganisk materiale, med lavt TC- og TN-innhold. De målte verdiene var i likhet med tidligere publiserte studier. TC- og TN-innholdet viste en statistisk signifikant forskjell mellom bresystemene, Austre Brøggerbreen og Vestre Brøggerbreen. Det høyeste TC- og TN-innholdet ble bestemt i prøver fra Vestre Brøggerbreen. Det ble ikke observert statistisk signifikante forskjeller i TC (%) og TN (%) konsentrasjoner mellom kryokonitt og supraglasiale materiale fra Austre Brøggerbreen.

Statistisk signifikante forskjeller i TC (%) og TN (%) konsentrasjon ble observert mellom kryokonitt og supraglasiale materiale fra Vestre Brøggerbreen. $SUVA_{254}$-verdier av snøprøver og smeltevann var i området for hydrofile substanser, og ingen verdier indikerte noen nivåer av hydrofobe- og aromatiske substanser. $SUVA_{254}$ viste ingen statistiske forskjeller mellom de to ulike bresystemene.

Langsiktig miljøovervåking av de ulike bresystemene og flere innsamlede data er nødvendig for å diskutere sammenhengen mellom ulike isbrematerialer som kryokonitt og supraglasiale materiale kryokonittalderen og deres evne til akkumulering av elementer, partikler fra forskjellige kryokonitthull og dybder, prøvetakingssted, størrelse på bre og bretype, elementspecier, for å analysere sporelementer, miljøforurensning og deres innvirkning på miljøet, ettersom det globale klimaet er i endring.

Preface

This project was written in the spring semester of 2023 as my master's thesis in the study program Sustainable Chemical and Biochemical Engineering, at the Department of Chemistry at NTNU Trondheim. This master's thesis is a direct extension of a specialisation project in analytical chemistry completed in the autumn semester of 2022. Contents from the specialisation project can therefore be found to be reused in this master's thesis, with more comprehensive methods and analysis. This has been necessary for this project to be possible to complete.

Pauline Verula Braaten

Trondheim, June 2023

Acknowledgements

The last two years of the master's program have been educational and interesting. There are several people I would like to thank for making me enjoy the last two years as a student.

At the beginning of the final year of my master's studies, I had the opportunity to go on fieldwork to Ny-Ålesund in Svalbard to collect samples for the specialisation project and master's thesis that I have been working on. Thank you to my supervisor, Øyvind, and fellow master students; Sofie, Margrethe, Lorenzo, Josy, and Anna for a great experience.

Special thanks to my supervisor, Øyvind Mikkelsen, who is always engaging, in a positive mood, and has provided good advice and guidance throughout the master's project. Not to forget, the waffle Fridays have been a great motivation every week.

I would also thank Kyyas Seyitmuhammedov for helping me with the sample preparation such as freeze-drying and UltraClave for the ICP-MS samples.

I would like to extend a special thanks to the wonderful people I have met in Trondheim, and shared experiences with - especially the short coffee breaks, the longer coffee breaks, the skiing trips, Chinese New Year, and board games gatherings. These are some of many good moments I appreciate.

To my roommates at Ila B&B, as this semester has included shared breakfasts and countless yatzy evenings - "as we all love", Thank you for making the last semester so cozy and including.

Lastly, I would also thank my family, for always supporting me and giving me advice.

Contents

List of Figures

List of Tables

1 Introduction

The Arctic region has experienced higher temperatures in response to climate change. The higher temperatures in the Arctic have been recorded from 1971- 2019 [1, 2], and the temperature has increased three times faster than the global temperature [2, 4]. This is the region with predicted fastest increasing temperatures on Earth [4, 5]. Glaciers that are melting are an important consequence of the increasing temperature. In 1967, the Norwegian Polar Institute began a program of observation of glaciers on Svalbard. The mass balance of different glaciers has been measured annually from the startup until the present [3]. All regions of the Arctic indicate a net loss of glaciers [2, 6], and the increase of this rate has been at its highest in the past decades [2].

One of the most drastic trends was seen at Austre Brøggerbreen in the Ny-Ålesund area, where the net mass balance decreased by almost 40 m between 1912 and 1990 [3]. The same research also came to the conclusion that this negative mass balance increases year after year. Greater quantities of clay and soil material are also released into the glacier-fed rivers Bayelva as an outcome of the significant negative mass balance, in addition to large volumes of water [7] and further into Kongsfjorden where it has an effect on both physical conditions and chemical conditions. Both supraglacial debris and particles stored inside glaciers are the sources of this particulate matter [8].

Supraglacial debris is particulate matter that occurs at the surface of a glacier, direct on the surface, in snowpack and cryoconite holes. Supraglacial material is transported particulate matter and accumulates on the surface of a glacier from local sources, such as rock and debris avalanches from the local terrain, weathering of rocks and debris eroded from the glacier bedrock, and distance sources, such as wind deposition of dust and long-range transported particles [9–11].

In order to increase the knowledge about the chemical compositions of the snow and particulate matter related to glacier systems on Svalbard, this project will study snow and particulate matter collected from the two glacier systems, Austre Brøggerbreen and Vestre Brøggerbreen in Brøggerdalen, Ny-Ålesund. Collecting sample materials such as snow, cryoconite hole sediment, flow sediment released from the glacier in major glacier melting water outlets, and particulate matter, such as supraglacial debris, directly from the surfaces of the two glacier systems.

This project is a direct extension of a specialisation project in analytical chemistry completed in the autumn semester of 2022. Contents from the specialisation project can therefore be found to be reused in this master's thesis, with more comprehensive methods and analysis. This has been necessary for this project to be possible to complete [12]. The aim of this project is to study potential differences between the chemical compositing of particulate matter collected from different sources at the individual glaciers and study potential differences between the two glacier systems, Austre Brøggerbreen and Vestre Brøggerbreen. All samples will be analysed for element component analysis using inductively coupled plasma mass spectrometry (ICP-MS). Water and snow samples will be analysed by high temperature combustion with Non-Dispersive Infrared detection (NDIR) for Total Carbon (TC), Total Inorganic Carbon (TIC) and Total Organic Carbon (TOC) using Shimadzu Total Organic Carbon Analyser (TOC-L) instrument. Sediment samples will be analysed by high temperature combustion with Non-Dispersive Infrared detection (NDIR) for Total Carbon (TC), Total Nitrogen (TN) using PrimacsSNC-100 instrument. After decomposing freeze-dried material with UltraClave Microwave Autoclave (Milestone). Decomposition by use of HNO_3 will be included [12].

2 Theory

In this chapter, the theory that has a relation to the analysis of supraglacial debris and particulate matter released from glaciers is described. Theory about the sample preparation and analysis as ICP-MS, TOC, TN/TC, UV-Vis spectrophotometry and SUVA is described to illustrate the analysis used in this project.

2.1 Svalbard

Svalbard is the common name of the archipelago of the Arctic islands located between 74° - 81° north latitude, and 10° - 35° east longitude, with the total landmass of 61 022 km^2 [13, 14]. Svalbard is a part of Norway, and at present, Svalbard has a total population of 2530 inhabitants [15]. About 60% of the landmass of Svalbard is covered by glaciers. The largest island in Svalbard is Spitsbergen. This island is also the most important island in Svalbard, where the largest settlement, Longyearbyen, and the research settlement, Ny-Ålesund, are located. These settlements were traditionally associated with the mining industry [12, 13].

Svalbard is exposed to long-range transport pollution mainly through the atmosphere and ocean currents. Local sources of pollution in Svalbard come from the mining industry, the settlements, local traffic, research, airport and tourism [16, 17]. The settlement and research station, Ny-Ålesund, is located on Brøggerhalvøya, a peninsula on the north-western Spitsbergen [18, 19]. The total landmass of Brøggerhalvøya is about 221 km^2, where approximately 25% is covered by glaciers. With its average annual air temperature of -5.7 °C, the climate in Ny-Ålesund is typically warmer than other places in Svalbard at the same latitude [12, 18].

2.2 Glaciers

Glaciers are a part of the cryosphere, which comes from the Greek word "kryo", meaning cold [20]. Glaciers cover 10% of the land surface on Earth and play an important role in many landscapes. They release melting water, are cooling the weather in the summer, and travel down valleys or into increased basins [21]. Glaciers are sensitive to climate change. Weather conditions such as snowfall, and changes in temperature make the glaciers constantly increase and melt [20]. Concerns about increased risks from avalanche and flood outbreaks, disappearing water supplies, and changes in sea level have been raised in the last decades due to decreasing of the global ice volume. The glaciers are now frequently thought of as a threatened species, suffering from anthropogenic climate change [12, 20].

Enormous landscape areas of the Earth's surface have been shaped by glaciers, which have removed rock and sediment and left behind thick accumulations of glacial debris. The moraines which have formed like tidemarks at the edges of former glaciers are important sources of knowledge about former glacier activity as well as climatic change. Greenland, Antarctica, and also smaller glaciers and ice caps have preserved ice that is a rich source of information about previous environmental conditions [20]. Glaciers can be divided into different zones, with different temperatures and physical characteristics [12, 22].

2.3 Supraglacial Debris and Cryoconite Holes

Supraglacial debris is debris that is transported on the surface of the glaciers. Globally, supraglacial debris occurs in most regions of glaciers and is more often found in mountainous regions. With increasing glacier size, the amount of debris is decreasing [9]. This debris commonly originates from sources such as dust particles transported by wind, rock avalanche debris, rockfall, soil, and snow avalanches from surrounding mountains [10, 11]. Studies show that supraglacial debris also consists of organic matter produced by glacier organisms. This debris is often called cryoconite [10, 12].

The term cryoconite is combined with two ancient Greek words for cold and dust, and was first presented by the arctic explorer Adolf Erik Nordenskiöld, during his exploration of Greenland Ice Cap in 1870 [23, 24]. Cryoconite is granular sediment that contains both a mineral and organic fraction found on glacier surfaces [24–26], typically on the ice surface of the glacier ablation zone [27]. The majority of the cryoconite composition, about 85-90 %, is mineral fractions. The remaining fraction contains organic matter. This mineral dust on the ice surface works as a substrate for microbial growth and the formation of bio-films, which structure and darken the produced sediment [26]. Because of its dark colour, cryoconite absorbs solar radiation efficiently and makes holes that can be tens of centimeters deep into the glacier ice surface, and are filled with its own meltwater [27]. Cryoconite holes are common features on perforating ice surfaces around the world [24, 25]. In areas of the glacial cryosphere where melt rates are high, the cryoconite holes are unstable. This means the holes can melt into streams and accumulate into new deposits and can create new holes [12, 27].

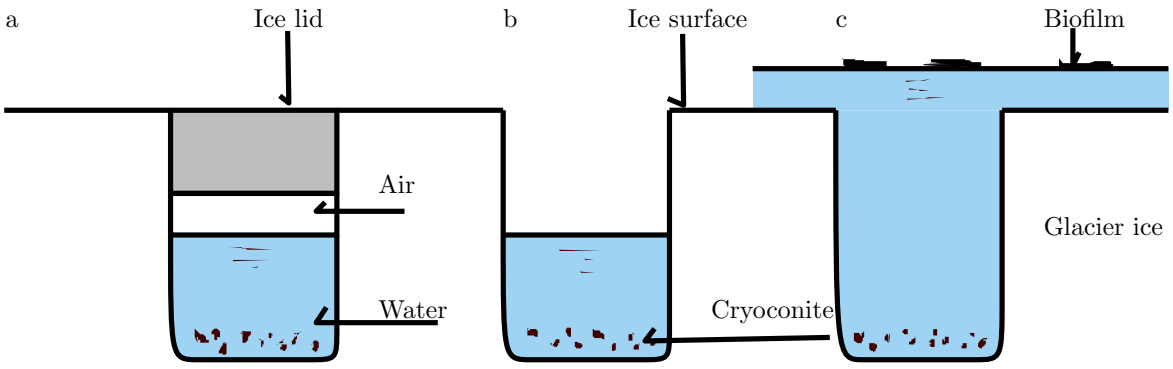

Figure 2.1: Cryoconite holes of a) a closed hole, b) an open hole and c) a submerged hole. Modified from "Glacial ecosystems", by Hodson et al. [2008].

Cryoconite holes can be categorised into three types; open holes, submerged holes, and closed holes. The three different types are illustrated in figure 2.1. The surface heat balance and the availability of surface water cause the creation of these three different types of cryoconite holes. Cryoconite holes can consist of more life than in the snowpack. Bacteria, algae, and fungi are the majority of life that occurs in cryoconite holes [12, 27, 28].

Only a limited research has been done on the correlations between the composition of cryoconite, the glacial environment, and atmospheric depositional fluxes. Both natural and anthropogenic atmospheric emissions exist on glaciers and snow. Because pollutants that have accumulated

in the ice over the past few decades are being remobilised, the thawing of glaciers presents major problems. Cryoconite may participate in this process due to its physical and chemical characteristics. The adsorption and accumulation of both organic and inorganic materials in cryoconite may be increased by the fine mineral material and organic matter that are already present. Data from the few studies that have been conducted so far indicate something similar is occurring. The cryoconite material can therefore impact what will happen to the pollutants found in the glaciers as the glaciers are shrinking [26]. Analysing the composition of supraglacial debris and cryoconite can give a better understanding of the dynamics which control these processes. Studies have shown that cryoconite can accumulate elemental carbon, specific elements, and radioactive isotopes. Atmospheric emissions play an important role on the influence of the composition of cryoconites. There have been found high amounts of isotopes as ^{210}Pb, which have occurred from the atmosphere. Although previous studies show that atmospheric deposition cannot be directly due to this accumulation alone. Meltwater is the one logical place to look for impurities besides direct atmospheric pollutants. When looking at the glacier, with the snow, and ice, as well as their impurities and pollutants, the glacier can be viewed as a temporary storage site for emissions from the atmosphere. Through meltwater, debris and other matter that has been preserved in the glacier is mobilised by ablation and released into the environment. Some amounts of pollutants will deposit annually on the glaciers. When there is a melting season, a part of these amounts will mobilise and be transported down to the debris and cryoconite, on the surface of the glacier. The only available substrate where anthropogenic and natural compounds can be accumulated is cryoconite. It can therefore be assumed that a part of all impurities that are transported with meltwater on the glaciers are being retained in cryoconite and the debris [12, 26].

2.4 Organic matter in Supraglacial Debris and Cryoconite Holes

Glacier ecosystems are changing quickly. The fast melting of glacier ice from the Earth's surface, particularly in the Arctic indicates that there will eventually be a transition from glacial to proglacial environments. Carbon will be captured and cycled in a different way in this proglacial environment, compared to the glaciers. Therefore, measuring the current biogeochemical carbon cycle in glacial ecosystems is important for determining carbon flow and predicting how the future will change [28, 29].

Sunlight is an important energy source for photosynthesis, as well as an energy source for melting glaciers. As mentioned in chapter 2.3, cryoconite holes contain microbial growth and other organic and inorganic matter. This microbial growth usually consists of heterotrophic - and phototrophic bacteria and algae. The energy sources for these microbial growths are organic carbon and light. Carbon and inorganic carbon are sources for growth in these microbial communities [27, 29]. Through primary production and respiration, supraglacial environments will have the potential to influence local and potentially even global carbon budgets. These phototrophic microorganisms have a significant impact to change the chemical environment of cryoconite holes, through photosynthesis. In closed cryoconite holes, the pH is increased and the pCO_2 is lowered, compared to open systems [28]. Present studies are limited to measurements from local glaciers and are limited to estimation on a larger scale [29].

There have been used different analytical methods to determine the quality of glacial organic matter. These are methods such as spectrofluorometric analysis that can be used to determine between organic material resistant to decomposition and easily decomposable carbon. This method may also reveal the origin of the organic matter. The use of nuclear magnetic resonance techniques reveals the composition and the origin of the organic matter. Quality and quantity of organic carbon in supraglacial debris have also been determined by using high-temperature combustion, chromatographic, spectrophotometric, and microscopic methods [29].

Research on smaller glaciers in the Himalayas, Tibet and the Arctic, reports the C:N molar ratio to be between 8-14 [30]. A study on the debris on the Greenland ice sheet from Stibal et al. 2010, reported TOC and TN content found within the same range of the smaller glaciers, as the study of Takeuicki, 2002, cited in Stibal et al. 2010 [29]. Stibal et al. 2010 recorded most of the samples with a C:N molar ratio of 8-9, which is also a typical value found in soils (according to Cleveland and Liptzin, 2007, as cited in Stibal et al. 2010 [29]), [12].

2.5 Trace elements

There are 90 naturally occurring elements on the earth. The main elements of the Earth's crust are O, Si, Al, Fe, Ca, Na, K, and Mg. While in river water, elements such as Ca^{2+}, Na^{2+}, Mg^{2+} and K^{+} are presented dominantly in decreasing order [31].

The elements in biological systems can be divided into major elements, which include elements such as C, H, N, O, and minor elements; which include the elements Ca, Cl, Mg, P, K, Na, and trace elements which are the remainder elements [31]. Multi-element methods such as inductively coupled plasma mass spectrometry (ICP- MS) and neutron activation analysis (NAA) can be used to measure elements on levels as low as < 0.01 µg kg^{-1} [31].

Trace elements can be divided into essential, non-essential, and toxic elements, all depending on parameters such as concentrations, speciation of the element, pH, redox properties, and other physical and chemical properties. These elements are important due to their association with problems related to the environment, plants, animals, and human health [31, 32].

In plants, trace elements are essential when their function cannot be substituted with other elements in their specific biochemical role. They also have a direct influence on the organisms' ability to grow and its metabolic processes [31].

There are many different sources of trace elements, both natural and anthropogenic [32]. In human and animal systems, trace elements are considered essential if depletion consistently results in a deficiency syndrome and repletion specifically reverses the abnormalities. Trace elements including As, Co, Cr, Cu, F, Fe, I, Mn, Mo, Ni, Se, Si, Sn, V, and Zn are met by these criteria. Non-essential elements are elements that have no proof of being essential for metabolic processes. Some trace elements are categorised as toxic. Pb, Hg, and Cd are examples of toxic elements. Depending on the concentration levels of the elements, and whether the levels are exceeding the limits of safe exposure, all trace elements can be predominantly classified as toxic. These levels differ from one element to another [31].

The entire role of trace elements in living organisms is directly associated with their interaction within all environmental, geological, biological, or marine systems. The trace element concentration in soils may influence the elemental composition of vegetation, which will also have an effect on the food chain through animals and human tissue [31].

The majority source of all the natural trace elements in the various environmental, geological, biological and marine systems come from the earth's crust [31].

2.6 Trace element contamination and pollution

There are varying degrees of all trace elements within every compartment of the environment. An increase in a trace element in relation to the natural elemental occurrence refers to environmental pollution. Although this increase can relate to natural occurrences, it is linked to anthropogenic activities. Activities from industry and agriculture are typically contributing to more environmental trace element contamination, compared to natural natural occurrence [31].

2.6.1 Air pollution

Air pollution is generally related to gaseous emissions into the atmosphere. This includes gas such as carbon monoxide, carbon dioxide, hydrocarbons, halocarbons, sulphur dioxide, hydrogen sulphide, nitrogen oxides, NO, NO_2, N_2O, and ammonia. Trace element or heavy metal contamination can result primarily through atmospheric particles or particulates. The main sources are coal, and fuel power generation plants, metal processing and smelting, transportional combustion, waste incineration, and aerosol sprays (halo-carbons). Petroleum refineries, the production of chemicals, chloro-alkali and cement, and non-ferrous metal and aluminium smelters are the sources of majority of the industrial emissions. In overall, most trace elements or heavy metals can be released through industrial emissions, although the major examples are Ca, Mg, Ba, Cd, Pb, F, Br, Ti, V, Mn, Fe, Cu, Cr, Ni and Zn [31].

2.6.2 Long-range atmospheric transport

Long-range atmospheric transport is the movement of air pollutants, including trace elements, over long distances through the atmosphere. This may be pollution from different sources such as industrial emissions, volcanic emissions, fossil fuel combustion, and waste burning, soil-derived dust [17, 31]. Wind patterns and atmospheric circulation are transporting the trace elements to remote areas, including the Arctic [4, 17].

2.6.3 Long-range atmospheric transported trace elements in the Arctic

Long-range transport of contaminants to the Arctic can occur in four major ways. These contaminant pathways include the atmosphere, ocean currents, and the riverine. As a result, the Arctic may act as a reservoir storage or sink for contaminants. These contaminants are removed by a number of processes from the atmosphere, oceans, and rivers and make access to animals and plants [33].

Toxic substances also occur in the long-range atmospheric transport of pollution to the Arctic. These substances can have a huge impact on ecosystems and human health and are substances such as mercury or persistent organic pollutants [4, 31]. Pollution in the Arctic is primarily originating from southerly latitudes [4, 33]. The fastest and most direct transportation from the source of pollution is through the atmosphere. This transfer may take a few days or weeks to complete [33, 34]. The atmospheric transport patterns are depending on the seasonal weather. The Arctic front is being pushed south by a strong high-pressure system over Siberia. This makes industrialised polluted areas of Eurasia within the Arctic airmass and can move contaminants across the pole [33, 34]. As a result, compared to the summer and autumn, contaminants carried by the atmospheric wind occur more frequently in the winter. In the summertime, the high-pressure systems break up, and the weakening of low-pressure systems over the oceans occurs. As a result, the transportations of pollutants are less significant in the summer [33, 34]. When the temperature is warmer, promotes the development of clouds and rain which can remove the contaminants from the air before transportation [33]. With cold temperatures, the natural decomposition of contaminant compounds decreases, which makes the contaminants intact and increases their persistence [35].

There is small local pollution in the Arctic [4]. Pollution includes volcanic emissions from the volcanic regions in Alaska and the Kamchatka Peninsula, Northeast of Russia, and anthropogenic emissions from urban areas such as Murmansk which is primarily notable in the northern part of Russia. Also, emissions from the oil industry and shipping are sources of local pollution in the Arctic [4]. Trace elements such as Pb, Cd, and Zn are heavy metals that can often be released into the atmosphere from anthropogenic activities, such as high-temperature processes. These

metals are often released in greater quantities, through water runoff, dumping and sanitary discharges [34].

There are limited studies of monitoring atmospheric deposition of trace elements in the Arctic [36]. However, different methods of monitoring long-range transported elements have been done in both wet deposition and dry deposition [36,37]. Since moss has no roots and depends primarily on a source of nutrients from the atmosphere, analysing trace elements in moss is an effective method to study the atmospheric deposition of trace elements [37,38].

2.7 Theoretical methods

2.7.1 Sample preparation

Theory about the sample preparation related to analysis as ICP-MS, TOC, TN/TC, UV-Vis spectrophotometry and SUVA is described to illustrate the sample preparation used in this project.

2.7.1.1 Freeze drying

Freeze drying is the most reliable method used to dry labile materials. Water is removed from the material by sublimation, where it will go from a solid phase to a gas phase. This is the main principle in the freeze-drying process. Figure 2.2 illustrates a typical phase diagram for a compound, such as water, with three phases: solid, liquid and gas. Where the vertical line from point A is the phase of sublimation [39]. The freeze-drying process consists of three stages; freezing, primary drying and secondary drying. The first stage consists of freezing the material. The aim of the primary drying phase is to make the water sublimate by lowering the pressure and supplying enough heat to the material. About 95% of the water in the material is sublimated in this drying phase. In the secondary drying phase, the temperature is set higher than in the primary drying phase to remove the unfrozen water molecules which are still bonded to the material [12,40,41].

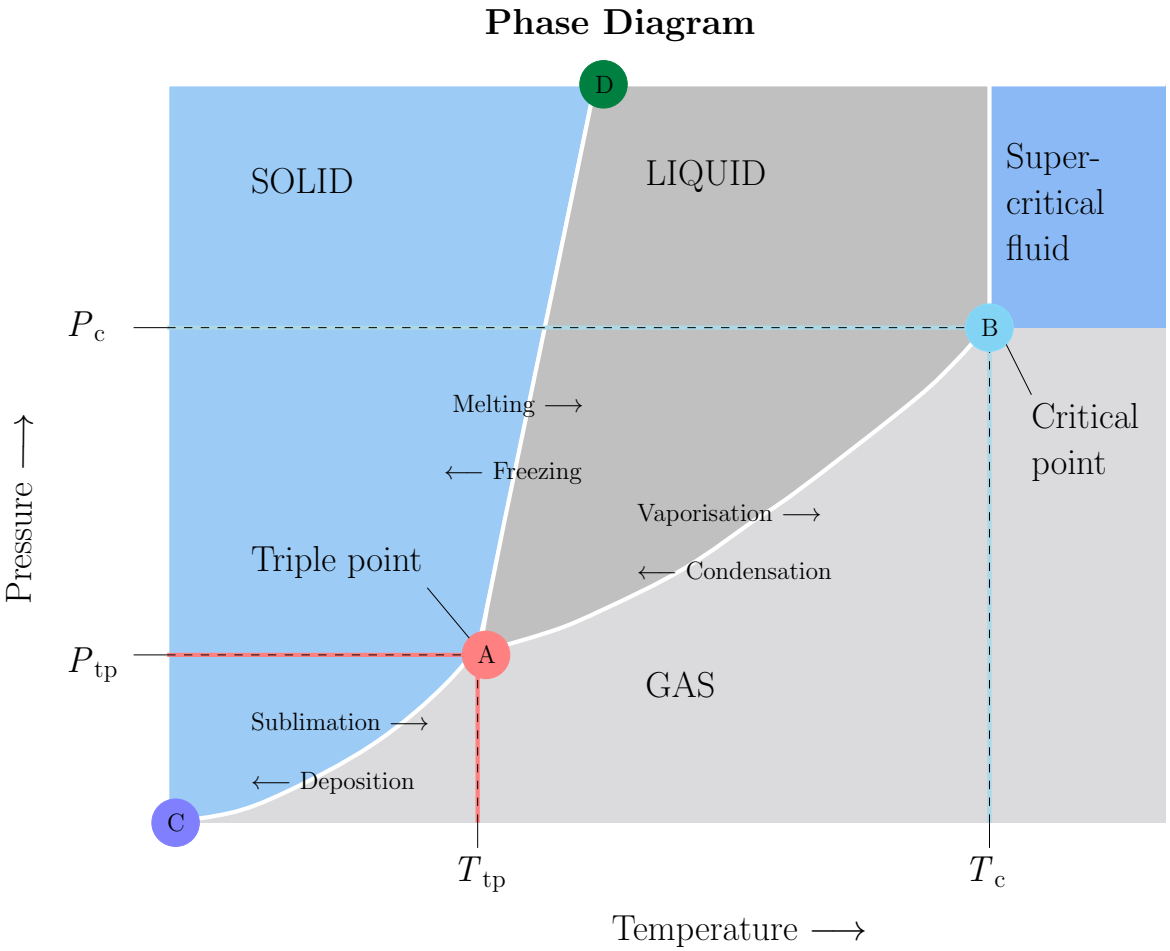

Figure 2.2: An example of a phase diagram for a compound with three phases. Solid phase, liquid phase, and gas phase, as well as a supercritical region. Modified from "Phase Diagram: Pressure and Temperature", by Westin [2021]. [39].

2.7.1.2 Microwave-assisted digestion

Microwave-assisted digestion is a method where organic and inorganic samples are decomposed with the use of concentrated acid. By using oxidising acids, organic samples are digested to produce a solution that should be applicable to the analysis that follows using a wide range of analytical techniques (e.g. ICP - MS). The primary acid used for digestion in a broad range of samples is concentrated nitric acid (HNO_3). The use of closed vessels will increase the boiling temperature of the digestion mixture. This method improves the digestion efficiency of organic compounds. There is some microwave equipment currently available that support temperatures of about 300 °C and pressure of 200 bar [42]. An example of microwave-assisted digestion in a closed vessel can be done by Milestone UltraCLAVE [42, 43]. Nitric acid can be combined with nonoxidising acids like hydrochloric and hydrofluoric acids to digest inorganic samples [42].

In order to digest organic samples, heated nitric acid is generally used, and the majority of analytes are soluble in the completed digest. The boiling temperature of nitric acid is relatively low, at atmospheric temperature. Long digestion times are the outcome, particularly when open vessels are used. Using a mixture of nitric acid and sulfuric acid (H_2SO_4) increases the temperature of digestion up to around 338 °C, and the digestion time will be reduced [12, 42].

2.7.2 Analytical methods

2.7.2.1 Inductively coupled plasma-mass spectrometry (ICP-MS)

Inductively coupled plasma-mass spectrometry (ICP-MS) has been a fast-growing technique of determination analysis of elements [44,45]. The system is based on the principles of an ICP-torch connected to a mass spectrometer (MS), where the sample is usually in liquid form. The sample is pumped into a nebuliser, and is converted into a fine aerosol with argon gas. Using a spray chamber, the fine droplets of aerosol, which is about 1- 5% of the sample, are separated from the larger drops. A sample injector feeds the aerosol into the plasma torch after it exits the exit tube of the spray chamber [45, 46]. Figure 2.3 illustrates a basic ICP-MS instrument setup [46].

ICP torch: The plasma torch is used to produce ions with a positive charge, in the ICP MS system. The plasma torch in ICP-MS is formed by the interaction of an intense magnetic field, which is produced by radio frequency (RF) passing through a copper coil, on a flow of gas, usually argon, through a concentric quartz tube, which is the torch. This step is ionising the gas. When this gas collides with a source of accelerated electrons from a high-voltage spark, a temperature of about 6000 - 10 000 K is generated [45, 46].

MS interface region: When the ions are produced in the plasma, they are led into the mass spectrometer via the interface region, which is in a vacuum. There are two cones in the interface region; a sampler and a skimmer cone. Both cones have a small opening where ions can pass through to the ion optics, leading them into the mass separation device [46].

Ion optics: When the ions are extracted from the interface region, they are fed into ion optics using electrostatic lenses, focusing the ion beam towards the mass separation device, as well as preventing detection of neutral species, photons, and particulates [46].

Mass separation device: The ion beam with all the analyte and matrix ions leaves the optics and enters into the mass spectrometer, known as the mass separation device, which is in a vacuum. ICP-MS systems have different mass separation devices. One of the most common mass separation devices is the quadrupole. This method separates the analyte ions of a mass per charge ratio (m/z) and detects the ions subsequently. All interfering, non-analyte and matrix ions are rejected. Quadrupole instruments usually also have collision cells, reaction cells or interfaces. This technology can reduce polyatomic ion interferences [46].

Ion detection and measurement: Ions are converted to an electrical signal by an ion detector in the final step of the process. The data management system transforms this electronical signal in a standard way, by using the ICP-MS calibration standard and converts it into analyte concentrations [46]. A number of detection instruments can handle a large dynamic range and determine analyte concentrations from ppt to ppm levels [45, 46]. Therefore, one of the most sensitive techniques available used for elemental analysis is ICP-MS [31].

The detection limit of ICP-MS is low, and can also be possible to quantify at high parts per million level [46].

ICP-MS interferences can occur, as isobars, abundance sensitivity, polyatomic, doubly charged, physical inreferences, memory interferences and ionisation interferences [45].

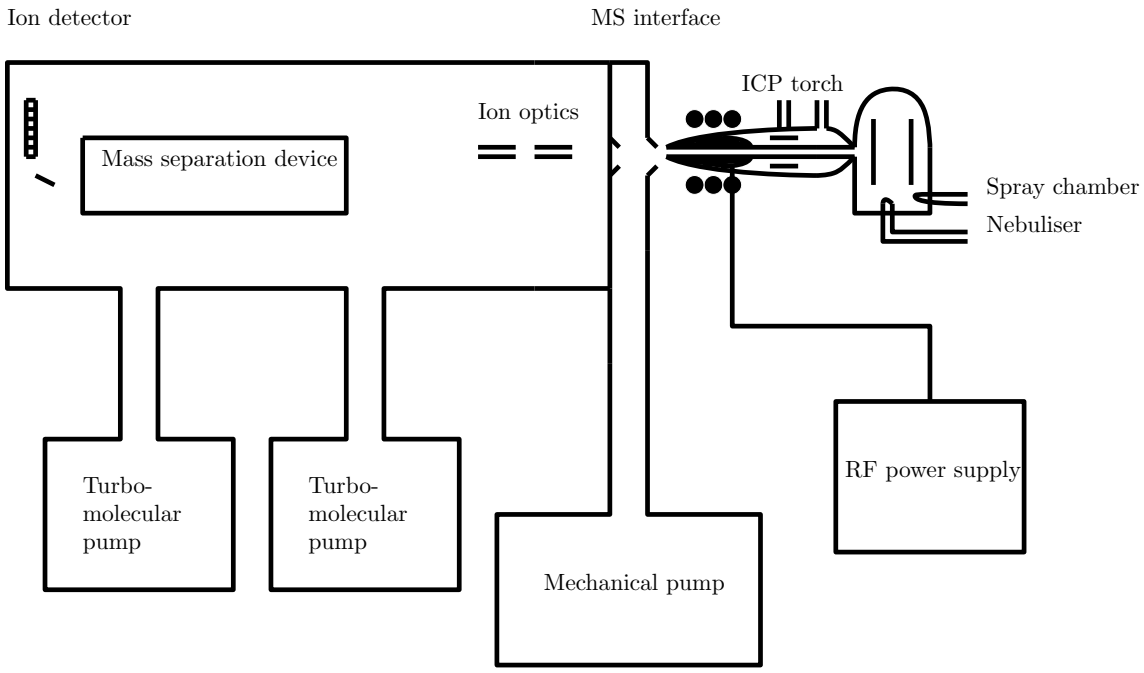

Figure 2.3: A diagram of a typical ICP-MS instrument system. Modified from "Practical Guide to ICP-MS", by Thomas [2008]. [46].

2.7.2.2 Determination of Total Carbon (TC), Total Inorganic Carbon (TIC) and Total Organic Carbon (TOC)

Determination of total organic carbon can be determined in different research areas. Examples of determination of carbon are in sediments, in liquid water, and even extracts [47]. Carbon is normally divided into two forms, such as inorganic carbon (TIC) and organic carbon (OC). Organic compounds are formed when total organic carbons (TOC) make bonds with hydrogen or oxygen [48]. In water, inorganic carbon (TIC) is represented by carbon dioxide, carbonic acid, and its dissociation products. Calcite particles are also present [47]. Total carbon (TC) is the combination of the two forms of carbon; the connection between them is represented by the expression TOC= TC - TIC [48].

Total Organic Carbon can be analysed with the use of a combustion instrument. The sample goes inside the Total Carbon (TC) combustion tube, which is heated to 680 °C and has an oxidation catalyst inside. In the combustion tube, the sample is burned. This turns the sample's TC components into carbon dioxide [49].

The sample combustion products are transported from the combustion tube to an electronic dehumidifier by carrier gas, which flows through the combustion tube at a rate of 150 mL/ min. The gas is cooled and dehydrated in this electronic dehumidifier. To remove halogens and chlorine, the gas carries the sample combustion products through a halogen scrubber. Finally, the sample combustion products are then transported by the carrier gas to the cell of a non-dispersive infrared (NDIR) gas analyser. This is where the carbon dioxide is detected. An analog detection signal with a peak is produced by the NDIR. The TOC-Control L software measures the peak area. [48].

This peak correlates with the sample's TC concentration. A calibration curve equation can be created by analysing various TC standard concentrations and showing the relation between peak area and the concentration of TC mathematically. Through analysing the sample to access the peak and then using the peak in the calibration curve equation, the TC concentration in the sample can be obtained [48].

The carbon in carbonates and carbon dioxide dissolved in water make up the TIC as determined by TOC analysis. All carbonates convert to carbon dioxide CO_2, by adding hydrochloric acid to the sample. This will acidify the sample, and the pH will be lower than 3. This is expressed as the reactions, R1 and R2:

$$Me_2CO_3 \; + \; 2\,HCl \; \rightarrow \; CO_2 \; + \; 2\,MeCl \; + \; H_2O \tag{R1}$$

$$MeHCO_3 \; + \; HCl \; \rightarrow \; CO_2 \; + \; MeCl \; + \; H_2O \tag{R2}$$

Bubbling pure air or nitrogen gas, which is free of carbon dioxide, through the sample, will volatilise dissolved carbon dioxide, and carbon dioxide in the sample are [12, 48].

2.7.2.3 Determination of Total Carbon (TC) and Total Nitrogen (TN)

Total Nitrogen (TN) is defined as all compounds in a sample that contain nitrogen. TN includes both inorganic nitrogen (IN) and organic Nitrogen (ON). TN is represented as the total mass of nitrogen per amount of sample [49].

Determination of total carbon (TC) and total nitrogen (TN) content in sediment material can be determined through the combustion of the sample in oxygen (ultra-pure grade, 99.995% purity) at a temperature of 1200°C. After the combustion, the gas mixture of CO_2 and NOx is led by a carrier gas through a splitter. This is where part of the combustion gas is collected. The remaining gas is led through an IR detector, in which the CO_2 content is measured. The collected gas mixture is led by a carrier gas of helium (nitrogen-free, 99.995% purity) through a copper reduction oven to reduce NOx to N_2. The carrier gas is then led through scrubbers to separate CO_2 and water. Following scrubbing, the carrier gas is finally led through a TCD detector to analyse the nitrogen content [12, 49].

2.7.2.4 UV/VIS- spectrophotometry

The technique of measuring the attenuation of electromagnetic radiation by an absorbing substance is known as ultraviolet and visible absorption spectrophotometry (UV/VIS- spectrophotometry) [50]. The spectral range of this radiation is about 190–800 nm. By measuring only the absorbance, accurate measurements of the attenuation can be made. Within certain limits, the absorbance is correlated with the concentration of the target analyte and the length of the light's path through the sample during irradiation. This correlation is called Beer's Law and is written as shown in equation 2.1.

$$A = \epsilon \times b \times c \tag{2.1}$$

A means absorbance, epsilon is the molar absorbance coefficient (1/(mol × cm)), b is the path length in cm and c is the concentration of absorber (mol/L) [50].

2.7.2.5 Specific UV absorbance (SUVA)

Specific UV absorbance (SUVA) is the UV absorbance of water at a given wavelength, measured in inverse meters (m^{-1}), divided for dissolved organic carbon (DOC) concentration (mg L^{-1}), given by the equation 2.2.

$$SUVA = \frac{UV_{254}(cm^{-1}) \times 100}{DOC(mgL^{-1})} \tag{2.2}$$

The amount of aromatic structures is correlated with SUVA measured at the wavelength of 254 nm. SUVA is a useful method for determining the amount of dissolved aromatic carbon in water samples. $SUVA_{254}$ values of > 4.0 L/mg $\times$ m of natural water are defined with high $SUVA_{254}$ values and have a high content of hydrophobic and aromatic structures. Water with low $SUVA_{254}$ values has an $SUVA_{254}$ of < 2.0 L/mg $\times$ m and are representing hydrophilic materials [12, 51, 52].

2.8 Quality control (QC) and Quality assurance (QA)

Quality control (QC) and quality assurance (QA) are important and should be included in all environmental chemical analysis. Weak quality assurance and quality control can lead to incorrect data, and when used improperly, it can result in poor environmental decisions. The definition of quality assurance is used to describe the procedures and handling made to verify the representativeness and validity of samples as well as the accuracy and reliability of the analytical test results [53]. This includes the use of validated methods, skilled personnel, calibration of the equipment and instruments, use of certified reference material (CRMs) and use of replicates [54]. The steps that measure and observe the performance of quality assurance procedures in relation to set objectives are referred to as quality control. Quality control can involve the use of duplicate sampling, analysing field and laboratory blank, replicates, and certified reference materials, and testing the cleanliness of the equipment [53].

It might be particularly difficult to detect a systematic error in an analytical method. To identify and correct for a systematic error in an analytical method, a combination of the steps presented in chapter 2.8.2 and 2.8.4 can be taken [12, 55].

2.8.1 Quality control in sampling, sampling plan and analysis

Fieldwork and collecting samples should be done in accordance with a plan which ensures that they are represented in the way they naturally occur. There are variables that need to be taken into account when producing a sampling plan [31]. When sampling river water and sediment, guidelines for the planning of the sampling, and how to handle the sample techniques can be followed in accordance with ISO 5667-1:2020 Water quality - Sampling - Part 1: Guidance on the design of sampling programs and sampling techniques [56]. Guidance on the preservation and how to handle the water samples are described in ISO 5667-3:2020 Part 3: Preservation and handling of water samples and ISO 5667-15:2009 Part 15: Guidance on preservation and handling of sludge and sediment samples, respectively [57]. Quality control and quality assurance of the water and sediment samples are described in ISO 5667-14:2014 Part 14: Guidance on quality assurance and quality control of environmental water sampling and handling.

A strategic sampling plan should be initiated. There are different types of sampling that can be done, depending on the sampling location [31]. Random sampling can be done where no obvious patterns of analyte exist. One practical form of random sampling for a surface is to collect the samples in a pattern of a "W" across the sampling area. This method involves systematically collecting samples in a zigzag or "W" pattern to cover larger areas and to minimize sampling bias. This method is useful in initial surveys and can provide information on the general distribution of an analyte while using a limited number of samples [31].

A proper sampling technique should be obtained to avoid contamination. Disposable gloves should be worn during the sampling procedure, in order to prevent sample contamination and to

avoid being in contact with the sample. It is important to avoid cross-contamination from one sample location to another by handling protective clothing and sampling equipment in such a way as to avoid cross-contamination [58].

Sample handling and storage techniques are important to avoid contamination during transport and storage [59]. Sampling equipment, such as sampling containers, cups, tubes, and syringes should be cleaned before use. When sampling water, the bottle should be rinsed three times, and collecting should be done facing up streams towards the water flow [58]. When the analyte to be studied are trace elements, in sediment and water samples, metal-free plastic containers should be used, to prevent metal contaminations in the samples [57].

Water and sediment samples should be kept cool or frozen, to increase the time of transport and storage. When transporting the samples, a sampling plan in accordance with ISO 5667-1:2020 should include; the time between sampling and the start of transport, transport time, and a starting time for the analysis in the laboratory. The containers with the samples should be protected from breakage during the transport, by the appropriate package. The samples should be transported as soon as possible after sampling [59, 60].

Each sample container should be clearly labeled, to make it able to identify the sample, and may include information such as sample number, sample material, date and time, sampling point, preservation, and pretreatment [60]. Markers with solvent must be avoided, which can risk contamination of the sample. Easily recognisable types of sample containers for various analysis parameters can be used to prevent cross-contamination[60].

The storage of water samples and sediment samples in the laboratory varies on which specific analysis methods are being used. Samples must not be stored for a longer period than described in ISO 5667-3. Water samples and sediment samples, before it is dried, should be stored in refrigerators with a temperature of 3 ± 2 °C. If the samples are preserved in a freezer, the temperature should be below -18 °C [59, 60]. When sediment samples have been dried, they can be stored at ambient temperature [59]. Water samples analysed for trace elements should be preserved with HNO_3, to acidify the sample to $pH < 2$ [57].

2.8.2 Standards

Certified reference materials (CRMs) are standard materials certified to contain specific concentrations of one or more analytes. Analysing CRMs is the best method for determining the systematic error of an analytical method. Certified reference materials can be provided in different ways. Synthesis can alternatively be used to obtain CRMs. Another option is to procure CRMs from various governmental and industrial sources [53, 55], such as the National Institute of standards and Technology (NIST), the National Research Council of Canada (NRC), and the International Atomic Energy Agency (IAEA) [53]. Over 1300 CRMs, such as rocks, sediments, river sediments, and more, are available from these institutes [12, 55].

2.8.3 Internal standard

An internal standard is a compound that is added to a sample and standards in a specific and defined quantity. This internal standard should result in greater accuracy and must have the same conditions as the sample that is tested and [31].

2.8.4 Blanks

The reagents and solvents used in a determination are present in a blank, but the analyte is absent. To recreate the analyte environment, as well known as the sample matrix, many of

the sample's components are typically added. In a blank determination, the blank material is exposed to each step of the analysis. In order to correct the sample measurements, the results are then applied. Errors caused by interfering contaminants from the reagents and containers used for analysis are revealed by blank determinations [12, 55].

2.8.5 Limit of detection

The Limit of detection (LOD) is the definition of the lowest concentrations of an analyte that is reliable, with predefined conditions of the test, where detection is possible to achieve [61, 62]. The concentration is not necessarily quantified [62].

2.8.6 Limit of quantification

The limit of quantification (LOQ) is the lowest concentration where an analyte can be reliably detected and predefined qualifications have been obtained for bias and imprecision. The limit of quantification can be at a much higher concentration than the limit of detection, or at the same concentration [61, 62].

2.9 Statistics and data analysis

2.9.1 Mean

The sample mean $\bar{x}$, is the mathematical average of a limited sample taken from a set of data. The sum of the measurement values divided by the total number of measurements is known as the sample mean and is expressed by equation 2.3. Where x_i represents the individual values of x, and N represents the number of measurements in the sample set [12, 55].

$$\bar{x} = \frac{\sum_{i=1}^{N} x_{\mathrm{i}}}{N} \tag{2.3}$$

2.9.2 Standard deviation

The population standard deviation σ, which is a measure of the precision of the data set, is given by the equation 2.4. N represents the number of data points in the sample set [12, 55].

$$\sigma = \sqrt{\frac{\sum_{i=1}^{N} (x_i - \bar{x})^2}{N-1}} \tag{2.4}$$

2.9.3 Normal distribution

The normal distribution is an important distribution method used when working with analytical data [31, 63]. Though there are some exceptions, replicate analytical measurements are typically assumed to have a normal distribution [31]. In order to determine if the samples in a data set are normal distributed, Shapiro- Wilk test can be used [64].

If the values in the data sets are normal distributed, the means can be compared by using a parametric method. In a data set with two normal distributed means being compared, a parametric method, such as the Student t-test can be used. If a data set with three or more means are being compared, the one-way analysis of variance (ANOVA) can be used [65]. When the data set is not normally distributed, a non-parametric method, such as Mann-Whitney U-test, should be used [12, 66].

2.9.4 Box plot

The box plot is a common technique used to visually present data sets. This type of plot contains a lot of information and allows easier thought and understanding of the data results. As illustrated in figure 2.4, the box plot is typically divided into quartiles of data distribution. The quartiles are divided into four equal parts. The locations of the upper and lower quartiles are shown in a box [67, 68]. The area between the upper and lower quartiles, which makes up half of the distribution, is defined by the inner quartile range in the interior of the box. In order to eliminate extreme outlines, lines are applied to the extreme points of the distribution, either the maximum and minimum limit values in the data set, or to a multiple of the inner quartile range. These lines are also sometimes called whiskers. Outliners are often represented as a symbol (e.g. circular points). The line which divides the box into two parts represents the median of the data set [12, 68].

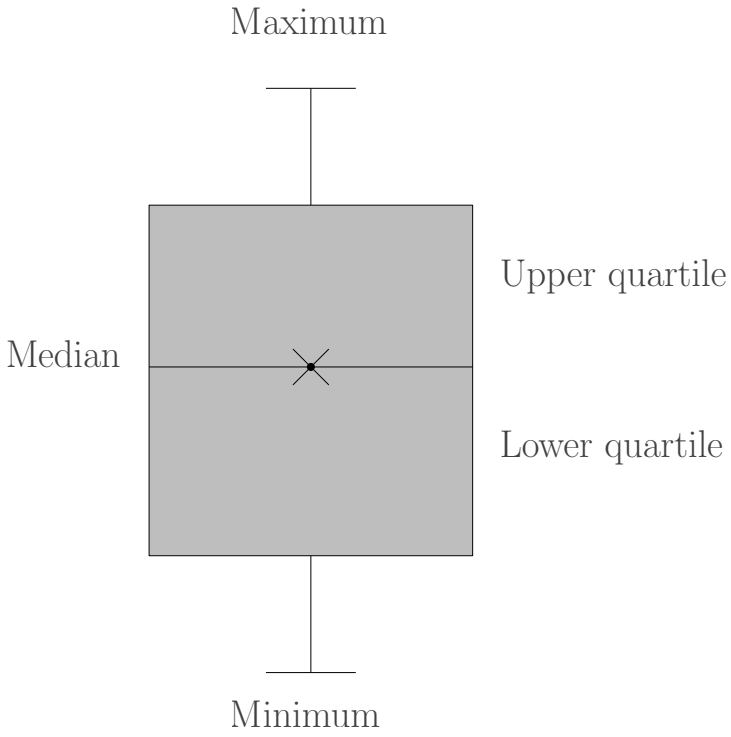

Figure 2.4: An illustration of the construction of a box plot. Modified from "Methods for Presenting Statistical Information: The Box Plot", by Potter et al. [2006] [68].

2.9.5 Multivariate Data Analysis

There are different types of multivariate data analysis and can be used for several different purposes. The different methods that can be used, depend on what type of outcome the results are wanted. Therefore a formulation of data analytical problem should be well formulated, and the collected data is suited to reach these objectives [69].

2.9.6 Principal component analysis

Principal component analysis (PCA) is one of the most widely used multivariate data analysis techniques [69, 70]. In accordance with the principles of PCA, a data matrix, X, is divided into two parts, where one part is of structure and one of noise. The X matrix is often called the data set and consists of n objects and p variables. The objects can be observations, samples, and experiments, while the variables can be typical measurements for each object [70].

The principal component analysis aims to extract important data from the data table. The data set is reduced and made simpler, by only keeping the most important information. The structure of the observations and variables are analysed. This information is expressed as a set of new linear combinations, made of the original variables, and called principal components. The first principal component (PC 1) must have the largest variance. The second principal component (PC 2) is calculated under the constraint of being orthogonal to the first principal component and must have the most inertia. The same formula is used to calculate the following principal components. Factor scores refer to the values of the new variables for the observations. These factor scores can be geometric applied as projections of the results to the principal components [70].

3 Experimental

The method used in this project is presented in this chapter. The sediment samples in this project were analysed by high-temperature combustion with Non-Dispersive Infrared detection (NDIR) for Total Carbon (TC) and Total Nitrogen (TN) content using Primacs$^{SNC-100}$ instrument and by Inductively coupled plasma mass spectrometry (ICP-MS) for elemental analysis. The water samples in this project were analysed by Inductively coupled plasma mass spectrometry (ICP-MS) for elemental analysis, and high-temperature combustion with Non-Dispersive Infrared detection (NDIR) for Total Carbon (TC), Total Inorganic Carbon (TIC) and Total Organic carbon (TOC) using Shimadzu Total Organic Carbon Analyzer (TOC-L), followed by measuring of the UV absorbance at 254 nm, for determining the Specific UV absorbance (SUVA) [12].

3.1 Fieldwork

Fieldwork and sampling for this project were carried out 25th - 26th of August 2022 at different locations on the glacier systems, as well as the melting water outlets, of Austre Brøggerbreen and Vestre Brøggerbreen at Ny-Ålesund area in Svalbard [12].

3.1.1 Geology of the Ny-Ålesund area

Ny-Ålesund is located on Brøggerhalvøya, southwest of Kongsfjorden, and is surrounded by dominantly terrestrial glaciers, such as Austre Brøggerbreen, Vestre Brøggerbreen, and Midtre Lovénbreen, and low-elevation mountains [19]. Austre brøggerbreen is a cold base glacier [71, 72], while Vestre Brøggerbreen is a polythermal valley glacier. Polythermal glaciers have cold ice and temperature surface layer during the summer and winter [72]. There are rocks in this area of a thick succession of Caledonian basement units and a post-Caledonian Lower Carboniferous to Lower Triassic cover sequence. There are remains of preserved Tertiary basin in the area of Ny-Ålesund [19]. A map of the geological structure of Brøggerhalvøya and the area Vestre Brøggerbreen and Austre Brøggerbreen is presented in figure 3.1. The numbers presented on the map are listed with the description of the rocks and minerals in table 3.1, with further description of their composition in table 3.2.

On the southeast of Brøggerhalvøya, the geology of the mountains mostly consists of phyllites with beds of quartzite. This can be found on the summit of Lundryggen (27), southeast of Austre Brøggerbreen. South of the phyllites (29) more strongly metamorphosed rocks can be found. This is such as mica schists with garnet and amphibole [73]. Mica is a type of Aluminium silicate mineral that can contain K, Na, Fe, Mg, and rarely Li or Cr [74]. There are also some areas with beds of marble (28) [73]. Sedimentary rocks of the Middle and Upper Carboniferous and Permian age are the main geology on the northern side of Brøggerhalvøya (11-16) [73]. Reddish sandstone can be seen near the glaciers, Austre Brøggerbreen and Vestre Brøggerbreen. Red glacier meltwater can be seen and occurs from these rocks. Smaller areas south and west of Ny-Ålesund contain Lower Tertiary beds, and these areas are surrounded by Upper Carboniferous and Permian rocks. The majority of these rocks consist of sandstones with minor conglomerates (10). Shales and coal are also found in the lower part (8,9) [73].

Around the Ny-Ålesund area, the bedrock appears visible on the ridges, whereas slopes are mainly covered by deposits from the slopes. Glaciers and moraines have covered the bedrock

of the main valley area of Ny-Ålesund [75]. In the main valleys in the area, bedrock is covered by glaciers and moraines. The bedrock has been weathered and partially covered by stream deposits and glacial deposits, at the ends of the glaciers, on the flat coastline level [75]. The geology of the bedrock in the area of Ny-Ålesund mostly consists of rocks such as limestone, shale, sandstone, and glacial till [75, 76].

At the main glacier outlets, such as Austre Brøggerbreen and Vestre Brøggerbreen, large rivers, Bayelva, and outwash plains are formed. Streams in size cross the terrain in the Ny-Ålesund area, and they can be identified by their broad braided paths [75].

There are some anthropogenic landforms and deposits in the area, and these originate from the coal mining industry from 1916 - 1963 [13, 75]. As a result of activities associated with the international research stations in Ny-Ålesund established in recent years, there are currently, dams, channels, temporary quarries, and anthropogenic deposit embankments in the area [75].

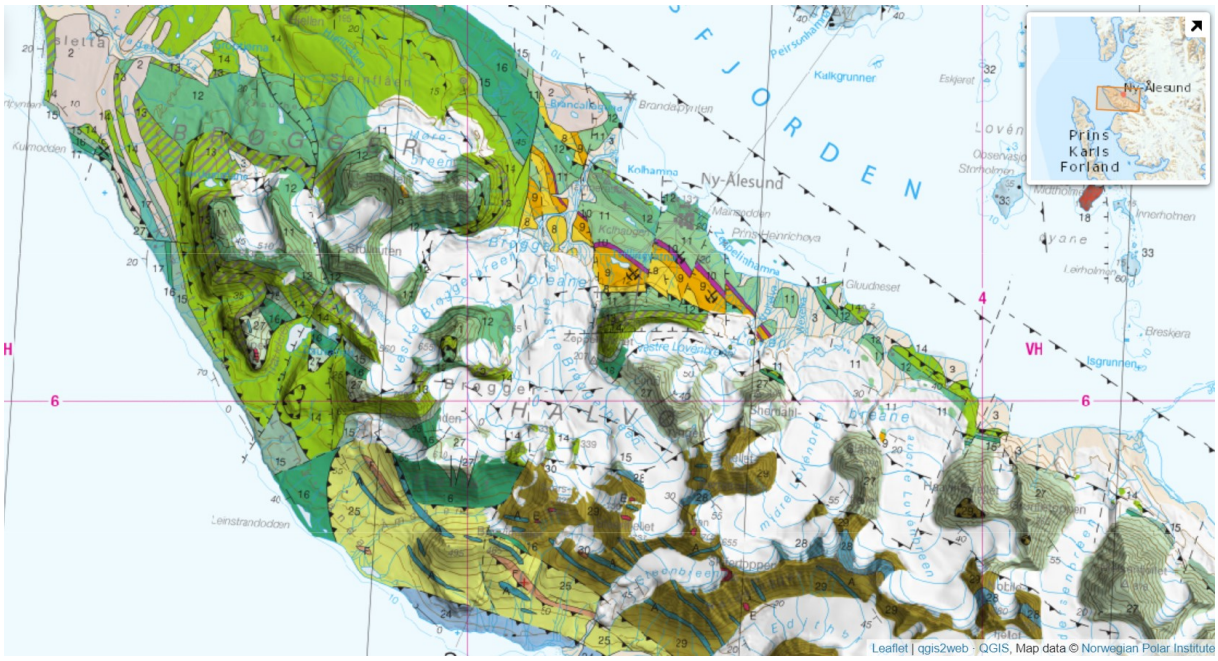

Figure 3.1: Geologicial map of Svalbard, sheet A7G Kongsfjorden. Source: © Norwegian Polar Institute n.d.[77].

Table 3.1: Descriptions of the numbers referred to on the geological map of Svalbard [78].

Number	Minerals / rock
8	Sandstone, shale, Conglomerate, coal
9	Sandstone, shale, Conglomerate, coal
10	Sandstone, shale
11	Limestone, sandstone
12	Dolomite breccia, dolomite, Limestone, marl
13	Dolomite, limestone
14	Limestone, dolomite
15	Carbonate rocks, sandstone
16	Conglomerate, sandstone, shale
27	Phyllite with interlayered quartizite
28	Marble
29	Mica-schist, garnet-mica-schist, Quartz-carbonate-schist

Table 3.2: Descriptions of the numbers referred to on the geological map of Svalbard [78].

Names	Rock or mineral composition
Sandstone	Siliclastic sedimentary rock, mainly quartz and/or feldspar [79]
Shale	Sedimentary rock, predominantly of siliciclastic materials by mixtures of clay and particle size or powder [79]
Conglomerate	existing rocks and mineral fragments of fine-grained matrix [74]
Coal	C, O and H, N, S (anthracite and bituminous coal) [79]
Dolomite	Mineral, mainly consisting of calcium magnesium carbonate ($CaMg(CO_3)_2$) [79]
Limestone	Sedimentary rock mainly composed of calcite, high content of silica, dolomite, and clay [79]
Carbonate rocks	Cacite ($CaCO_3$), Magnesite ($MgCO_3$), dolomite($CaMg(CO_3)_2$, ankerite Ca, (Fe, Mg, Mn)$(CO_3)_2$, smithsonite ($ZnCO_3$), cerussite ($PbCO_3$), rhodochrosite ($MnCO_3$) [79]
Phyllite	Quartz, mica, sericite, and chlorite [74]
Schist	Chlorite, mica, staurolite, talc, quartz, garnet, feldspar, kyanite [74]
Quartzite	Monomineral metamorphic rock, mainly quartz [79]
Marble	Monomineralic, mainly of calcite [74]
Mica	Aluminiumsilicate of K/Na, Fe/Mg and rarely Li or Cr [79]
Quartz	SiO2 [79]

3.2 Sampling

In total 65 samples were collected, and in total 11 sediment samples were collected from cryoconite holes, 20 snow samples, and 20 supraglacial debris samples were collected from the glaciers Austre Brøggerbreen and Vestre Brøggerbreen. There were collected 6 unfiltered samples from glacier melting water outlets, 2 filtered samples from glacier melting water outlets and 6 flow sediment samples from the melting water outlets. Figure 3.2 is a map of the sampling site at Ny-Ålesund. The figures 3.3 and 3.4 are maps of the locations for the sample collection on Vestre Brøggerbreen and Austre Brøggerbreen, respectively. Table A.1 in appendix A.1 provides more detailed information about the sample GPS- positions, sample materials, sampling containers and sample ID [12].

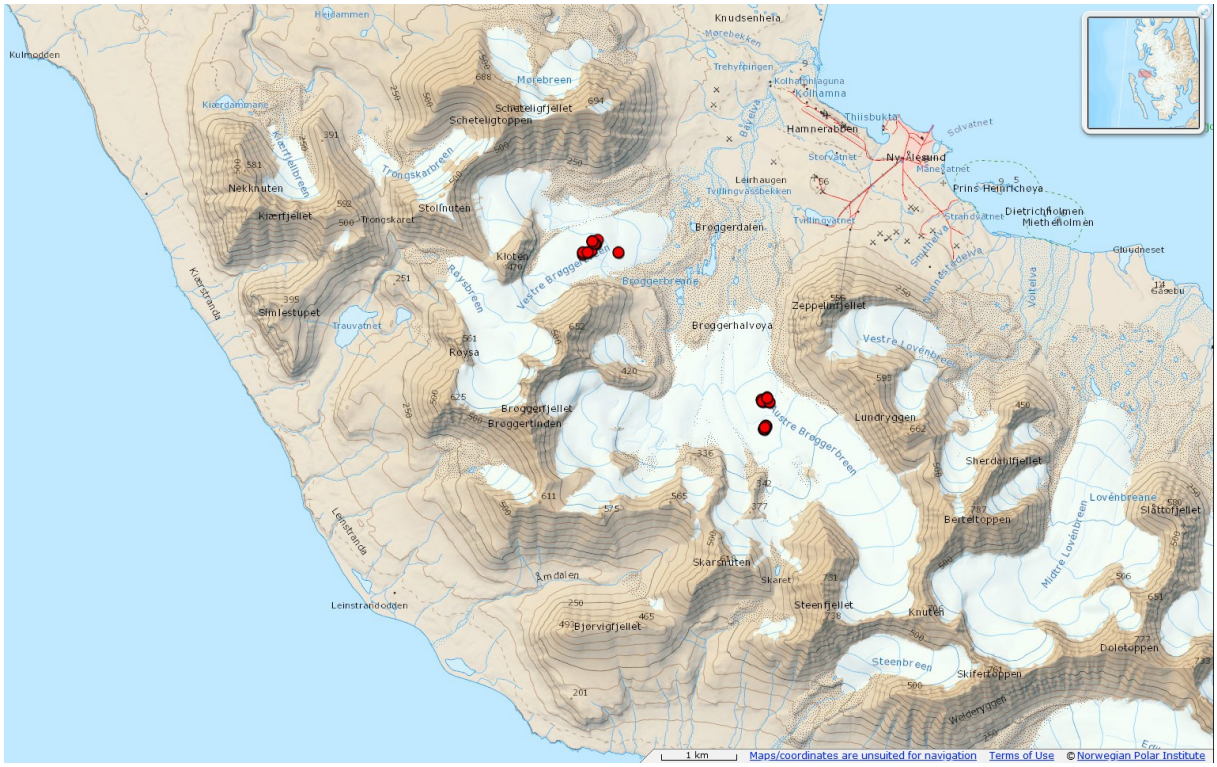

Figure 3.2: Map of the two sampling locations, Vestre Brøggerbreen (VB) from left and Austre Brøggerbreen (AB), at Ny-Ålesund area. Source: © Norwegian Polar Institute n.d. [12, 80].

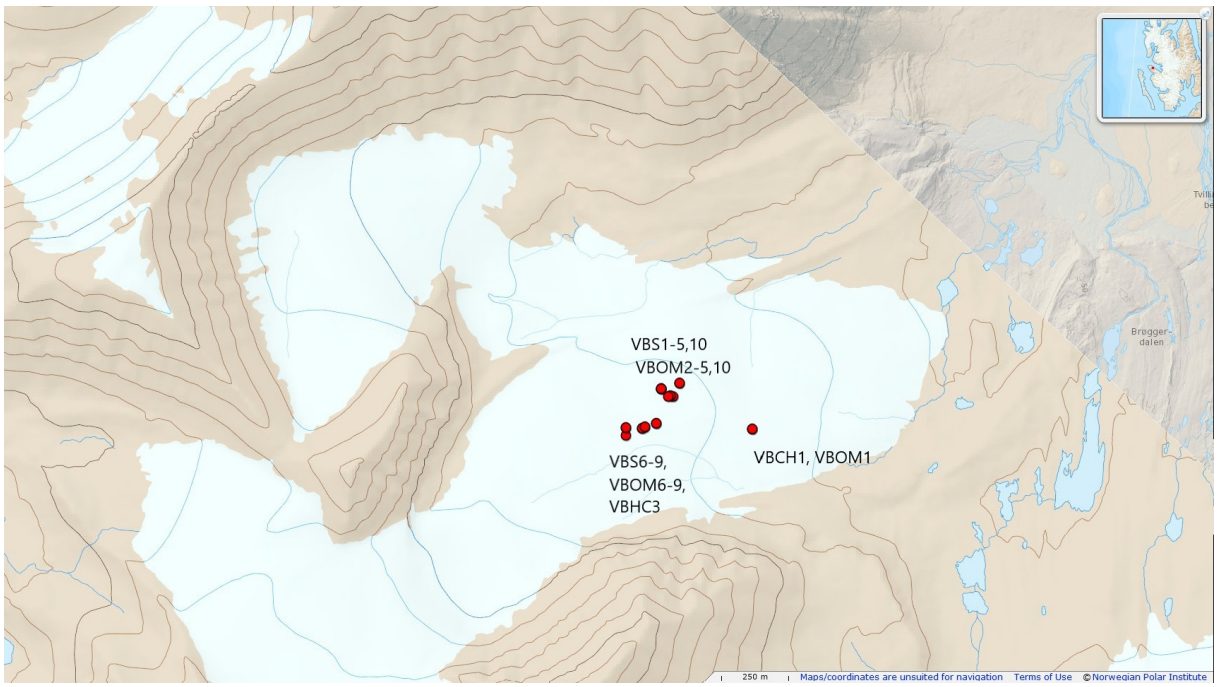

Figure 3.3: Map of the sampling locations on the glacier, Vestre Brøggerbreen (VB) at Ny-Ålesund area. Source: © Norwegian Polar Institute n.d. [12, 80].

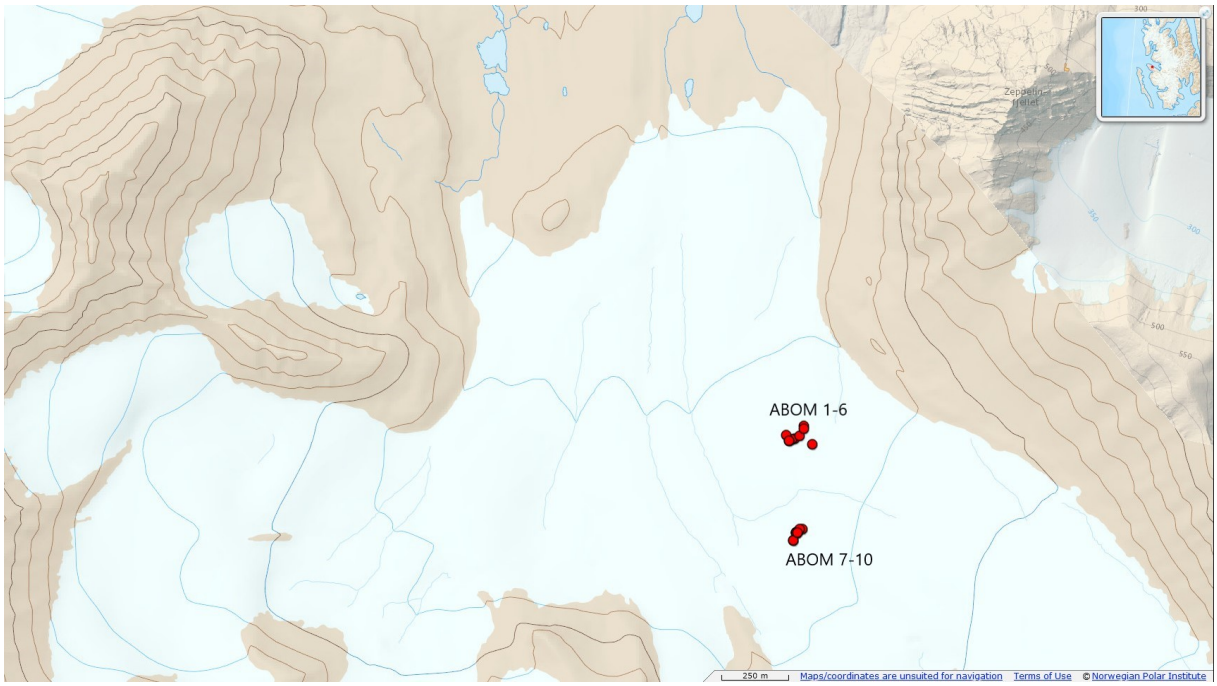

Figure 3.4: Map of the sampling locations on the glacier, Austre Brøggerbreen (AB) at Ny-Ålesund area. Source: © Norwegian Polar Institute n.d. [12, 80].

3.2.1 Sample collection

The samples were collected on the glacier systems Austre Brøggerbreen and Vestre Brøggerbreen and the melting water outlet of both glacier systems. All sampling and fieldwork of this project were carried out in accordance with ISO 5667-1:2020 Water quality — Sampling — Part 1: Guidance on the design of sampling programs and sampling techniques [56]. The samples were

handled and collected using Nitrile gloves and stored in metal-free 30 mL cc-cups or 50 mL PP tubes to avoid contamination. Table 3.3 provides information on the material and suppliers of the equipment used for the sample collection of this project [12].

Particulate matter, such as cryoconite, was collected from cryoconite holes on both Austre Brøggerbreen and Vestre Brøggerbreen. These samples were collected by the use of a pre-cleaned 25 mL plastic syringe and stored in metal-free 30 mL cc-cups. Both plastic syringes and cc-cups were cleaned with water from the cryoconite hole, before collecting the particulate matter. The snow- samples and sediment samples were stored in the freezer until further preparations in the laboratory. The water samples were stored in the refrigerator until further preparations in the laboratory [12].

Water samples collected from the melting water outlet of Austre Brøggerbreen and Vestre Brøggerbreen were sampled and collected in 50 mL PP tubes where all tubes were cleaned with the sample source, before collecting the water samples. One sample from both Austre Brøggerbreen and Vestre Brøggerbreen was collected with a 25 mL plastic syringe and filtrated with a 0.45 µm filter into a 15 mL PP tube. This sample was acidified with 3 drops of 65% ultrapure HNO_3, in accordance with ISO 5667-3:2018 Water quality - Sampling - Part 3: Preservation and handling of water samples, before analysing by ICP-MS [57]. Figure 3.5 and 3.6 are illustrations of the sampling locations of the melting water outlets [12].

Figure 3.5: Melting water outlet of Austre Brøggerbreen.

Figure 3.6: Melting water outlet of Vestre Brøggerbreen.

Snow samples were collected from the upper surface of both Austre Brøggerbreen and Vestre Brøggerbreen using 50 mL PP tubes. 10 samples from each glacier were collected and stored in the freezer until further work in the laboratory [12].

In accordance with ISO 5667-3:2018 Water quality - Sampling - Part 3: Preservation and handling of water samples, Snow-samples collected on Austre Brøggerbreen and Vestre Brøggerbreen were thawed to separate the water phase and the particulate matter [57]. The water in the tubes was decanted into new 50 mL PP tubes. The particles that were left in the original tubes were stored in metal-free 30 mL cc-cups. Table A.3 in appendix 3.2.1 is showing the merging of the samples [12].

The water phase was prepared for ICP-MS analysis by filtrating the samples with using a syringe with a 0.45 µm filer, and stored in 15 mL PP tubes. This sample was acidified with 3 drops of 65% ultrapure HNO_3, before analysing by ICP-MS [12].

Supraglacial material samples were collected in metal-free 30 mL cc-cups. 10 samples from each glacier, Austre Brøggerbreen and Vestre Brøggerbreen were collected. The samples were stored in the freezer until further preparations in the laboratory. Figure 3.7a and 3.7b are examples of supraglacial debris collected on the surface of Vestre Brøggerbreen and Austre Brøggerbreen [12].

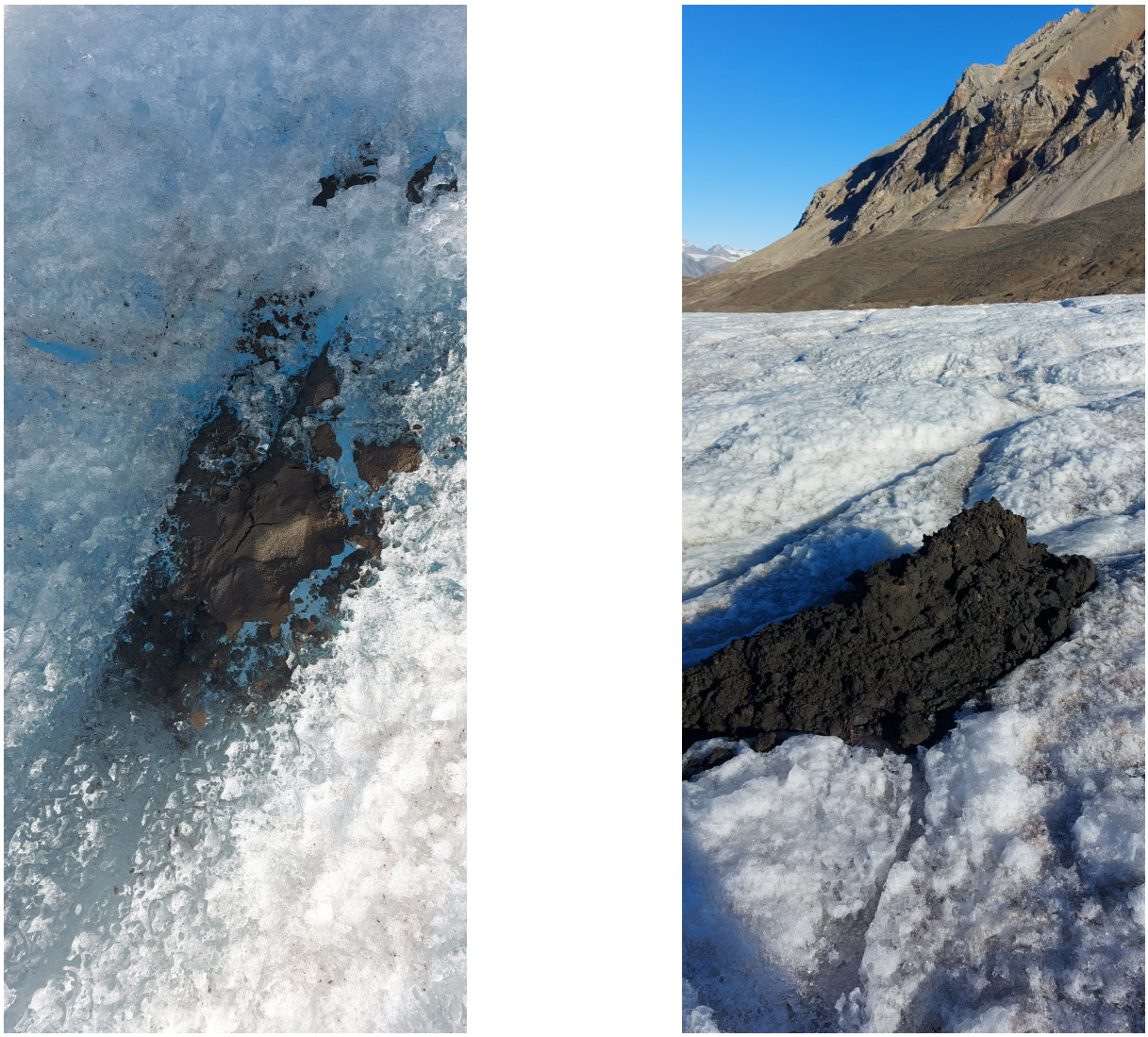

(a) *(b)*

Figure 3.7: Supraglacial debris from the surface of a) Vestre Brøggerbreen and b) Austre Brøggerbreen.

Table 3.3: List of the equipment used for the sample collection.

Equipment	Type/Material	Supplier
Nitrile gloves	EN ISO 374-1 Type B (KTP), EN ISO 374-5 VIRUS	VWR Chemicals
50 mL Plastic tube	PP Centrifuge Tubes, HDPE cap	VWR Chemicals
15 mL Plastic tube	PP Centrifuge Tubes, HDPE cap	VWR Chemicals
20 mL Syringe	PP barrel, PE piston	HSW HENKE-JECT
0.45 µL Filter	PES membrane	VWR Chemicals

3.3 Sample preparation

This chapter describes all the methods for the sample preparation that has been done in this project.

3.3.1 Freeze-drying

Supraglacial material samples, cryoconite hole materials, snow surface material samples collected in 30 mL cc-cups and flow sediments from melting water outlet collected in 50 mL PP tubes, were covered with parafilm to avoid cross-contamination. Small holes were made in the parafilm to let the water vaporise out of the sample during the freeze-drying. Samples were then freeze-dried according to ISO 16720:2005 Soil quality- Pretreatment of samples by freeze-drying for subsequent analysis, in a Christ Alpha 1-4 Ld Plus Freeze-dryer for 48 hours, under a vacuum of 0.94 mbar. All samples were weighed before and after freeze-drying, and stored in 30 mL cc-cups and 50 mL PP tubes at room temperature after freeze-drying [12].

3.3.2 Microwave assisted digestion

In total 52 samples, cryoconite samples, sediment samples and supraglacial debris samples were microwave-assisted digested in two batches by using Milestone UltraCLAVE [12].

Teflon vials were rinsed three times with Milli-Q water. Samples were weight to between 250 mg- 350 mg in Teflon vials, using a plastic spatula covered in plastic film. The samples were then digested with 9 mL of 50% v/v HNO_3. The samples were then placed in a Teflon container containing 300 mL Milli-Q water, 2 mL concentrated sulfuric acid (H_2SO_4) and 30 mL hydrogen peroxide (H_2O_2). Further, the samples were digested according to the temperature profile shown in figure A.2 in appendix A.2, by Milestone UltraCLAVE instrument. Following digestion, the samples were then diluted to 108 mL (109.8 g $\pm$ 0.5 g) and transferred to 15 mL Polypropylene-tubes for ICP-MS analysis [12].

For the quality control procedure, three Certified reference material samples (CRM MODAS-2 Bottom Sediment (M-2 BotSed) 50 g FOR TRACE ANALYSIS no. 0382) and three blanks (50% v/v HNO_3) were run parallel per batch of digested sediment samples [12].

3.4 Analysis

3.4.1 Element analysis by Inductively coupled plasma mass spectrometry (ICP-MS)

Element analysis of snow samples, melting water samples, supraglacial debris, and cryoconite samples were obtained using an 8800 Triple Quadrupole inductively coupled plasma mass spectrometry (ICP-MS) system (Agilent, USA) equipped with prepFAST M5 autosampler (ESI, USA). The ICP-MS parameters during analysis are listed in table 3.4 for snow and water samples, and in table 3.5 for the sediment samples. More comprehensive tables of the system tune mode parameters for the sediment and water analysis are listed in table B.1 and B.2, in appendix B.

Table 3.4: ICP-MS parameters for the snow and water samples

General parameters	
RF Power	1500 W
Nebuliser Gas	0.79 L/min
Makeup Gas	0.38 L/min
Sample depth	8.0 mm
Ion lenses	x- lens
H_2 mode	
H_2 gas flow	4.5 mL/min
He gas flow	1.0 mL/min
O_2 mode	
O_2 gas flow	0.45 mL/min
He gas flow	1.0 mL/min

Table 3.5: ICP-MS parameters for the sediment samples

General parameters	
RF Power	1600 W
Nebuliser Gas	0.78 L/min
Makeup Gas	0.38 L/min
Sample depth	8.0 mm
Ion lenses	s- lens
H_2 mode	
H_2 gas flow	7.5 mL/min
He gas flow	3.5 mL/min
O_2 mode	
O_2 gas flow	0.6 mL/min
He gas flow	2.0 mL/min

3.4.2 Determination of Total Carbon (TC) and Total Nitrogen (TN) content in sediment material

Freeze-dried cryoconite, supraglacial debris and flow sediment samples from Austre Brøggerbreen and Vestre Brøggerbreen were analysed for total carbon and total nitrogen content according to ISO 17184:2014(E) Soil quality — Determination of carbon and nitrogen by high-temperature combustion with near-infrared spectrometry (NIRS). The samples were analysed in two batches [12].

90.45 - 100.18 mg of samples were weight in ceramic crucibles (2SN100370 pkg/20) and analysed by using Primacs^{SNC100} instrument through the combustion of the sample in oxygen (ultra-pure grade, 99.995% purity) at a temperature of 1200°C. After the combustion, the gas mixture of CO_2 and NOx was led by a carrier gas through a splitter. This is where part of the combustion gas is collected. The remaining gas was led through an IR detector, which analysed the CO_2 content. The collected gas mixture was led by a carrier gas of helium (nitrogen-free, 99.995% purity) through a copper reduction oven to reduce NOx to N_2. The carrier gas was then led through scrubbers to separate CO_2 and water. Following scrubbing, the carrier gas was finally led through a thermal conductivity detector (TCD), used to analyse the nitrogen content [12].

A seven-point calibration curve was made for each batch, by using seven crucibles (2SN100370) and weight out glycine (carbon content 32.00%, nitrogen content 18.66%) as calibration standard material. The standards were weight to 6, 10, 20, 40, 80, 120 and 160 mg. The exact weights for the calibration standards are presented in table C.4 and C.5 in appendix C.2. The standard calibration curves for determination of TC and TN are plotted in the figures C.1 - C.4 in appendix C.2 [12].

3.4.3 Determination of Total Carbon (TC), Total Inorganic Carbon (TIC) and Total Organic Carbon (TOC) content in water

6 snow samples and samples from glacier melting water outlets were analysed according to ISO 8245:1999(E) Water quality — Guidelines for the determination of total organic carbon (TOC) and dissolved organic carbon (DOC), by high-temperature combustion with Non-Dispersive Infrared detection (NDIR) for Total Carbon (TC), Total Inorganic Carbon (TIC) and Total Organic Carbon (TOC) content using Shimadzu Total Organic Carbon Analyzer (TOC-L) instrument [12].

For quality control, pre-made standard solutions for TC and TIC were used to make a calibration curve. Standard solutions for TC were prepared by measuring 2.125 g of reagent-grade potassium hydrogen phthalate and transferred into a 1 L volumetric flask. Milli-Q water, which is absolutely free of carbon and nitrogen, was added to the 1 L mark. The solution was then mixed well. The carbon concentration of the solution is 1000 mg C / L, equivalent to 1000 ppm carbon. This solution is the standard stock solution [12].

Standard solutions for TIC were prepared by measuring 7.219 g of reagent-grade sodium hydrogen carbonate and 4.412 g of sodium carbonate into a 1 L volumetric flask. Milli-Q water was added to the 1 L mark, and well mixed. The carbon concentration in this standard stock solution was equivalent to 1000 ppm carbon/L = 1000 ppm carbon [12].

The calibration curve was made of dilutions of 0.5, 1, 2, 5, 10 and 20 ppm of the standard stock solution for TIC and TOC [12].

3.4.4 Specific UV absorbance (SUVA)

Snow samples and melting water samples from Austre Brøggerbreen and Vestrebrøggrbreen were analysed with a UV/Vis-spectrophotometer (Shimadzu UV mini 1240) according to NS 9462:2006 Water quality — Determination of UV-absorbance [81]. The samples were analysed in quarts cuvettes, for measuring the UV absorbance at 254 nm (UV_{254}). Between each measurement, the cuvettes were cleaned with the sample solutions [12].

3.5 Statistical treatment and data analysis

Statistical treatment and data analysis, including the formation of box plots and standard calibration curves, were performed using Microsoft Excel. In order to determine if the samples were normally distributed, Shapiro- Wilk test was used. The significance level was set to $p < .05$. In a data set where two independent normal distributed means were compared, a Student t-test was used, with a significance level set to $p < .05$. In a data set where two independent means not being normal distributed were compared, the Mann-Whitney U test was used. The significance level was set to $p < .05$ [12]. In order to extract information from a data set with multivariate parameters, principal component analysis was performed, using Aspen Unscrambler V12.1.

4 Results and discussion

The results obtained from the determination of elemental analysis by ICP-MS, TC and TN content, TOC, UV-vis and SUVA are presented in order to increase the knowledge about the chemical composition of cryoconite (CH), supraglacial debris from the surface (SGD), supraglacial debris separated from the snow (SGD-S), flow sediment (FS), snow (S) and melting water (W) from the two different glacier systems, Austre Brøggerbreen and Vestre Brøggerbreen in Svalbard.

4.1 Determination of elemental composition of snow, meltwater, cryoconite, supraglacial debris, and flow sediment samples

A total of 50 elements were analysed by ICP-MS in cryoconite, supraglacial debris, flow sediment, meltwater and snow samples from Austre Brøggerbreen and Vestre Brøggerbreen. Nine elements were selected for further analysis. The elements as Na, Mg, Al, Fe and Ca were selected as they are sources of local rock and minerals (table 3.2) [74]. The heavy metals As, Cd, Cr, and Pb were selected due to their categorisation as toxic elements [31]. Hg was not selected due to all samples were under the detection limit. Zn was selected as it can be a source of anthropogenic activity, a natural source [74], and a long-range transported element [38]. A summary of the mean concentrations ± standard deviation (SD), with the range of minimum and maximum values of the collected samples, are presented in tables 4.1, for cryoconite and flow sediment samples, in table 4.2, for supraglacial debris, and in table 4.3, for snow and meltwater samples. Concentrations for cryoconite, flow sediment, and supraglacial debris were measured in µg/g, while snow and meltwater concentrations were measured in µg/L. Additional information of the results from the measured samples by ICP-MS are listed in tables C.1, C.2 and C.3 in appendix C.

The mean concentrations of the elements in the cryoconite (CH) samples from both glacier systems were in the following order: Fe > Al ≫ Mg ≫ Ca ≫ Na ≫ Zn > Pb > As ≫ Cd. Similarities in the elemental concentrations between cryoconite, supraglacial debris (SGD) and supraglacial debris separated from the snow samples (SGD-S), with some variaties between the locations, were observed. Supraglacial debris (SGD) and supraglacial debris separated from the snow samples (SGD-S) from Austre Brøggerbreen was detected in the decreasing order: Fe > Al ≫ Mg ≫ Ca > Na ≫ Zn > Pb > As ≫ Cd. Mean concentrations of Al were higher in the samples from Vestre Brøggerbreen, with the following decreasing order: Al > Fe ≫ Mg ≫ Ca ≫ Na ≫ Zn > Pb > As ≫ Cd. The similarity of these concentrations can be a cause of the materials originating from the same source [10]. This is expected results, due to the local rocks and minerals surroundings around Austre Brøggerbreen, such as shale and reddish sandstone [73, 74].

For both locations, Austre Brøggerbreen and Vestre Brøggerbreen, concentrations of the snow samples for both glaciers were dominated by Ca, Na and Mg concentrations. The concentrations of the elements in the snow samples for both glaciers were in the following decreasing order: Ca > Na > Mg > Fe ≫ Al > Zn > Pb > As ≫ Cd. This is the same order as the reported results in a previous study of snow samples collected on the same glaciers, except Na was reported with a higher concentration than Ca [82]. The concentrations of the elements were detected in different ranges between the samples. For example, in snow samples, concentrations of Mg and Ca varied from 10.9 µg/L - 100 µg/L and 25.2 - 356 µg/L - 100 µg/L, respectively, collected on Austre

Brøggerbreen. Concentrations from the meltwater of the sample from Austre Brøggerbreen were in the following order: Ca $\gg$ Mg $\gg$ Na $\gg$ Fe $>$ Al $>$ As $>$ Zn $\gg$ Cd $\gg$ Pb. The measured Pb concentration from the meltwater sample from Austre Brøggerbreen was detected under the detection limit. For the meltwater sample from Vestre Brøggerbreen, Zn was in higher concentration than As compared with Austre Brøggerbreen and the elemental concentrations were in the order: Ca $\gg$ Mg $\gg$ Na $\gg$ Fe $>$ Al $\gg$ Zn $\gg$ As $\gg$ Cd $\gg$ Pb. It is important to say, that only one sample per location were analysed for the meltwater. With only one measurement, there were not possible to make any statistical tests for these samples. Although in three previous studies of meltwater and water emerging from Austre Brøggerbreen and Vestre Brøggerbreen, observated higher levels of Ca and Mg in samples from Vestre Brøggerbreen compared with samples from Austre Brøggerbreen. In the same studies Al, Fe, and Mn concentrations in meltwater and water emerging from Austre Brøggerbreen had significantly higher concentrations than meltwater and water emerging from Vestre Brøggerbreen [83–85].

For the flow sediment samples collected on Austre Brøggerbreen, the mean concentrations of the elements were in the following order: Al $>$ Fe $\gg$ Ca $\gg$ Mg $\gg$ Na $\gg$ Zn $>$ Pb $>$ As $\gg$ Cd. The flow sediment samples from Vestre Brøggerbreen had higher concentrations of Ca and Mg, which gives the following order for the mean concentrations of the elements: Ca $\gg$ Mg $\gg$ Al $>$ Fe $>$ Na $\gg$ Zn $>$ Pb $>$ As $>$ Cd. When comparing the elemental concentrations in the flow sediments with cryoconite and supraglacial debris, the concentration is generally lower in the flow sediment samples. Except for the Ca concentration, as the element concentrations is dominating in the flow sediment sample composition.

The differences in mean concentrations of the different sample materials were tested for normal distribution using the Shapiro-Wilk test. Differences in mean concentrations between samples from Austre Brøggerbreen and Vestre Brøggerbreen were tested for statistical significance using a t-test for normal distributed samples and the Mann-Whitney U test for non-normal distributed samples. The significance was set to $p<0.05$ for all tests. Summary of the samples tested for normal distribution and statistical significant differences are listed in tables E.1 and E.3, respectively, in appendix E.

Table 4.1: Summary table of values as mean, standard deviation (SD), range with the minimum and maximum values of elemental concentrations for cryoconite and flow sediment samples from Austre Brøggerbreen (AB) and Vestre Brøggerbreen (VB). Where n represents the number of samples, and the concentrations are measured in µg/g.

Element	Location	Cryoconite		Flow sediment	
		AB; n = 6, VB; n = 5		n = 4	
		Mean ± SD (µg/g)	Range (µg/g)	Mean ± SD (µg/g)	Range (µg/g)
Na	AB	700 ± 88.6	581 - 803	374 ± 86.3	286 - 449
	VB	596 ± 24.9	561 - 630	203 ± 5.19	198 - 210
Mg	AB	14100 ± 620	13200 - 14900	6130 ± 38900	5740 - 6680
	VB	8840 ± 319	8550 - 9360	38900± 5960	33300 - 46600
Al	AB	42900 ± 2250	40100 - 45800	28493 ± 4770	23700 - 33302
	VB	38400 ± 1910	3610 - 41040	10300 ± 1230	9290 - 1190
Ca	AB	4650 ± 658	3890 - 5660	7880 ± 521	7410 - 8420
	VB	1580 ± 47.5	1540-1660	121000 ± 11660	110000 - 134000
Fe	AB	47300 ± 1600	45200 - 48800	27300 ± 1620	25300 - 29300
	VB	32500 ± 849	31400 - 33600	8980 ± 458	8520 - 9560
Zn	AB	95.0 ± 5.36	87.7 - 101	48.2 ± 3.12	44.9 - 52.4
	VB	75.2 ± 1.42	73.01 - 77.0	37.3 ± 3.97	33.4 - 42.5
As	AB	10.4 ± 13.7	4.25 - 38.4	5.07 ± 0.571	4.38 - 5.62
	VB	8.26 ± 0.200	7.99 - 8.52	3.04 ± 0.396	2.70 - 3.48
Cd	AB	0.0911 ± 0.0235	0.0719- 0.129	0.0486 ± 0.00178	0.0461 - 0.0504
	VB	0.0714 ± 0.0171	0.0434 - 0.0853	0.262 ± 0.00178	0.253 - 0.280
Pb	AB	34.4 ± 2.42	30.59 - 37.7	15.19 ± 2.50	11.7 - 18.2
	VB	64.2 ± 4.93	61.02 - 72.8	4.08 ± 0.0969	3.96 - 4.20

Table 4.2: Summary table of values as mean, standard deviation (SD), range with the minimum and maximum values of elemental concentrations and supraglacial debris from Austre Brøggerbreen (AB) and Vestre Brøggerbreen (VB). Where n represents the number of samples, and the concentrations are measured in µg/g.

Element	Location	SGD		SGD-S	
		n = 10		n = 3	
		Mean ± SD (µg/g)	Range (µg/g)	Mean ± SD (µg/g)	Range (µg/g)
Na	AB	749 ± 126	462 - 918	677 ± 53.5	641 - 738
	VB	658 ± 42.97	561 - 712	606 ± 86.0	518 - 690
Mg	AB	142 ± 1310	11900 - 16400	15600 ± 959	14600 - 16500
	VB	879± 325	8240 - 9230	8590 ± 180	8390 - 8750
Al	AB	43900 ± 4850	32500 - 48900	4610 ± 2990	43200 - 49200
	VB	39300 ± 1630	36600 - 41700	36700 ± 1910	35100 - 38800
Ca	AB	5364 ± 521	3590 - 8180	4000 ± 797	3390 - 4900
	VB	1630 ± 11700	1400 - 1950	1830 ± 341	1480 - 2160
Fe	AB	46900 ± 4620	38800 - 53500	52300 ± 5270	46500 - 56800
	VB	32500 ± 11600	30500 - 34600	31500 ± 1480	29900 - 32800
Zn	AB	95.0 ± 8.65	72.8 - 102	99.6 ± 5.67	93.7 - 105
	VB	75.9 ± 3.12	69.8 - 80.7	74.8 ± 4.73	70.0 - 79.5
As	AB	5.27 ± 2.83	2.03 - 12.09	3.21 ± 0.859	2.63 - 4.19
	VB	8.53 ± 0.731	7.12 - 9.59	8.09 ± 0.801	7.18 - 8.68
Cd	AB	0.101 ± 0.0305	0.0519 - 0.149	0.103 ± 0.0220	0.0877 - 0.128
	VB	0.0725 ± 0.0136	0.0535 - 0.0962	0.0618 ± 0.0072	0.0535 - 0.0666
Pb	AB	40.3 ± 23.4	22.3 - 105	35.4 ± 4.61	31.0 - 40.2
	VB	68.6 ± 7.02	56.9 - 80.1	60.0 ± 9.17	50.0 - 68.1

Table 4.3: Summary table of values as mean, standard deviation (SD), range with the minimum and maximum values of elemental concentrations for snow and meltwater samples from Austre Brøggerbreen (AB) and Vestre Brøggerbreen (VB). Where n represents the number of samples, and the concentrations are measured in µg/L.

Element	Location	Snow		Meltwater
		AB; n = 10, VB; n = 8		n = 1
		Mean ± SD (µg/L)	Range (µg/L)	Measured (µg/L)
Na	AB	90.7 ± 51.1	20.8 - 197	1590
	VB	92.9 ± 81.5	15.6 - 247	1690
Mg	AB	64.5 ± 51.1	10.9 - 178	8730
	VB	43.1 ± 27.4	11.7 - 91.5	7350
Al	AB	5.05 ± 2.98	1.79 - 11.3	1.98
	VB	4.79 ± 2.78	0.984 - 10.6	2.51
Ca	AB	115 ± 104	25.2 - 356	27700
	VB	96.2 ± 87.7	31.5 - 260	29900
Fe	AB	21.2 ± 24.2	4.90 - 67.9	0.3780
	VB	14.8 ± 13.5	2.54 - 50.0	0.351
Zn	AB	3.26 ± 1.15	0.817 - 4.85	0.0634
	VB	3.64 ± 5.04	0.967 - 17.8	0.6312
As	AB	0.0548 ± 0.0313	0.0191 - 0.112	0.0706
	VB	0.0345 ± 0.0250	0.00607 - 0.0772	0.0743
Cd	AB	0.00317 ± 0.00256	0.000133 - 0.00821	0.00546
	VB	0.00167 ± 0.00139	< LOD - 0.00452	0.00350
Pb	AB	0.177 ± 0.296	0.0126 - 0.804	<LOD
	VB	0.520 ± 0.783	0.0798 - 2.69	<LOD

4.2 Principal component analysis of snow, meltwater, cryoconite, supraglacial debris, and flow sediment samples

To compare the collected samples, sample material, and locations, the data sets of the samples from the ICP-MS analysis were analysed by using principal component analysis (PCA). In this analysis, for selecting an element for PCA the criteria of at least 70 % of the variables should be over the detection limit. Principal component analysis was carried out in three separate runs. The results from the first run included 67 of the samples collected from Austre Brøggerbreen and Vestre Brøggerbreen, and 34 elements. The samples were divided into two categories, one for sample material and one for locations, in order to see if the different categories would give different results.

The first run of PCA is illustrated in the PCA plots of the scores and loadings of the 67 samples in figures D.1 and D.2, respectively, in the appendix D. PC 1 makes up 75 % of the total variance, and PC 2 makes up 9 % of the total variance. The factor scores plot of PC 1 and PC 2 showed that there were four outliners in the PCA. These four samples represent the flow sediment samples from Vestre Brøggerbreen. The flow sediments collected at the meltwater outlets of the glaciers Austre Brøggerbreen and Vestre Brøggerbreen are significantly different from the materials collected on the glaciers. When comparing the scores plot with the loadings plot, it is showing a correlation between the element concentration of Ca. This can be assotiated with strong correlation to the geomorphology in the area as carbonate rocks, e. g. dolomite and limestone [73, 74].

The PCA plot of all samples showed that most of the materials collected from Austre Brøggerbreen and Vestre Brøggerbreen are correlating. There are clear clusters of the samples from the two locations, Austre Brøggerbreen and Vestre Brøggerbreen. The PCA loadings plot is showing a strong association between mineral components such as Fe, Al and Mn [74], as well as As, Sb, and Na. Fe, Al and Mn are elements in minerals are represented in the geomorphology in the local area, as shown in figure 3.1 and listed in tables 3.1 and 3.2 [73, 74, 77]. The Snow samples have generally lower concentrations of the elements compared with the material samples such as cryoconite, supraglacial debris, and flow sediments.

4.3 Principal component analysis of cryoconite, supraglacial debris, and flow sediments

A second PCA run was done with a reduced data set, where all samples of sedimentary material were extracted from the first data set. This PCA included the categories of sample material and locations. The PCA Scores plot of the sediment material samples collected from Austre Brøggerbreen and Vestre Brøggerbreen, and loadings plot of the elemental concentrations are presented in figures 4.2 and 4.3, respectively. PC 1 and PC 2 explain 78 % of the variance.

Clear clusters between sample locations can be observed in the scores plot, in figure 4.2. The samples placed in the right of the scores plot got a higher concentration of the elements right in the loadings plot. When comparing the scores plot with the loadings plot, the supraglacial debris samples (SGD and SGD-S) and cryoconite samples (CH) is showing a clear association with parent materials, such as Al, Na, K and Zn [74].This shows a stronger correlation of these elements in sample materials from Austre Brøggerbreen compared with samples from Vestre Brøggerbreen. The same can be observed for the samples placed in the left side of the scores plot. As described in previous studies where supraglacial debris samples from Midtre Lovénbreen, Vestre Brøggerbreen and Austre Brøggerbreen were analysed, the suggestion of the higher levels of K, Na, Ca, Fe, Al Li, Cr in the samples from Austre Brøggerbreen originated from local minerals and rocks such as from mica, feldspar and quartz [72, 83]. There is possible to assume

that the levels of these elements in the samples from Austre Brøggerbreen origin from the same source.

The flow sediments are strongly associated with Ca, Mg, And Cd concentrations. The loadings plot shows a higher correlation of these elements in the flow sediments from Vestre Brøggerbreen than in the flow sediment samples from Austre Brøggerbereen. As Ca, Mg and Cd are parent materials, reported in the geology of the location, this can indicate a higher concentration of parent material in the flow sediment samples from Vestre Brøggerbreen than Austre Brøggerbreen [73, 74].

As and Pb is strongly correlating with supraglacial debris and cryoconite samples from Vestre Brøggerbreen. This is of similarity to reported findings of Pb concentrations from a previous study of cryoconite samples from Vestre Brøggerbreen [82].

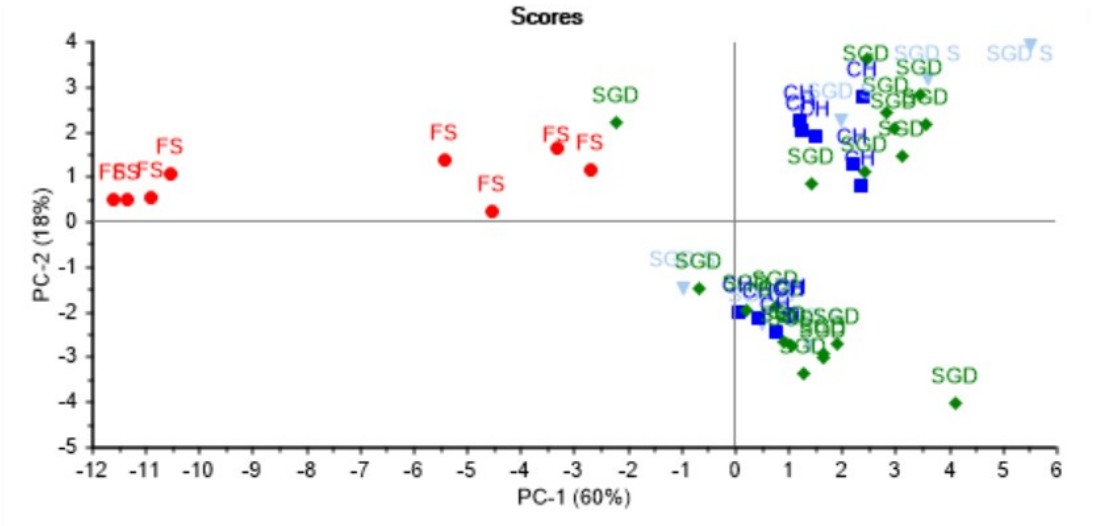

Figure 4.1: Principal component analysis (PCA) scores plot of all the sediment material samples and components. PC 1 makes up 60 % of the total variance, and PC 2 makes up 18 % of the total variance.

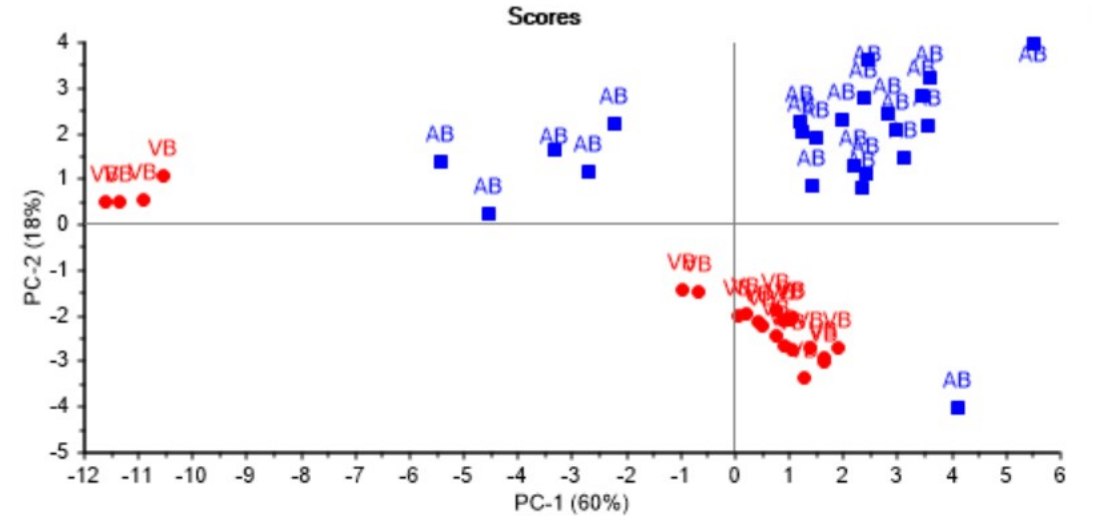

Figure 4.2: Principal component analysis (PCA) scores plot of all the sediment material samples and components. PC 1 makes up 60 % of the total variance, and PC 2 makes up 18 % of the total variance

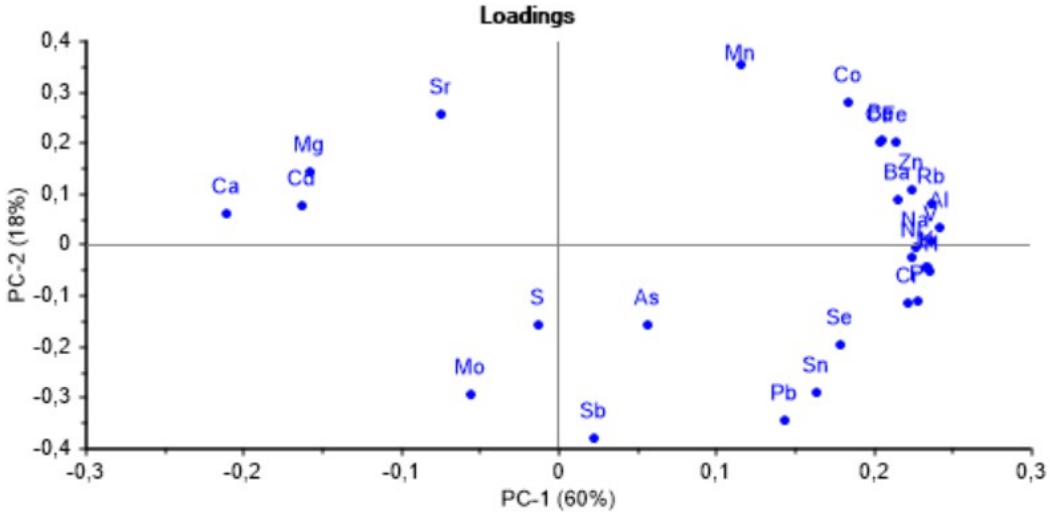

Figure 4.3: Principal component analysis (PCA) loadings plot of all sediment material samples and components. PC 1 makes up 49 % of the total variance, and PC 2 makes up 15 % of the total variance

4.4 Elemental compositions in cryoconite, supraglacial debris, and flow sediment between locations

To compare the difference in elemental concentrations in cryoconite, supraglacial debris, and flow sediment samples between the two locations, Austre Brøggerbreen and Vestre Brøggerbreen, statistical analysis of the Ca, Na, Mg, Fe, Al, Zn, Pb, As and Cd concentrations were done. The elemental concentration varied between the sample material and location. The elemental concentrations of Fe, Al, Mg, and Ca in cryoconite, supraglacial debris, and flow sediment samples were dominating. these elements are the same elements which are dominating in the upper continental crust, after O and Si [86, 87]. These elements are represented in parent materials located in the surroundings of the glacier systems [73, 74].

Significant differences of the element concentrations were observed between the cryoconite and supraglacial debris samples collected at the locations Austre Brøggerbreen and Vestre brøggerbreen. Statistical data for the results of this project is shown in the appendix E. Shapiro-Wilk test was used to test if the mean concentrations were normal distributed. A table of the p-values from the data sets tested for normal distribution is listed in table E.1 in appendix E.1. The student t-test was used to calculate if the mean concentrations between the locations were statistical significant, when the means were normal distributed. When the mean concentrations of the snow samples were not normal distributed, the Mann-Whitney U test was used to calculate if the two mean concentrations of the snow samples from the two locations Austre Brøggerbreen and Vestre Brøggerbreen show any statistically significant difference. A table of the statistical significance is listed in table E.3 in appendix E.

Nine elements were tested for statistical significant differences between cryoconite samples collected on the different galciers Austre Brøggrebreen and Vestre Brøggerbreen. In cryoconite samples, all elements except, Cd showed statistical significal differences between samples from Austre Brøggerbreen and Vestre Brøggerbreen ($p = 0.07706$ for Cd, $p = 0.016319$ for Na, $p<.00001$ for Mg, Ca, and Fe, $p = 0.003258$ for Al, $p <.0001$ for Zn, Student- t test and, $p = 0.04113$ for As, $p= 0.002165$, Mann-Whiteny U test). Of the selected elements, examples of the sample concentrations of Zn, Pb and Ca in cryoconite samples are presented as box plots in figures 4.4, 4.6, and 4.8.

In supraglacial debris samples, all elements showed statistical significal differences between samples from Austre Brøggerbreen and Vestre Brøggerbreen ($p = 0.007021$ for Cd, $p = 0.02257$ for Na, $p<.00001$ for Mg, Ca, and Fe, $p = 0.004438$ for Al, and, $p = 0.001228$ for As, Student-t test and $p = 0.0005$ for Zn, $p= 0.0007523$ for Pb, Mann-Whiteny U test). Of the selected elements, examples of the sample concentrations of Zn, Pb and Ca in supraglacial debris samples are presented as box plots in figures 4.5, 4.7, and 4.9. The cryoconite samples and the supraglacial debris samples compared between the two locations did show a trend in the two different sample materials. Higher concentrations of Ca and Zn were observed in the samples from Austre Brøggerbreen. And higher concentrations of Pb could ble observed on the samples from Vestre Brøggerbreen.

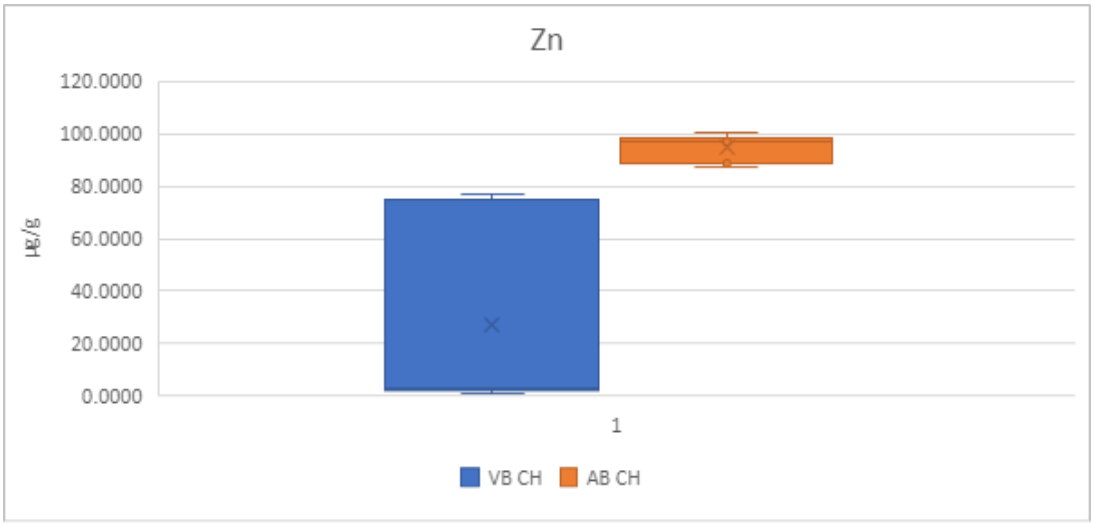

Figure 4.4: Box plot of the Zn concentration (µg/g) from cryoconite samples collected on Austre Brøggerbreen (AB, n = 6) and Vestre Brøggerbreen (VB, n = 5). (p<.0001, Student-test).

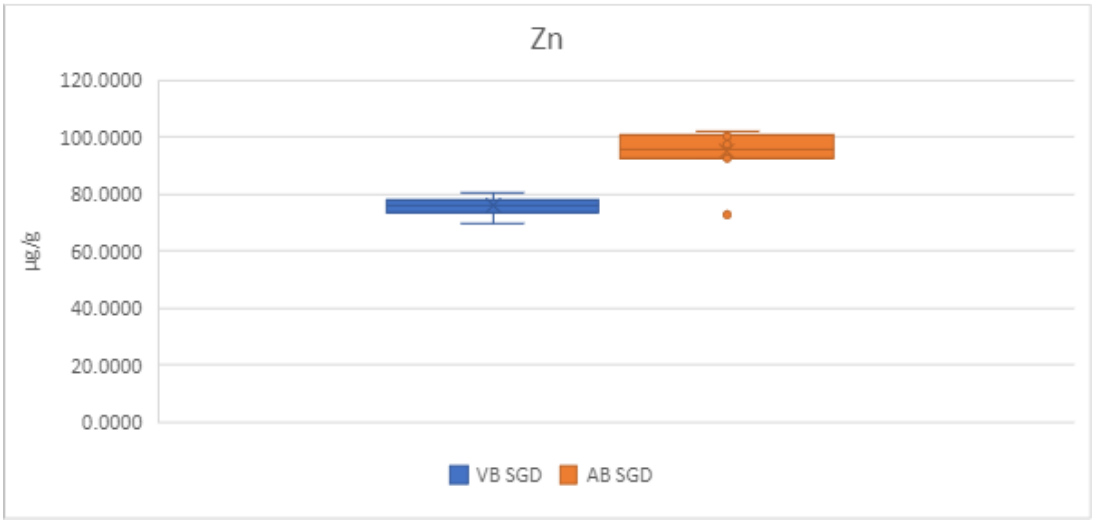

Figure 4.5: Box plot of the Zn concentration (µg/g) from supraglacial debris samples collected on Austre Brøggerbreen (AB, n = 10) and Vestre Brøggerbreen (VB, n = 10). (p=0.000525 , Mann-Whitney U test).

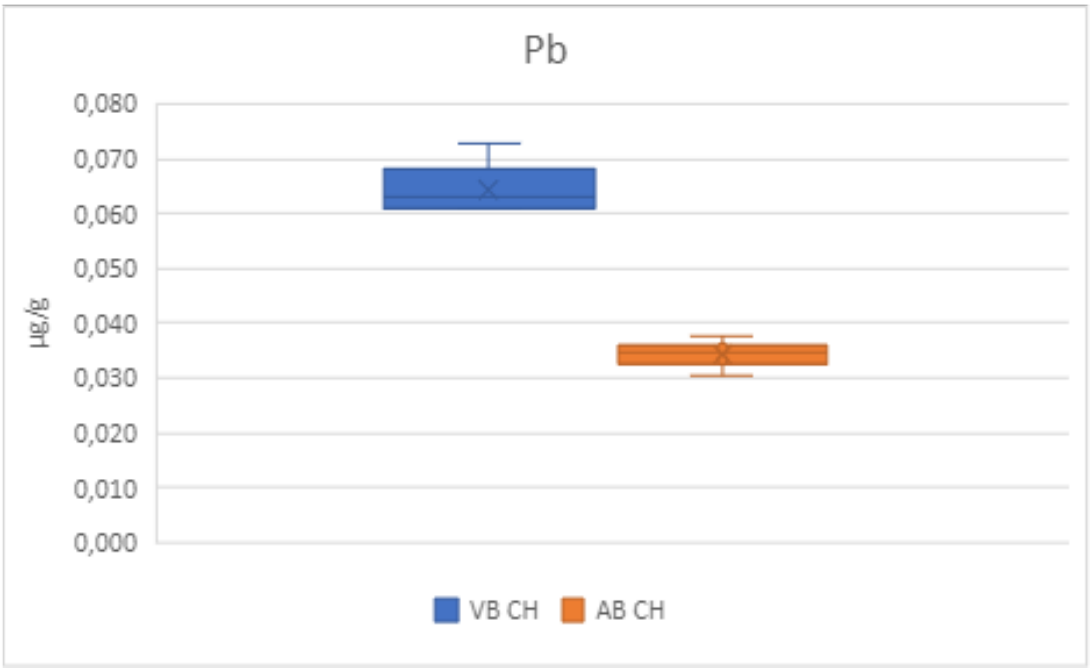

Figure 4.6: Box plot of the Pb concentration (µg/g) from cryoconite samples collected on Austre Brøggerbreen (AB, n = 6) and Vestre Brøggerbreen (VB, n = 5). (p=0.002165, Mann-Whitney U test).

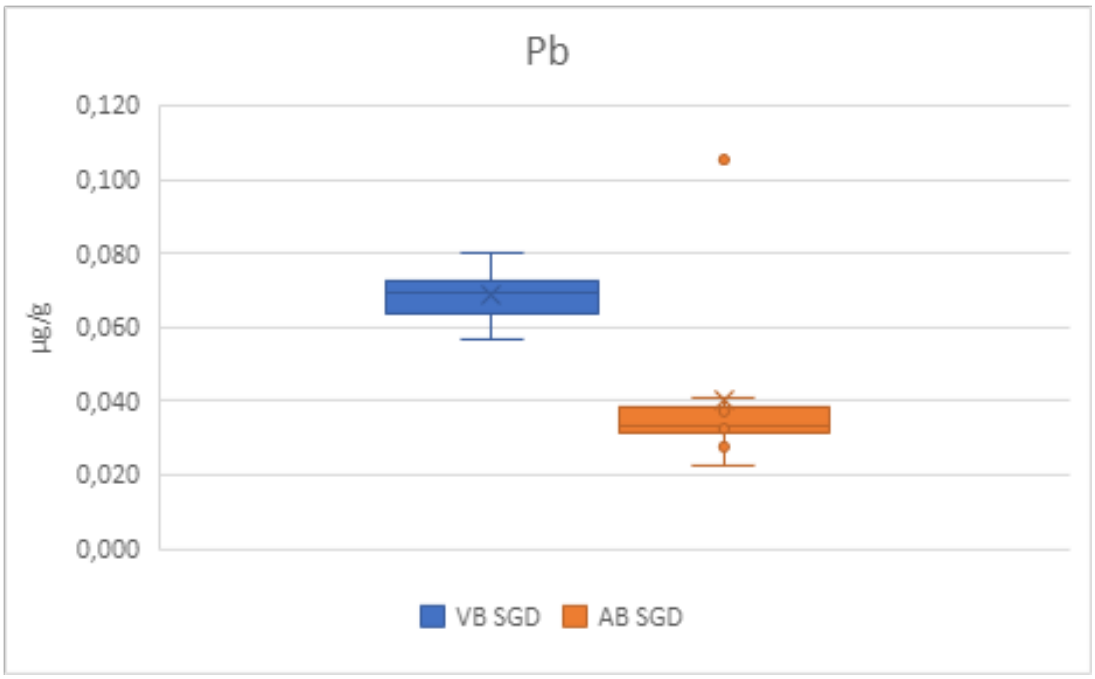

Figure 4.7: Box plot of the Pb concentration (µg/g) from supraglacial debris samples collected on Austre Brøggerbreen (AB, n = 10) and Vestre Brøggerbreen (VB, n = 10). (p=0.0007523, Mann-Whitney U test).

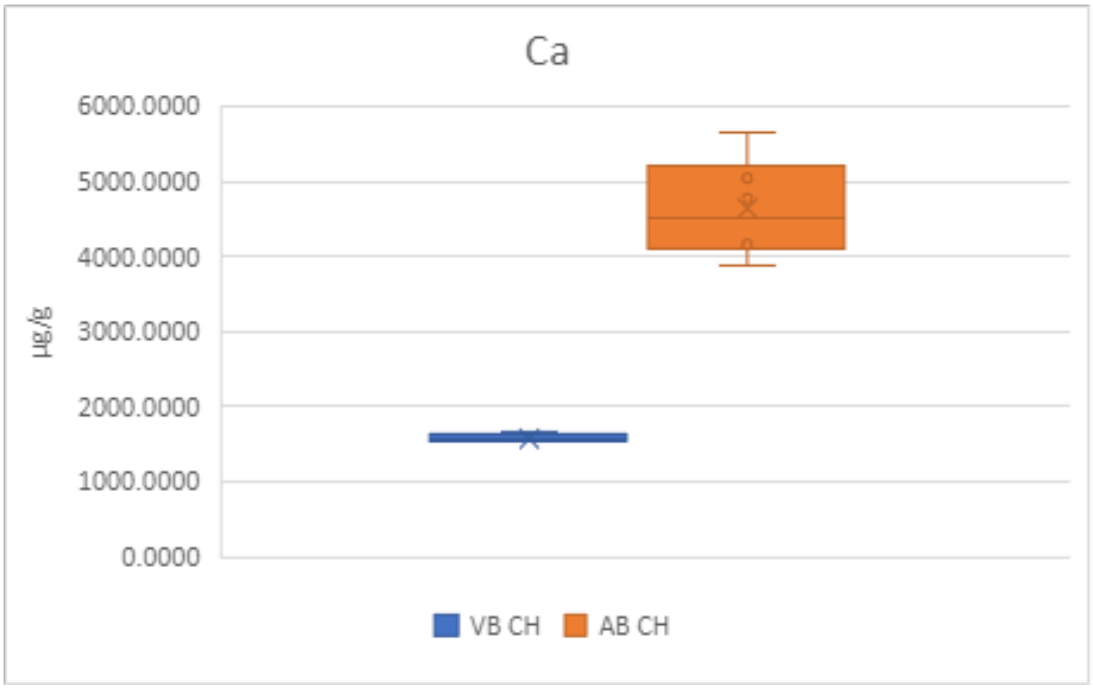

Figure 4.8: Box plot of the Ca concentration (µg/g) from cryoconite samples collected on Austre Brøggerbreen (AB, n = 6) and Vestre Brøggerbreen (VB, n = 5). (p<.00001, Student t-test).

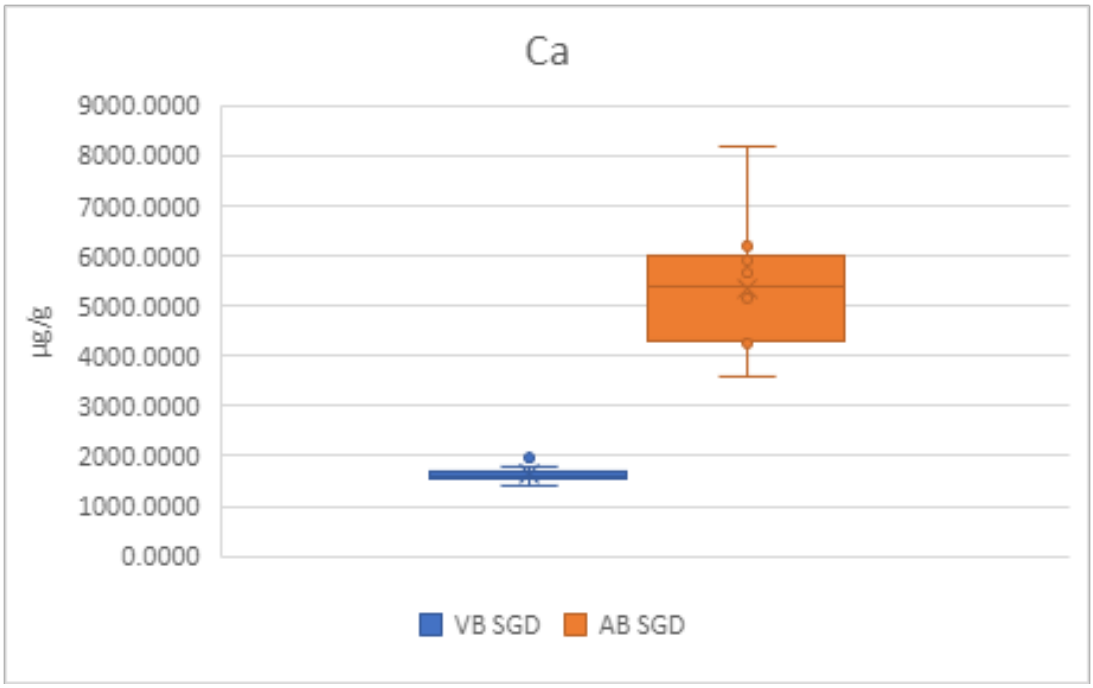

Figure 4.9: Box plot of the Ca concentration (µg/g) from supraglacial debris samples collected on Austre Brøggerbreen (AB, n = 10) and Vestre Brøggerbreen (VB, n = 10). (p<.00001, Student t-test).

4.5 Principal component analysis of snow samples

The third PCA run was done by extracting all snow samples from the first data set and including the location category. As observed from the PCA scores plot and loadings plot in figures 4.10 and 4.12, the samples are quite assosiating between the two locations. The PC 1 and PC 2 makes up 49 % and 15 % of the total variance.

The scores and loadings plots is showing that the samples from both locations have strong similarities in elemental concentrations, and generally low concentrations. Although, three snow samples, ABS 7, ABS 8 and ABS 9, collected from Austre Brøggerbreen, stands out as outliners. When comparing the scores plot in figure 4.11 with the loadings plot in figure 4.12, the three samples are correlating with the elements As, Co Li. When collecting these samples, the snow could clearly be observed as a more yellow colour compared with the other snow samples. Figure A.1 in appendix A illustrates the colour of the snow samples, ABS 7, ABS 8 and ABS 9. A higher concentration of these elements shows that these samples do not contain pure minerals [74]. In a study of atmospheric trace element deposition in moss samples, concentrations of Co were detected. In that study, Co was strongly correlated to elements such as As, Ni and Cu [38]. The same correlations of these elements are found in the scores and loadings plots of the snow samples. The study suggested that the major source of these elements in the detected location originates from the copper-nickel refinery on the Kola peninsula [38]. Although conducted concentrations of As are lower than the mean concentrations detected in moss over Norway, the source of the elements can be assumed to origin from anthropogenic activities of either local or long-ranged atmospheric transport [38].

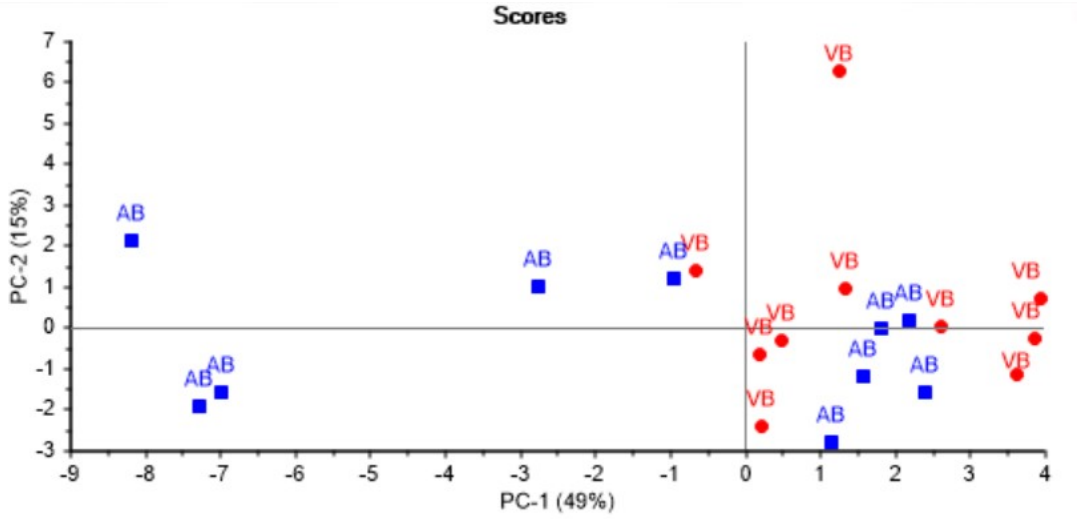

Figure 4.10: Principal component analysis (PCA) scores plot of all snow samples and components. PC 1 makes up 49 % of the total variance, and PC 2 makes up 15 % of the total variance

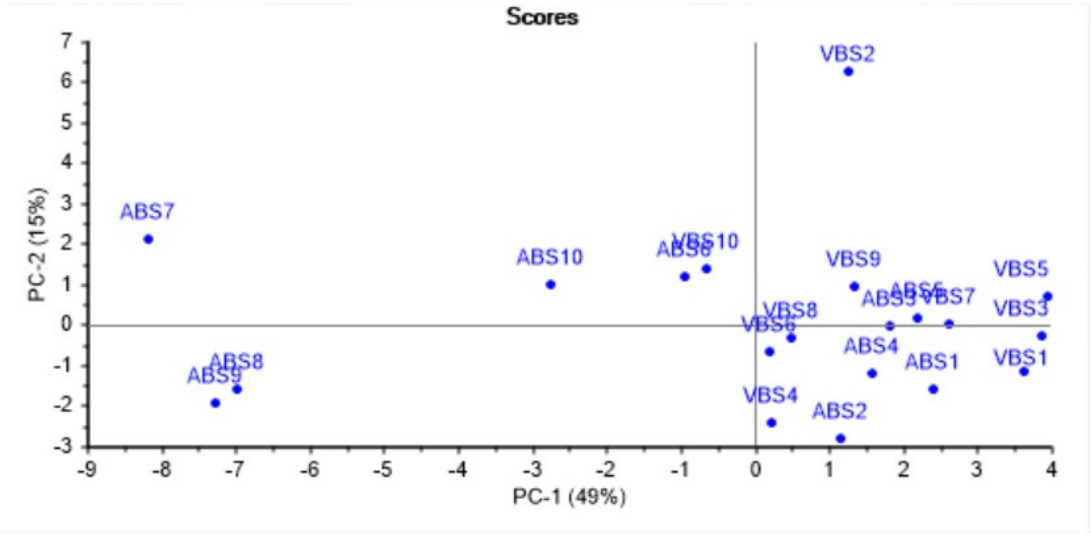

Figure 4.11: Principal component analysis (PCA) scores plot of snow samples and components. PC 1 makes up 49 % of the total variance, and PC 2 makes up 15 % of the total variance.

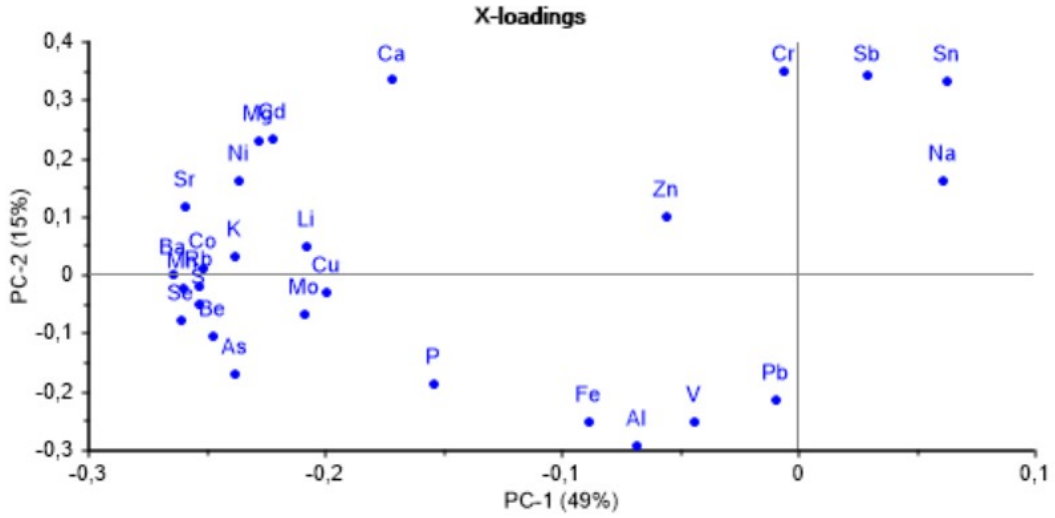

Figure 4.12: Principal component analysis (PCA) loadings plot of snow samples and components. PC 1 makes up 49 % of the total variance, and PC 2 makes up 15 % of the total variance.

4.6 Elemental composition of snow and meltwater between locations

To compare the difference in elemental concentrations in snow samples between the two locations, Austre Brøggerbreen and Vestre Brøggerbreen, statistical analysis of the Ca, Na, Mg, Fe, Al, Zn, Pb, As and Cd concentrations were done. The elemental concentration varied between the sample material and location. As mentioned in section 4.1, the elemental concentrations of Ca, Mg and Na in snow samples and meltwater samples were dominating. Described in a study, the elements of Na, Ca and Mg could be reflected as atmospheric transport from marine environment [38].

Significant differences of the element concentrations were observed between the snow samples collected at the locations Austre Brøggerbreen and Vestre brøggerbreen. Statistical data for

the results of this project is shown in the appendix E. Shapiro-Wilk test was used to test if the mean concentrations were normal distributed. A table of the p-values from the data sets tested for normal distribution is listed in table E.1 in appendix E.1. The student t-test was used to calculate if the mean concentrations between the locations were statistical significant, when the means were normal distributed. When the mean concentrations of the snow samples were not normal distributed, the Mann-Whitney U test was used to calculate if the two mean concentrations of the snow samples from the two locations Austre Brøggerbreen and Vestre Brøggerbreen show any statistically significant difference. A table of the statistical significance is listed in table E.3 in appendix E. Out of the selected elements, mean concentrations of Pb and Zn in showed a statistically significant difference between the two locations in the snow samples. Where p = 0.007345, of Pb and p = 0.03763, of Zn, using Mann Whitney U test. The detected concentrations show a statistical significant difference between the concentrations of Pb, with higher concentrations detected in the samples from Vestre Brøggerbreen.

Figure 4.13 presents a box plot of the lead concentrations of the snow samples from Vestre Brøggerbreen (VB S) and Austre Brøggerbreen (AB S). The lead concentrations are significantly different between the two locations (p= 0.007345, Mann-Whitney U test), where the concentration is higher in the samples collected from Vestre Brøggerbreen (VB S).

Figure 4.14 presents a box plot of the sink concentrations of the snow samples from Vestre Brøggerbreen (VB S) and Austre Brøggerbreen (AB S). The sink concentrations are significantly different between the two locations (p= 0.03763, Mann-Whitney U test), where the concentration is higher in the samples collected from Austre Brøggerbreen (VB S).

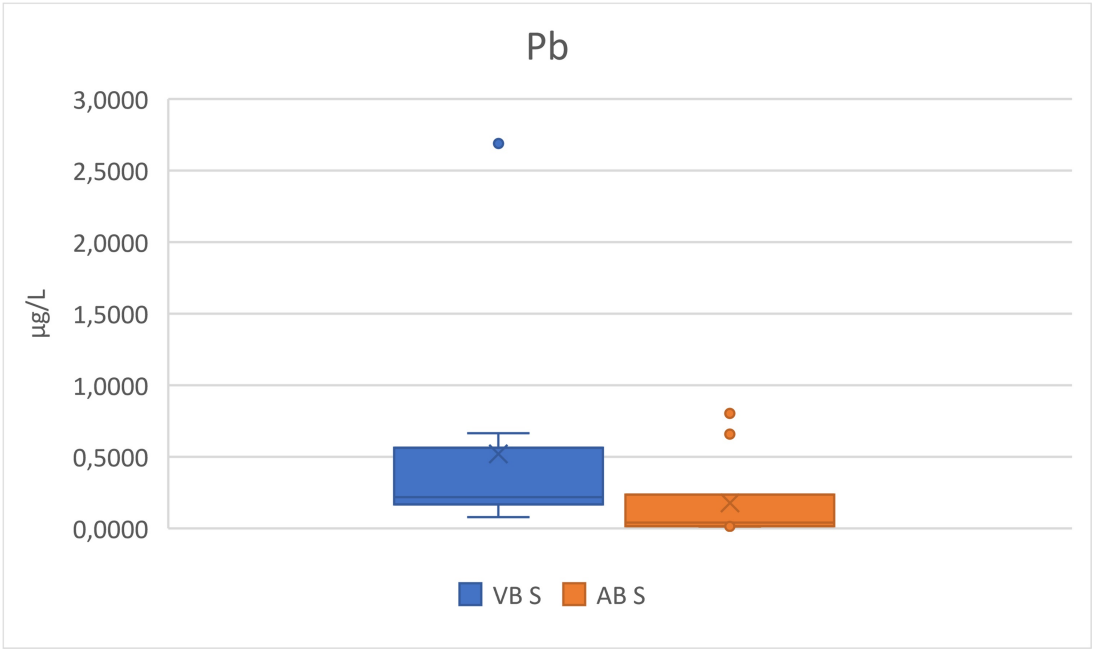

Figure 4.13: Box plot of the Pb concentration (µg/L) from snow samples collected on Austre Brøggerbreen (AB, n = 10) and Vestre Brøggerbreen (VB, n = 10). (p= 0.007345, Mann-Whitney U test).

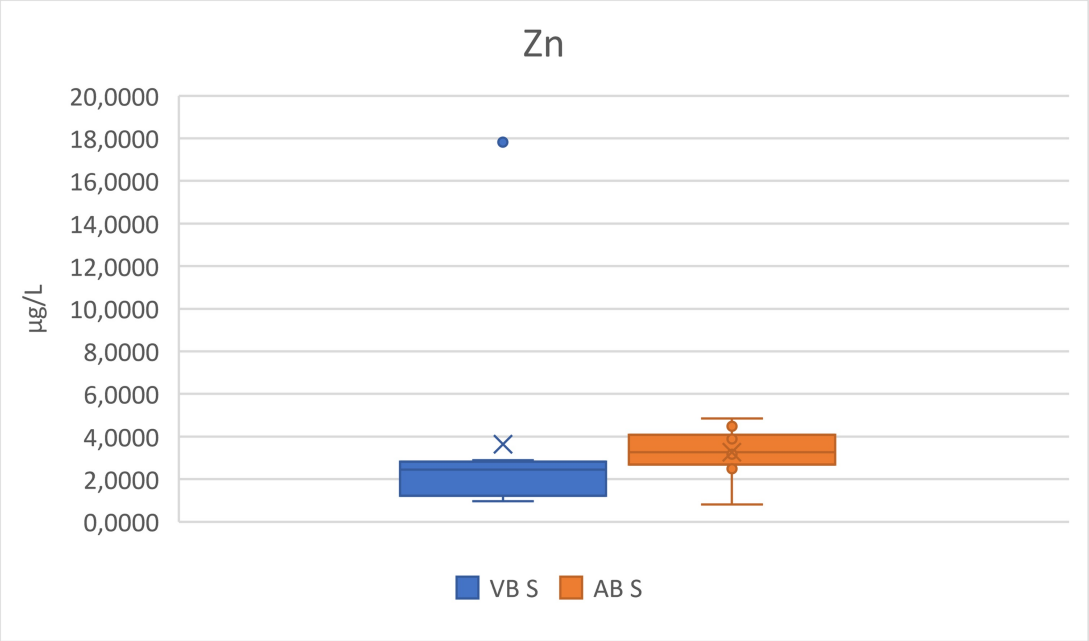

Figure 4.14: Box plot of the Zn concentration (µg/L) from snow samples collected on Austre Brøggerbreen (AB, n = 10) and Vestre Brøggerbreen (VB, n = 8). (p= 0.03763, Mann-Whitney U test).

4.7 Determination of Total Carbon (TC) and Total Nitrogen (TN) content in cryoconite, supraglacial debris and flow sediment

Samples of cryoconite, supraglacial debris and flow sediment collected on locations from the glacier systems Austre Brøggerbreen and Vestre Brøggerbreen were analysed for total carbon (TC) and total nitrogen (TN) by high-temperature combustion with near-infrared spectrometry (NIRS).

Table 4.4: TC and TN in percentage composition by weight for measured samples of cryoconite, supraglacial debris and flow sediments from Austre Brøggerbreen (AB) and Vestre Brøggerbreen (VB). Where n represents the number of samples.

Sample material	n	TC (%)	TN (%)
Cryoconite (AB) Mean ± SD	6	1.4 ± 0.3	0.12 ± 0.02
Cryoconite (VB) Mean ± SD	10	3.0 ± 0.7	0.24± 0.06
Supraglacial debris (AB) Mean ± SD	10	1.7 ± 0.8	0.12 ± 0.07
Supraglacial debris (VB) Mean ± SD	10	3.4 ± 0.6	0.25 ± 0.04
Flow sediment (AB) Mean	1	5.0×10^{-1}	<LOD
Flow sediment (VB) Mean	1	6.5	0.019

The list with the mean concentration and standard deviation of TC and TN in percentage concentrations are presented in table 4.4. Where n represents the number of samples. Samples marked with AB are samples from locations from the glacier system Austre Brøggerbreen. The samples marked with VB are samples from locations on the glacier system, Vestre Brøggerbreen.

A list with the results of the TC and TN content of all samples analysed in this project is shown in the tables C.4 and C.5 in the appendix C.2.

For the samples collected on Austre Brøggerbreen, the TC and TN content of the cryoconite samples were found at 1.4 % ± 0.3 % and 0.12 % ± 0.02 %, respectively. The TC and TN content of the supraglacial debris were found at 1.7 % ± 0.8 % and 0.12 % ± 0.07 %, respectively. The TC content of the flow sediment from Austre Brøggerbreen was at 5.0×10^{-1} %. The TN content for the flow sediment was under the limit of detection.

For the cryoconite samples collected on Vestre Brøggerbreen, the TC and TN content were found at 3.0 % ± 0.7 % and 0.24 % ± 0.06 %, respectively. The TC and TN content of the supraglacial debris collected on Vestre Brøggerbreen were found at 3.4 % ± 0.6 % and 0.25 % ± 0.04 %, respectively. The TC and TN content of the flow sediment from Vestre Brøggerbreen was at 6.5 % and 0.019 %, respectively.

4.7.1 Comparing the Total Carbon (TC) and Total Nitrogen (TN) content of cryoconite and supraglacial debris from different locations

In order to compare different particulate matter collected on locations from the same glacier system, the data sets were first tested for normal distribution by using Shapiro- Wilk test. The data set tested for normal distribution are listed in table E.2 in appendix E.1.

As the data sets were normally distributed, a Student t-test was used to compare the calculated means from the samples of cryoconite and supraglacial debris collected on Austre Brøggerbreen, to obtain if there were a significant difference between the two materials from Austre Brøggerbreen. The significance was set to $p<.05$ for all tests that have been done. The data set tested for statistically significant differences are listed in table E.4 and E.5 in appendix E.

The data sets were all normally distributed, and comparing the means of TC and TN content in cryoconite and supraglacial debris did not show a significant difference, on Austre brøggerbreen (where $p=.2$ for the TC content, and $p=.5$ for the TN content, Student t- test). This suggests that melted cryoconite holes are the source of supraglacial debris on Austre Brøggerbreen.

The data sets were all normally distributed, and comparing the means of TC and TN content in cryoconite and supraglacial debris collected on Vestre Brøggerbreen did show a significant difference, in the TC content (where $p=.005$ for the TC content, Student t-test). The test shows that there is a statistical significance difference where there indicates an increase in TC (%) content in the supraglacial debris compared with cryoconite. Where the TC (%) content of cryoconite and supraglacial debris were found at 3.0 % ± 0.7 and 3.4 % ± 0.6 %, respectively, It is reasonable to assume that these differences are marginal. For the TN (%) content, no significant differences were obtained (where $p=.02$, Student t-test).

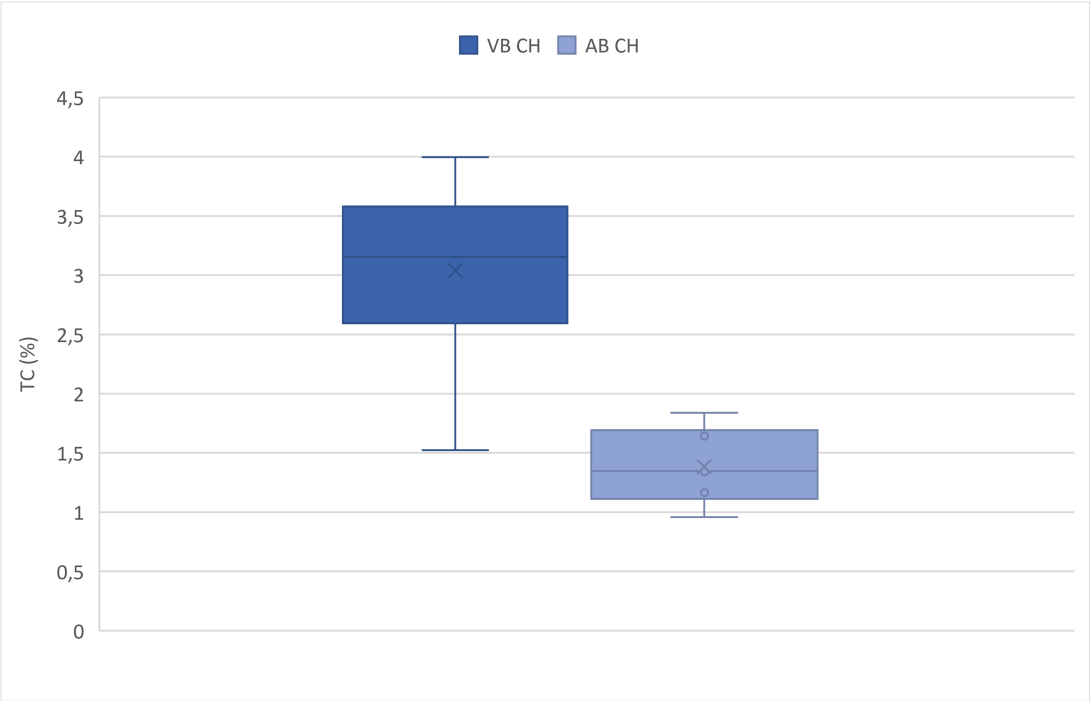

Figure 4.15: Box plot of the TC (%) concentration from cryoconite samples collected on Austre Brøggerbreen (AB, n = 6) and Vestre Brøggerbreen (VB, n = 10). VB CH are cryoconite samples collected from Vestre Brøggerbreen. AB CH are cryoconite samples collected from Austre Brøggrbreen. (p <.001, Student-t test).

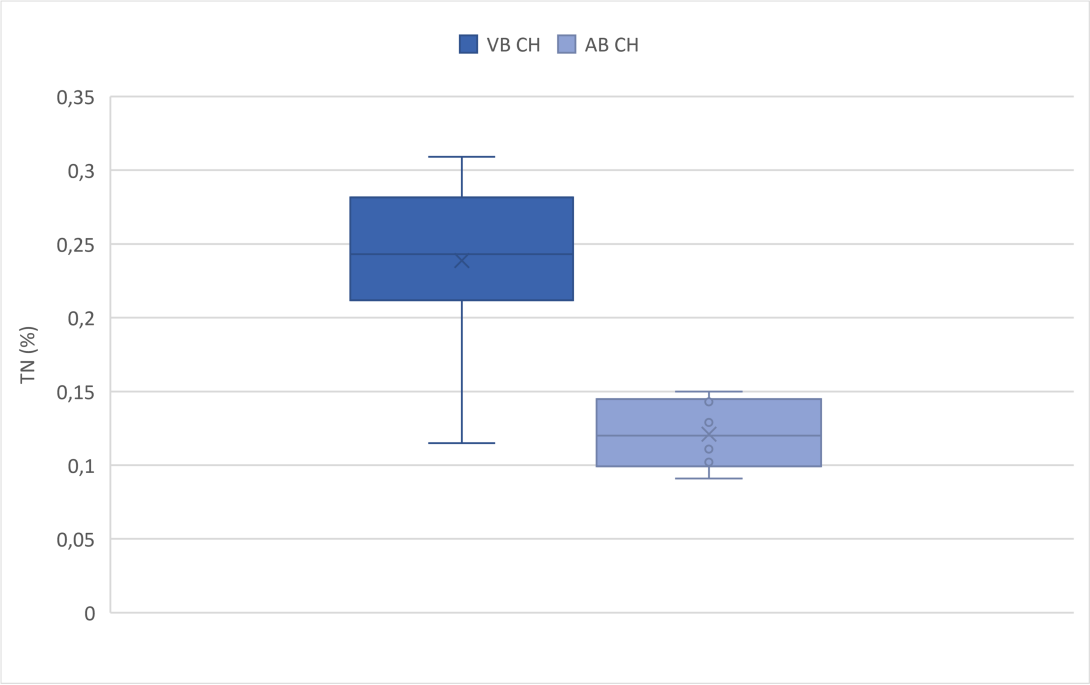

Figure 4.16: Box plot of the TN (%) concentration from cryoconite samples collected on Austre Brøggerbreen (AB, n = 6) and Vestre Brøggerbreen (VB, n = 10). VB CH are cryoconite samples collected from Vestre Brøggerbreen. AB CH are cryoconite samples collected from Austre Brøggrbreen. (p <.001, Student-t test).

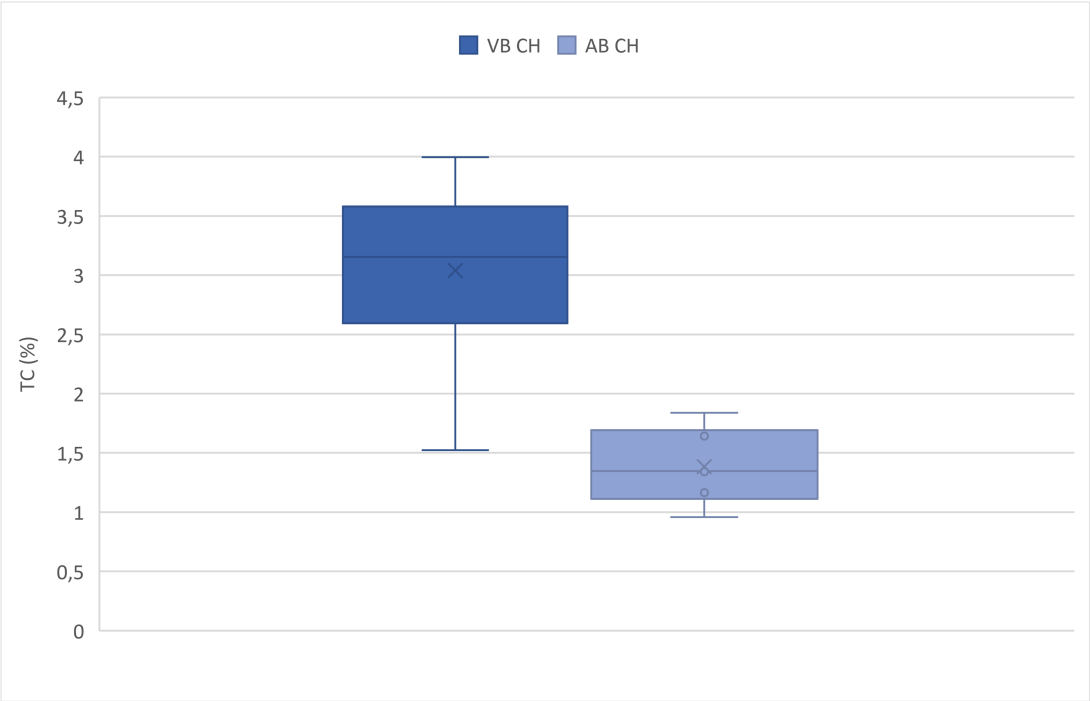

Figure 4.17: Box plot of the TC (%) concentration from supraglacial debris samples collected on Austre Brøggerbreen (AB, n = 10) and Vestre Brøggerbreen (VB, n = 10). VB OM are supraglacial debris samples collected from Vestre Brøggerbreen. AB OM are supraglacial debris samples collected from Austre Brøggrbreen. (p <.001, Student-t test).

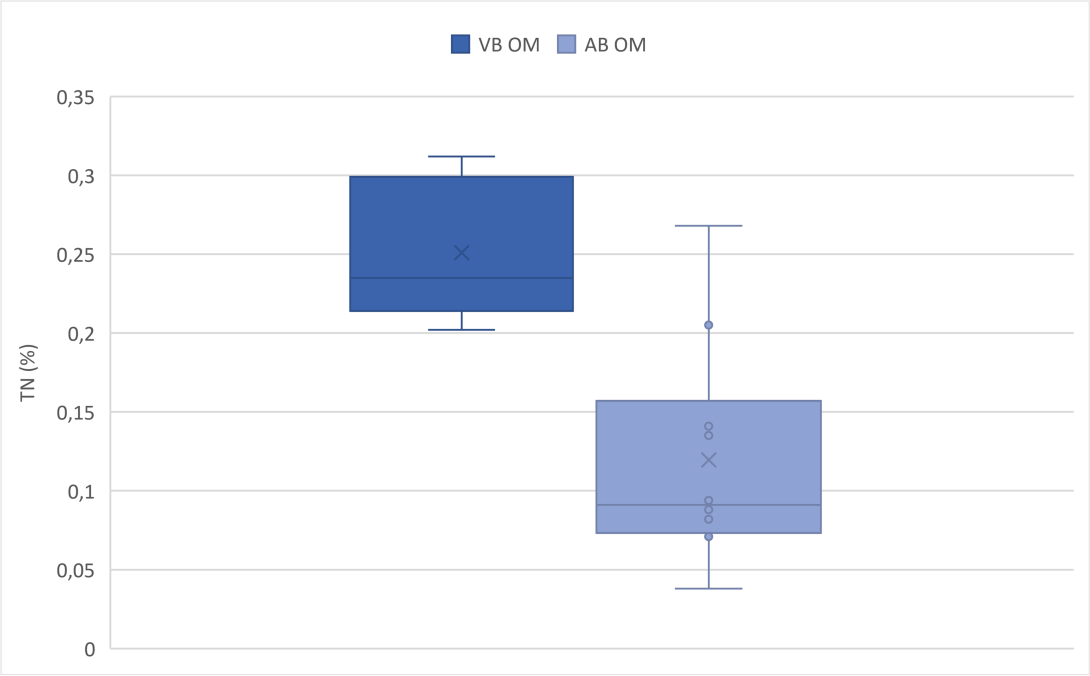

Figure 4.18: Box plot of the TN (%) concentration from supraglacial debris samples collected on Austre Brøggerbreen (AB, n = 10) and Vestre Brøggerbreen (VB, n = 10).VB OM are supraglacial debris samples collected from Vestre Brøggerbreen. AB OM are supraglacial debris samples collected from Austre Brøggrbreen. (p <.001, Student-t test).

Comparison of the means of the TC (%) content and TN (%) content in both cryoconite and supraglacial debris samples of different locations (Vestre Brøggerbreen and Austre Brøggerbreen) did show a statistically significant difference. (Where p <.001 for all tests, Student-t test). This indicates a significant decrease in TC (%) and TN (%) content from measurements of both cryoconite and supraglacial debris samples from Vestre Brøggerbreen to Austre Brøggerbreen.

The Box plots of the TC (%) and TN(%) concentrations from cryoconite samples collected on Austre Brøggerbreen and Vestre Brøggerbreen are presented in figure 4.15 and 4.16, respectively. VB CH are cryoconite samples collected from Vestre Brøggerbreen. AB CH are cryoconite samples collected from Austre Brøggrbreen. The Box plots of the TC (%) and TN(%) concentrations from supraglacial samples collected on Austre Brøggerbreen and Vestre Brøggerbreen are presented in figure 4.17 and 4.18, respectively. VC OM are supraglacial debris samples collected from Vestre Brøggerbreen. AB OM are supraglacial debris samples collected from Austre Brøggrbreen.

Previous findings in a study determined a carbon and nitrogen content in cryoconite of 0.54 - 4.37% and 0.11 - 0.42 %, respectively [30]. All samples determined from Austre Brøggerbreen and Vestre Brøggerbreen, for TC (%) content were within the same range as presented in the study [30]. As already mentioned in chapter 2.3, about 85-90 % of the cryoconite composition is mineral fractions [26]. As the measured TC (%) concentration were lowest in samples from Austre Brøggerbreen, measured at 1.4% ± 0.3 % at lowest in cryoconite samples and 1.7% ± 0.8 % in supraglacial debris samples. It can be indicated that the samples from locations on Austre Brøggerbreen contain a bigger fraction of inorganic carbon such as minerals and dust minerals from local areas, compared with samples from Vestre Brøggerbreen. Although there are statistical significances between the samples from the different glacier systems, the differences are marginal.

The C:N ratio of the cryoconite and supraglacial debris in this project was between 12.7 - 14.1, which is with similarities to reported findings conducted in a study of cryoconite on glaciers in the Arctic and Himalaya [30]. The observed C:N ratio in this project is close to the C:N ratio of general microbes [30].

4.8 Determination of TOC, UV-vis and SUVA

The aromaticity content of the water samples and snow samples listed in table 4.5 were determined by $SUVA_{254}$ analysis calculating TOC and UV-vis of the samples. Means and standard deviation of the $SUVA_{254}$ values of the snow samples are presented in table 4.6.

Determination of $SUVA_{254}$ on the snow samples ABS and VBS, from Austre Brøggerbreen and Vestre Brøggerbreen respectively did not show any significant difference in $SUVA_{254}$ values (When comparing the snow samples p=.5, and comparing the meltwater samples p=.8, Student t-test). Which the snow samples from both locations were determined to be 2.2 ± 0.4 L/mg×m. As previously mentioned in chapter 2.7.2.5, $SUVA_{254}$ values of > 4.0 L/mg×m of natural water is defined with high $SUVA_{254}$ values and have a high content of hydrophobic and aromatic structures. Water with low $SUVA_{254}$ values has an $SUVA_{254}$ of < 2.0 L/mg×m and are representing hydrophilic materials [51, 52].

All the samples determined have $SUVA_{254}$ values < 4.0 L/mg × m, which indicates low content of hydrophobic and aromatic structures. If the $SUVA_{254}$ values had been > 4.0 L/mg × m, there would be interesting to analyse the samples with further analysis, to determine the aromatic substances in the samples.

The lowest values were determined in the meltwater from the glacier systems. These samples had also $SUVA_{254}$ of < 2.0 L/mg × m and are representing hydrophilic materials. The snow samples were also decanted and there have not been used 0.45 µL filter to determine the DOC

Table 4.5: Values of TOC, UV-Vis and SUVA for measured snow samples and water samples from Austre Brøggerbreen and Vestre Brøggerbreen.

Sample ID	TOC [mg/L]	UV-vis [1/cm]	SUVA [L/mg × m]
AB5	0.242	0.004	1.655
VB5	0.471	0.005	1.062
ABS1	1.25	0.030	2.398
ABS2	2.94	0.049	1.666
ABS3	1.02	0.025	2.456
VBS1	1.67	0.032	1.913
VBS2	1.04	0.022	2.115
VBS3	0.576	0.015	2.606

Table 4.6: Mean SUVA values for measured snow samples and water samples from Austre Brøggerbreen and Vestre Brøggerbreen. Where Sample ID AB S represents the snow samples from Austre Brøggerbreen, and VB S represents snow samples from Vestre Brøggerbreen, and n represents the number of samples.

Sample ID	n	SUVA [L/mg × m]
ABS Mean ± SD	3	2.2 ± 0.4
VBS Mean ± SD	3	2.2 ± 0.4

values. Studies say that between 83- 96% of TOC values are DOC [51]. If a 0.45 µL filter had been used to determine the DOC, the $SUVA_{254}$ would have been different.

4.9 Further work

The discussions provides many assumptions and unanswered questions, as result of limitations in time, funding for this specific project, priorities made and of preformed analyses. There is currently limited research on the chemical composition of cryoconite. Studies have observed cryoconite accumulates elemental carbon, specific elements and radioactive isotopes [12, 26].

The findings of this project makes it clear that a long term environmental monitoring of the different glacial systems is needed. Some of the sediment samples which occur from the snow surface at Austre Brøggerbreen had higher concentrations of the elements S, As, and Li, which stands out from the other samples from the same location. This is showing how complex these materials from the same location can be. It is interesting to analyse more materials from this location to find the sources of these elements.

In order to discuss the connection between different glacial particulate matter, such as cryoconite and supraclacial debris, the cryoconite age and their abilities of accumulation of elements, particulate matter from different cryoconite holes and depth, sampling location, size of glacier and glacier type, element speciation, require more data to analyse trace elements, environmental contamination and their impact on the environment, as the global climate is in change.

5 Conclusion

Different particulate matter, such as cryoconite, supraglacial debris, flow sediment and snow, collected from the two glacier systems, Austre Brøggerbreen and Vestre Brøggerbreen in Brøggerdalen, Ny-Ålesund were determined in order to increase the knowledge about the chemical compositions of particulate matter related to glacier systems on Svalbard. Most of the samples were collected directly from the surface of the glaciers.

Differences in the chemical and physical properties of different sample materials collected within the same glacier system and between the two glacier systems have been observed. A variation of factors may be responsible for the differences in chemical and physical properties are a result of the local geology, the structure of the sample material, and sample location.

The major elemental composition in cryoconite, supraglacial debris, supraglacial debris collected from snow, flow sediment and snow differed. With dominating elements such as Fe, Al, Mg, Ca and Na in the cryoconite, supraglacial debris. The snow samples were dominated by Ca, Na and Mg concentrations. The supraglacial debris and cryoconite samples collected on Vestre Brøggerbreen showed a statistical significantly higher concentration of Pb concentrations. The supraglacial debris and cryoconite samples collected on Austre Brøggerbreen showed a statistical significantly higher concentration of Zn concentrations. This was with similarities as presented in previous studies, done in the same study area.

The supraglacial debris and cryoconite samples contained a higher level of inorganic material, with low total carbon and total nitrogen content. Although within the range of previously published research. The total carbon and total nitrogen content did show a statistically significant difference between the two glacier systems of Austre Brøggerbreen and Vestre Brøggerbreen. The highest total carbon and total nitrogen content were determined in samples from the glacier system of Vestre Brøggerbreen, compared to samples from the glacier system of Austre Brøggerbreen. There were not observed statistical significant differences in the TC (%) and TN (%) concentrations between cryoconite and supraglacial debris samples collected on Austre Brøggerbreen. Statistical significant differences in the TC (%) and TN (%) concentrations were observed between cryoconite and supraglacial debris samples collected on Vestre Brøggerbreen.

$SUVA_{254}$ values of snow samples and meltwater were in the range of hydrophilic substances, and no values did indicate any levels of hydrophobic and aromatic substances. The $SUVA_{254}$ did not show any statistical differences between the two glacier systems.

Long term environmental monitoring of the different glacial systems and more collected data is required in order to discuss the connection between different glacial particulate matter, such as cryoconite and supraclacial debris, the cryoconite age and their abilities of accumulation of elements, particulate matter from different cryoconite holes and depth, sampling location, size of glacier and glacier type, element speciation, to analyse trace elements, environmental contamination and their impact on the environment, as the global climate is in change.

Bibliography

[1] Jason E Box, William T Colgan, Torben Røjle Christensen, Niels Martin Schmidt, Magnus Lund, Frans-Jan W Parmentier, Ross Brown, Uma S Bhatt, Eugénie S Euskirchen, Vladimir E Romanovsky, et al. Key indicators of arctic climate change: 1971–2017. *Environmental Research Letters*, 14(4):045010, 2019.

[2] AMAP. Arctic climate change update 2021: key trends and impacts. summary for policy-makers. *Arctic monitoring and assessment programme (AMAP)*, page 16, 2021.

[3] Harald Svendsen, Agnieszka Beszczynska-Møller, Jon Ove Hagen, Bernard Lefauconnier, Vigdis Tverberg, Sebastian Gerland, Jon Børre Ørbøk, Kai Bischof, Carlo Papucci, Marek Zajaczkowski, Roberto Azzolini, Oddbjørn Bruland, Christian Wiencke, Jan-Gunnar Winther, and Winfried Dallmann. The physical environment of kongsfjorden–krossfjorden, an arctic fjord system in svalbard. *Polar Research*, 21(1):133–166, 2002.

[4] Kathy S Law and Andreas Stohl. Arctic air pollution: Origins and impacts. *science*, 315(5818):1537–1540, 2007.

[5] Marion Maturilli, Andreas Herber, and Gert König-Langlo. Surface radiation climatology for ny-ålesund, svalbard (78.9 n), basic observations for trend detection. *Theoretical and Applied Climatology*, 120:331–339, 2015.

[6] Marco Möller and Jack Kohler. Differing climatic mass balance evolution across svalbard glacier regions over 1900–2010. *Frontiers in Earth Science*, 6:128, 2018.

[7] Alexander M Milner, Lee E Brown, and David M Hannah. Hydroecological response of river systems to shrinking glaciers. *Hydrological Processes: An International Journal*, 23(1):62–77, 2009.

[8] Harald Svendsen, Agnieszka Beszczynska-Møller, Jon Ove Hagen, Bernard Lefauconnier, Vigdis Tverberg, Sebastian Gerland, Jon Børre Ørbøk, Kai Bischof, Carlo Papucci, Marek Zajaczkowski, et al. The physical environment of kongsfjorden–krossfjorden, an arctic fjord system in svalbard. *Polar research*, 21(1):133–166, 2002.

[9] Dirk Scherler, Hendrik Wulf, and Noel Gorelick. Global assessment of supraglacial debris-cover extents. *Geophysical Research Letters*, 45(21):11–798, 2018.

[10] Nozomu Takeuchi and Zhongqin Li. Characteristics of surface dust on ürümqi glacier no. 1 in the tien shan mountains, china. *Arctic, Antarctic, and Alpine Research*, 40(4):744–750, 2008.

[11] Peter L Moore. Stability of supraglacial debris. *Earth Surface Processes and Landforms*, 43(1):285–297, 2018.

[12] Pauline Verula Braaten. Study of supraglacial debris and particulate matter released from Austre Brøggerbreen and Vestre Brøggerbreen at Ny-Ålesund, Svalbard, 2022.

[13] Nils Petter Thuesen and Susan Barr. Svalbard i Store norske leksikon på snl.no, 2022.

[14] Borgar Aamaas, Carl Egede Bøggild, Frode Stordal, Terje Berntsen, KIM Holmén, and

Johan Strùm. Elemental carbon deposition to svalbard snow from norwegian settlements and long-range transport. *Tellus B: Chemical and Physical Meteorology*, 63(3):340–351, 2011.

[15] Statistisk sentralbyrå. Population of Svalbard, 2023.

[16] Sysselmesteren på Svalbard. Forurensning og avfall, 2022.

[17] Katharina Halbach, Øyvind Mikkelsen, Torunn Berg, and Eiliv Steinnes. The presence of mercury and other trace metals in surface soils in the norwegian arctic. *Chemosphere*, 188:567–574, 2017.

[18] Åshild Ønvik Pedersen, P Convey, Kevin K Newsham, Jesper Bruun Mosbacher, Eva Fuglei, Virve Ravolainen, Brage Bremset Hansen, Thomas Correll Jensen, A Augusti, Elisabeth Mackteld Biersma, et al. Five decades of terrestrial and freshwater research at ny-ålesund, svalbard. *Polar Research*, 41, 2022.

[19] FRIEDHELM Thiedig, KERSTIN Saalmann, and KARSTEN Piepjohn. Explanatory notes to the geological map of broggerhalvoya and blomstrandhalvoya 1: 40,000. *GEOLOGISCHES JAHRBUCH REIHE B*, pages 25–54, 2001.

[20] Douglas I Benn and David JA Evans. *Glaciers & glaciation*. Routledge, 2014.

[21] Kurt M Cuffey and William Stanley Bryce Paterson. *The physics of glaciers*. Academic Press, 2010.

[22] William Stanley Bryce Paterson. *Physics of glaciers*. Butterworth-Heinemann, 2000.

[23] Robert A Wharton Jr, Christopher P McKay, George M Simmons Jr, and Bruce C Parker. Cryoconite holes on glaciers. *Bioscience*, pages 499–503, 1985.

[24] Piotr Rozwalak, Paweł Podkowa, Jakub Buda, Przemysław Niedzielski, Szymon Kawecki, Roberto Ambrosini, Roberto S. Azzoni, Giovanni Baccolo, Jorge L. Ceballos, Joseph Cook, Biagio Di Mauro, Gentile Francesco Ficetola, Andrea Franzetti, Dariusz Ignatiuk, Piotr Klimaszyk, Edyta Łokas, Masato Ono, Ivan Parnikoza, Mirosława Pietryka, Francesca Pittino, Ewa Poniecka, Dorota L. Porazinska, Dorota Richter, Steven K. Schmidt, Pacifica Sommers, Juliana Souza-Kasprzyk, Marek Stibal, Witold Szczuciński, Jun Uetake, Łukasz Wejnerowski, Jacob C. Yde, Nozomu Takeuchi, and Krzysztof Zawierucha. Cryoconite – from minerals and organic matter to bioengineered sediments on glacier's surfaces. *Science of The Total Environment*, 807:150874, 2022.

[25] Joseph Cook, Arwyn Edwards, Nozomu Takeuchi, and Tristram Irvine-Fynn. Cryoconite: the dark biological secret of the cryosphere. *Progress in Physical Geography*, 40(1):66–111, 2016.

[26] Giovanni Baccolo, Biagio Di Mauro, Dario Massabò, Massimiliano Clemenza, Massimiliano Nastasi, Barbara Delmonte, Michele Prata, Paolo Prati, Ezio Previtali, and Valter Maggi. Cryoconite as a temporary sink for anthropogenic species stored in glaciers. *Scientific reports*, 7(1):1–11, 2017.

[27] Andy Hodson, Alexandre M Anesio, Martyn Tranter, Andrew Fountain, Mark Osborn, John Priscu, Johanna Laybourn-Parry, and Birgit Sattler. Glacial ecosystems. *Ecological monographs*, 78(1):41–67, 2008.

[28] Marek Stibal and Martyn Tranter. Laboratory investigation of inorganic carbon uptake by cryoconite debris from werenskioldbreen, svalbard. *Journal of Geophysical Research: Biogeosciences*, 112(G4), 2007.

[29] Marek Stibal, Emily C Lawson, Grzegorz P Lis, Ka Man Mak, Jemma L Wadham, and

Alexandre M Anesio. Organic matter content and quality in supraglacial debris across the ablation zone of the greenland ice sheet. *Annals of Glaciology*, 51(56):1–8, 2010.

[30] Nozomu Takeuchi. Optical characteristics of cryoconite (surface dust) on glaciers: the relationship between light absorbency and the property of organic matter contained in the cryoconite. *Annals of Glaciology*, 34:409–414, 2002.

[31] Frederick William Fifield and Peter J Haines. *Environmental analytical chemistry*, volume 2. Blackwell science London, 2000.

[32] Dalway J Swaine. Why trace elements are important. *Fuel Processing Technology*, 65:21–33, 2000.

[33] Arctic Monitoring and Assessment Programme. *Arctic pollution issues: A state of the Arctic environment report*. Amap, 1997.

[34] Robie W Macdonald, T Harner, and J Fyfe. Recent climate change in the arctic and its impact on contaminant pathways and interpretation of temporal trend data. *Science of the total environment*, 342(1-3):5–86, 2005.

[35] Frank Wania and Donald Mackay. Peer reviewed: tracking the distribution of persistent organic pollutants. *Environmental science & technology*, 30(9):390A–396A, 1996.

[36] Sigurd Rognerud, Trond Skotvold, Eirik Fjeld, Stephen A Norton, and Anders Hobæk. Concentrations of trace elements in recent and preindustrial sediments from norwegian and russian arctic lakes. *Canadian Journal of Fisheries and Aquatic Sciences*, 55(6):1512–1523, 1998.

[37] Jan Schaug, Jon P Rambæk, Eiliv Steinnes, and Ronald C Henry. Multivariate analysis of trace element data from moss samples used to monitor atmospheric deposition. *Atmospheric Environment. Part A. General Topics*, 24(10):2625–2631, 1990.

[38] Torunn Berg, Oddvar Røyset, Eiliv Steinnes, and Marit Vadset. Atmospheric trace element deposition: principal component analysis of icp-ms data from moss samples. *Environmental Pollution*, 88(1):67–77, 1995.

[39] Phase diagram pressure and temperature - energy changes in chemical reactions - mcat content, Aug 2021.

[40] Soham Shukla. Freeze drying process: A review. *International journal of pharmaceutical sciences and research*, 2(12):3061, 2011.

[41] Standard Norge. ISO 16720:2005(E). Soil quality — Pretreatment of samples by freeze-drying for subsequent analysis, 2005.

[42] Edson I. Müller, Márcia F. Mesko, Diogo P. Moraes, Maria das Graças A. Korn, and Érico M.M. Flores. Chapter 4 - wet digestion using microwave heating. In Érico Marlon de Moraes Flores, editor, *Microwave-Assisted Sample Preparation for Trace Element Analysis*, pages 99–142. Elsevier, Amsterdam, 2014.

[43] MILESTONE HELPING CHEMIST ultraclave microwave digestion system. https://www.milestonesci.com/microwave-digestion-solutions/ultraclave-microwave-digestion-system/. Accessed: 2022-12-07.

[44] Joseph Sneddon and Michael D Vincent. Icp-oes and icp-ms for the determination of metals: application to oysters. *Analytical Letters*, 41(8):1291–1303, 2008.

[45] Mostafa F Al-Hakkani. Guideline of inductively coupled plasma mass spectrometry “icp–ms”:

Fundamentals, practices, determination of the limits, quality control, and method validation parameters. *SN Applied Sciences*, 1(7):791, 2019.

[46] Robert Thomas. *Practical guide to ICP-MS: a tutorial for beginners*. CRC press, 2008.

[47] Isabella Bisutti, Ines Hilke, and Michael Raessler. Determination of total organic carbon – an overview of current methods. *TrAC Trends in Analytical Chemistry*, 23(10):716–726, 2004.

[48] Shimadzu Corporation. Shimadzu total organic carbon analyzer toc-lcph/cpn userś manual, May 2017.

[49] Skalar Analytical B.V. Primacs100 analyzer series for measurement of tn/tc/ic user manual, May 2019.

[50] Marieta L.C. Passos and M. Lúcia M.F.S. Saraiva. Detection in uv-visible spectrophotometry: Detectors, detection systems, and detection strategies. *Measurement*, 135:896–904, 2019.

[51] Tanju Karanfil, Mark A Schlautman, and Ilke Erdogan. Survey of doc and uv measurement practices with implications for suva determination. *Journal-American Water Works Association*, 94(12):68–80, 2002.

[52] Ceyda Senem Uyguner and Miray Bekbolet. Implementation of spectroscopic parameters for practical monitoring of natural organic matter. *Desalination*, 176(1):47–55, 2005. Seminar in Environmental Science and Technology: Evaluation of Alternative Water Treatment Systems for Obtaining Safe Water.

[53] G.E Batley. Quality assurance in environmental monitoring. *Marine Pollution Bulletin*, 39(1):23–31, 1999.

[54] Daniel MacDougall, Warren B Crummett, et al. Guidelines for data acquisition and data quality evaluation in environmental chemistry. *Analytical Chemistry*, 52(14):2242–2249, 1980.

[55] Douglas A Skoog, Donald M West, F James Holler, and Stanley R Crouch. *Fundamentals of analytical chemistry*. Cengage learning, 2013.

[56] Standard Norge. ISO 5667-1:2020. Water quality — Sampling — Part 1: Guidance on the design of sampling programmes and sampling techniques, 2020.

[57] Standard Norge. ISO 5667-3:2018. Water quality — Sampling — Part 3: Preservation and handling of water samples, 2018.

[58] Standard Norge. ISO 5667-6:2014. Water quality — Sampling — Part 6: Guidance on sampling of rivers and streams, 2014.

[59] Standard Norge. ISO 5667-15:2009. Water quality — Sampling — Part 15: Guidance on the preservation and handling of sludge and sediment samples, 2009.

[60] Standard Norge. ISO 5667-14:2014. Water quality — Sampling — Part 14: Guidance on quality assurance and quality control of environmental water sampling and handling, 2014.

[61] David A Armbruster and Terry Pry. Limit of blank, limit of detection and limit of quantitation. *The clinical biochemist reviews*, 29(Suppl 1):S49, 2008.

[62] Alankar Shrivastava, Vipin B Gupta, et al. Methods for the determination of limit of detection and limit of quantitation of the analytical methods. *Chron. Young Sci*, 2(1):21–25, 2011.

[63] Michael J Campbell, David Machin, and Stephen J Walters. *Medical statistics: a textbook for the health sciences*. John Wiley & Sons, 2010.

[64] B. W. Yap and C. H. Sim. Comparisons of various types of normality tests. *Journal of Statistical Computation and Simulation*, 81(12):2141–2155, 2011.

[65] Tae Kyun Kim. Understanding one-way anova using conceptual figures. *Korean journal of anesthesiology*, 70(1):22–26, 2017.

[66] Andrew J Vickers. Parametric versus non-parametric statistics in the analysis of randomized trials with non-normally distributed data. *BMC medical research methodology*, 5(1):1–12, 2005.

[67] Robert McGill, John W Tukey, and Wayne A Larsen. Variations of box plots. *The american statistician*, 32(1):12–16, 1978.

[68] Kristin Potter, Hans Hagen, Andreas Kerren, and Peter Dannenmann. Methods for presenting statistical information: The box plot. In *VLUDS*, pages 97–106, 2006.

[69] Kim H Esbensen, Dominique Guyot, Frank Westad, and Lars P Houmoller. *Multivariate data analysis: in practice: an introduction to multivariate data analysis and experimental design*. Multivariate Data Analysis, 2002.

[70] Hervé Abdi and Lynne J Williams. Principal component analysis. *Wiley interdisciplinary reviews: computational statistics*, 2(4):433–459, 2010.

[71] Aga Nowak and Andy Hodson. Changes in meltwater chemistry over a 20-year period following a thermal regime switch from polythermal to cold-based glaciation at austre brøggerbreen, svalbard. *Polar Research*, 33(1):22779, 2014.

[72] Arwyn Edwards, Alexandre M Anesio, Sara M Rassner, Birgit Sattler, Bryn Hubbard, William T Perkins, Michael Young, and Gareth W Griffith. Possible interactions between bacterial diversity, microbial activity and supraglacial hydrology of cryoconite holes in svalbard. *The ISME journal*, 5(1):150–160, 2011.

[73] Audun Hjelle. *Geology of Svalbard*. Norsk Polarinstitutt, 1993.

[74] Swapan Kumar Haldar and S. K. Kumar Haldar. *Introduction to Mineralogy and Petrology*. Elsevier Science, Saint Louis, 2013.

[75] Enrico Miccadei, Tommaso Piacentini, and Claudio Berti. Geomorphological features of the kongsfjorden area: Ny-ålesund, blomstrandøya (nw svalbard, norway). *Rendiconti Lincei*, 27:217–228, 2016.

[76] Synnøve Elvevold, Winfried Dallmann, and Dierk Blomeier. Svalbards geologi, 2007.

[77] Norwegian Polar institute. GeoSvalbard.

[78] Audun Hjelle. *Geological Map of Svalbard 1: 100,000: Sheet A7G Kongsfjorden*. Norwegian Polar Institute, 1999.

[79] Swapan Kumar Haldar. *Introduction to mineralogy and petrology*. Elsevier, 2020.

[80] Norwegian Polar institute. Toposvalbard.

[81] Standard Norge. NS 9462:2006. Water quality — Determination of UV— absorbance, 2006.

[82] Sara Johnson. Cryoconite Holes as Potential Tools for Environmental Monitoring in the Arctic. A Study of the Accumulation of Atmospherically Deposited Inorganic and Organic Pollutants in Cryoconite Holes from Three Glaciers in Ny-Ålesund. Master's thesis, NTNU, 2022.

[83] Maja Olava Lindmo Ryan. Particulate matter released from Austre Brøggerbreen; a study on the potential impact on chemical conditions in Bayelva and Kongsfjorden. Master's thesis, NTNU, 2021.

[84] Mats Nordum. Metaller og naturlig organisk materiale i arktiske elver på Svalbard. Master's thesis, NTNU, 2012.

[85] Sara Jenny Katrine Hald. Kartlegging og studie av metaller og naturlig organisk materiale i elver på Svalbard. Master's thesis, NTNU, 2014.

[86] Kent C Condie. Chemical composition and evolution of the upper continental crust: contrasting results from surface samples and shales. *Chemical geology*, 104(1-4):1–37, 1993.

[87] K Hans Wedepohl. The composition of the continental crust. *Geochimica et cosmochimica Acta*, 59(7):1217–1232, 1995.

Appendix

The appendix contains additional information related to the sample collection, sample preparation and the results.

Chapter A provides additional information on the experimental, sampling collection and sample preparations of this project. Chapter B provides additional information on the instrumental analysis parameters used in this project. Chapter C provides additional information on the results related to analysis by ICP-MS and the determination of Total carbon (TC) and Total Nitrogen (TN) content in sediment material from Austre Brøggerbreen and Vestre Brøggerbreen. Chapter E provides information of statistical data, as normal distributed data sets, and statistical significance between mean concentrations.

A Experimental

A.1 Sample collection data

Table A.1 provides information about the samples used in this project. There were collected samples such as cryoconite, supraglacial debris, flow sediment, snow and meltwater from the two locoation sites, Austre Brøggerbreen and Vestre Brøggerbreen. The samples were collected in different sample containers as 50 mL PP tube or 30 mL cc-cup. GPS- positions for the collected samples are listed in the table.

Table A.1: Table of sample information as sample material, sample location, container and GPS positions.

Sample ID	Sample type	Sample location	Sampling container	GPS position latitude	GPS position longitude
ABOM1	Supraglacial debris	Austre Brøggerbreen	30 mL cc-cup		
ABOM2	Supraglacial debris	Austre Brøggerbreen	30 mL cc-cup	N 78.894257	E 11.84112
ABOM3	Supraglacial debris	Austre Brøggerbreen	30 mL cc-cup	N 78.894445	E 11.842943
ABOM4	Supraglacial debris	Austre Brøggerbreen	30 mL cc-cup	N 78.894176	E 11.845188
ABOM5	Supraglacial debris	Austre Brøggerbreen	30 mL cc-cup	N 78.894769	E 11.843504
ABOM6	Supraglacial debris	Austre Brøggerbreen	30 mL cc-cup	N 78.894688	E 11.843504
ABOM7	Supraglacial debris	Austre Brøggerbreen	30 mL cc-cup	N 78.890915	E 11.842803
ABOM8	Supraglacial debris	Austre Brøggerbreen	30 mL cc-cup	N 78.891319	E 11.844346
ABOM9	Supraglacial debris	Austre Brøggerbreen	30 mL cc-cup	N 78.891319	E 11.843785
ABOM10	Supraglacial debris	Austre Brøggerbreen	30 mL cc-cup	N 78.891184	E 11.843504
VBOM1	Supraglacial debris	Vestre Brøggerbreen	30 mL cc-cup	N 78.911074	E 11.746142
VBOM2	Supraglacial debris	Vestre Brøggerbreen	30 mL cc-cup	N 78.912045	E 11.731552
VBOM3	Supraglacial debris	Vestre Brøggerbreen	30 mL cc-cup	N 78.912018	E 11.731271
VBOM4	Supraglacial debris	Vestre Brøggerbreen	30 mL cc-cup	N 78.912260	E 11.729868
VBOM5	Supraglacial debris	Vestre Brøggerbreen	30 mL cc-cup	N 78.912260	E 11.729868
VBOM6	Supraglacial debris	Vestre Brøggerbreen	30 mL cc-cup	N 78.910886	E 11.724116
VBOM7	Supraglacial debris	Vestre Brøggerbreen	30 mL cc-cup	N 78.910886	E 11.726922
VBOM8	Supraglacial debris	Vestre Brøggerbreen	30 mL cc-cup	N 78.910940	E 11.727483
VBOM9	Supraglacial debris	Vestre Brøggerbreen	30 mL cc-cup	N 78.911074	E 11.729447
VBOM10 (1-2)	Supraglacial debris	Vestre Brøggerbreen	30 mL cc-cup	N 78.912476	E 11.733095

Sample ID	Sample type	Sample location	Sampling container	GPS position latitude	GPS position longitude
AB1	Sediment	Austre Brøggerbreen	30 mL cc-cup		
AB2	Sediment	Austre Brøggerbreen	30 mL cc-cup		
AB3	Sediment	Austre Brøggerbreen	30 mL cc-cup		
AB4	Sediment	Austre Brøggerbreen	30 mL cc-cup		
AB5	water	Austre Brøggerbreen	50 mL PP tube		
AB6	water	Austre Brøggerbreen	50 mL PP tube		
AB7	water	Austre Brøggerbreen	50 mL PP tube		
AB8F	water	Austre Brøggerbreen	15 mL PP tube		
ABCH1	Cryoconite	Austre Brøggerbreen	30 mL cc-cup		
ABCH2	Cryoconite	Austre Brøggerbreen	30 mL cc-cup		
ABCH3	Cryoconite	Austre Brøggerbreen	30 mL cc-cup		
ABCH4	Cryoconite	Austre Brøggerbreen	30 mL cc-cup		
ABCH5	Cryoconite	Austre Brøggerbreen	30 mL cc-cup		
ABCH6	Cryoconite	Austre Brøggerbreen	30 mL cc-cup		
ABS1	Snow	Austre Brøggerbreen	50 mL PP tube	N 78.894338	E 11.842102
ABS2	Snow	Austre Brøggerbreen	50 mL PP tube	N 78.894311	E 11.84154
ABS3	Snow	Austre Brøggerbreen	50 mL PP tube	N 78.894257	E 11.84112
ABS4	Snow	Austre Brøggerbreen	50 mL PP tube	N 78.894445	E 11.840558
ABS5	Snow	Austre Brøggerbreen	50 mL PP tube	N 78.894445	E 11.842943
ABS6	Snow	Austre Brøggerbreen	50 mL PP tube	N 78.890915	E 11.842803
ABS7	Snow	Austre Brøggerbreen	50 mL PP tube	N 78.891184	E 11.843224
ABS8	Snow	Austre Brøggerbreen	50 mL PP tube	N 78.891184	E 11.843224
ABS9	Snow	Austre Brøggerbreen	50 mL PP tube	N 78.891184	E 11.843224
ABS10	Snow	Austre Brøggerbreen	50 mL PP tube	N 78.891184	E 11.843504

Sample ID	Sample type	Sample location	Sampling container	GPS position latitude	GPS position longitude
VB1	Sediment	Vestre Brøggerbreen	50 mL PP tube		
VB2	Sediment	Vestre Brøggerbreen	50 mL PP tube		
VB3	Sediment	Vestre Brøggerbreen	50 mL PP tube		
VB4	Sediment	Vestre Brøggerbreen	50 mL PP tube		
VB5	water	Vestre Brøggerbreen	50 mL PP tube		
VB6	water	Vestre Brøggerbreen	50 mL PP tube		
VB7	water	Vestre Brøggerbreen	50 mL PP tube		
VB8F	water	Vestre Brøggerbreen	15 mL PP tube		
VBCH1	Cryoconite	Vestre Brøggerbreen	30 mL cc-cup		
VBCH2	Cryoconite	Vestre Brøggerbreen	30 mL cc-cup		
VBCH3	Cryoconite	Vestre Brøggerbreen	30 mL cc-cup		
VBCH4	Cryoconite	Vestre Brøggerbreen	30 mL cc-cup		
VBCH5	Cryoconite	Vestre Brøggerbreen	30 mL cc-cup		
VBS1	Snow	Vestre Brøggerbreen	50 mL PP tube	N 78.912045	E 11.731552
VBS2	Snow	Vestre Brøggerbreen	50 mL PP tube	N 78.911937	E 11.732113
VBS3	Snow	Vestre Brøggerbreen	50 mL PP tube	N 78.912018	E 11.731271
VBS4	Snow	Vestre Brøggerbreen	50 mL PP tube	N 78.912260	E 11.729868
VBS5	Snow	Vestre Brøggerbreen	50 mL PP tube	N 78.912260	E 11.729868
VBS6	Snow	Vestre Brøggerbreen	50 mL PP tube	N 78.910886	E 11.724116
VBS7	Snow	Vestre Brøggerbreen	50 mL PP tube	N 78.910886	E 11.726922
VBS8	Snow	Vestre Brøggerbreen	50 mL PP tube	N 78.910940	E 11.727483
VBS9	Snow	Vestre Brøggerbreen	50 mL PP tube	N 78.911074	E 11.729447
VBS10	Snow	Vestre Brøggerbreen	50 mL PP tube	N 78.912476	E 11.733095

A.2 Sample preparations and analysis techniques

Below is table A.2 where all the samples collected from Austre Brøggerbreen, Vestre Brøggerbreen and the water melting outlets of the glacier systems are presented. This includes also the sampling preparations and analysing techniques that were used for each sample in this project:

Table A.2: Table of sample preparations and analysing techniques that were used for each sample in this project.

Sample ID	Sample type	Temperature [°C]	Conductivity [µS * cm^{-1}]	pH	Freeze drying	Digestion HNO_3	ICP-MS	TC/TN	TOC	UV/vis
AB1	Sediment	n/a	n/a	-	x	x	x	x	-	n/a
AB2	Sediment	n/a	n/a	-	x	x	x	-	-	n/a
AB3	Sediment	n/a	n/a	-	x	x	x	-	-	n/a
AB4	Sediment	n/a	n/a	-	x	x	x	-	-	n/a
AB5	water	0.6	231	7.554	n/a	x	x	-	x	x
AB6	water	0.6	231	7.554	n/a	x	x	-	x	x
AB7	water	0.6	231	7.554	n/a	x	x	-	x	x
ABCH1	Cryoconite	n/a	n/a	-	x	x	x	x	-	n/a
ABCH2	Cryoconite	n/a	n/a	-	x	x	x	x	-	n/a
ABCH3	Cryoconite	n/a	n/a	-	x	x	x	x	-	n/a
ABCH4	Cryoconite	n/a	n/a	-	x	x	x	x	-	n/a
ABCH5	Cryoconite	n/a	n/a	-	x	x	x	x	-	n/a
ABCH6	Cryoconite	n/a	n/a	-	x	x	x	x	-	n/a
ABS1	Snow	-	-	-	n/a	x	x	-	x	x
ABS2	Snow	-	-	-	n/a	x	x	-	x	x
ABS3	Snow	-	-	-	n/a	x	x	-	x	x
ABS1a	Sediment	n/a	n/a	-	x	x	x	-	-	n/a
ABS2a	Sediment	n/a	n/a	-	x	x	x	-	-	n/a
ABS3a	Sediment	n/a	n/a	-	x	x	x	-	-	n/a

Below is a table where all the samples collected from Austre Brøggerbreen, Vestre Brøggerbreen and the water melting outlets of the glacier systems are presented. This includes also the sampling preparations and analysing tecniques that were used for each sample in this project:

Sample ID	Sample type	Temperature [°C]	Conductivity [µS * cm^{-1}]	pH	Freeze drying	Digestion HNO_3	ICP-MS	TC/TN	TOC	UV/vis	
ABOM1	Supraglacial debris	n/a	n/a	-	x	x	x	x	x	-	n/a
ABOM1	Supraglacial debris	n/a	n/a	-	x	x	x	x	x	-	n/a
ABOM2	Supraglacial debris	n/a	n/a	-	x	x	x	x	x	-	n/a
ABOM3	Supraglacial debris	n/a	n/a	-	x	x	x	x	x	-	n/a
ABOM4	Supraglacial debris	n/a	n/a	-	x	x	x	x	x	-	n/a
ABOM5	Supraglacial debris	n/a	n/a	-	x	x	x	x	x	-	n/a
ABOM6	Supraglacial debris	n/a	n/a	-	x	x	x	x	x	-	n/a
ABOM7	Supraglacial debris	n/a	n/a	-	x	x	x	x	x	-	n/a
ABOM8	Supraglacial debris	n/a	n/a	-	x	x	x	x	x	-	n/a
ABOM9	Supraglacial debris	n/a	n/a	-	x	x	x	x	x	-	n/a
ABOM10	Supraglacial debris	n/a	n/a	-	x	x	x	x	x	-	n/a
VB1	Sediment	n/a	n/a	-	x	x	x	x	x	-	n/a
VB2	Sediment	n/a	n/a	-	x	x	x	x	-	-	n/a
VB3	Sediment	n/a	n/a	-	x	x	x	x	-	-	n/a
VB4	Sediment	n/a	n/a	-	x	x	x	x	-	-	n/a
VB5	water	0.6	221	8.465	n/a	x	x	x	-	x	x
VB6	water	0.6	221	8.461	n/a	x	x	x	-	x	x
VBCH1	Cryoconite	n/a	n/a	-	x	x	x	x	x	-	n/a
VBCH2	Cryoconite	n/a	n/a	-	x	x	x	x	x	-	n/a
VBCH3	Cryoconite	n/a	n/a	-	x	x	x	x	x	-	n/a
VBCH4	Cryoconite	n/a	n/a	-	x	x	x	x	x	-	n/a
VBCH5	Cryoconite	n/a	n/a	-	x	x	x	x	x	-	n/a
VBS1	Snow	-	-	-	n/a	x	x	x	-	x	x
VBS2	Snow	-	-	-	n/a	x	x	x	-	x	x
VBS3	Snow	-	-	-	n/a	x	x	x	-	x	x

Below is a table where all the samples collected from Austre Brøggerbreen, Vestre Brøggerbreen and the water melting outlets of the glacier systems are presented. This includes also the sampling preparations and analysing tecniques that were used for each sample in this project:

Sample ID	Sample type	Temperature[^{o}C]	Conductivity [µS * cm^{-1}]	pH	Freeze drying	Digestion HNO_3	TC/TN	TOC	UV/vis
VBS1a	Sediment	n/a	n/a	-	x	x	-	-	n/a
VBS2a	Sediment	n/a	n/a	-	x	x	-	-	n/a
VBS3a	Sediment	n/a	n/a	-	x	x	-	-	n/a
VBOM1	Supraglacial debris	n/a	n/a	-	x	x	x	-	n/a
VBOM2	Supraglacial debris	n/a	n/a	-	x	x	x	-	n/a
VBOM3	Supraglacial debris	n/a	n/a	-	x	x	x	-	n/a
VBOM4	Supraglacial debris	n/a	n/a	-	x	x	x	-	n/a
VBOM5	Supraglacial debris	n/a	n/a	-	x	x	x	-	n/a
VBOM6	Supraglacial debris	n/a	n/a	-	x	x	x	-	n/a
VBOM7	Supraglacial debris	n/a	n/a	-	x	x	x	-	n/a
VBOM8	Supraglacial debris	n/a	n/a	-	x	x	x	-	n/a
VBOM9	Supraglacial debris	n/a	n/a	-	x	x	x	-	n/a
VBOM10	Supraglacial debris	n/a	n/a	-	x	x	x	-	n/a
VBOM10	Supraglacial debris	n/a	n/a	-	x	x	x	-	n/a

Below is table A.3 of the snow samples merged for $SUVA_{254}$ analysis.

Table A.3: Table of samples merged for $SUVA_{254}$ analysis and ICP-MS analysis

Sample ID				
VBS1:	VeS1	VeS4	VeS10	
VBS2:	VeS6	VeS9	VeS2	
VBS3:	VeS3	VeS8	VeS7	VeS5
ABS1:	ABS1	ABS8	ABS6	
ABS2:	ABS3	ABS9	ABS7	
ABS3:	ABS2	ABS4	ABS10	ABS5

Figure A.1 visually presents the samples ABS 7, 8 and 9, and the colour of the snow samples.

Figure A.1: Snow samples ABS 7, ABS 8, and ABS 9, collected on Austre Brøggerbreen. The colour of the snow is clearly more yellow compared with the other snow samples collected on Austre Brøggerbreen And Vestre Brøggerbreen.

Figure A.2 illustrates the temperature profile of microwave-assisted digestion.

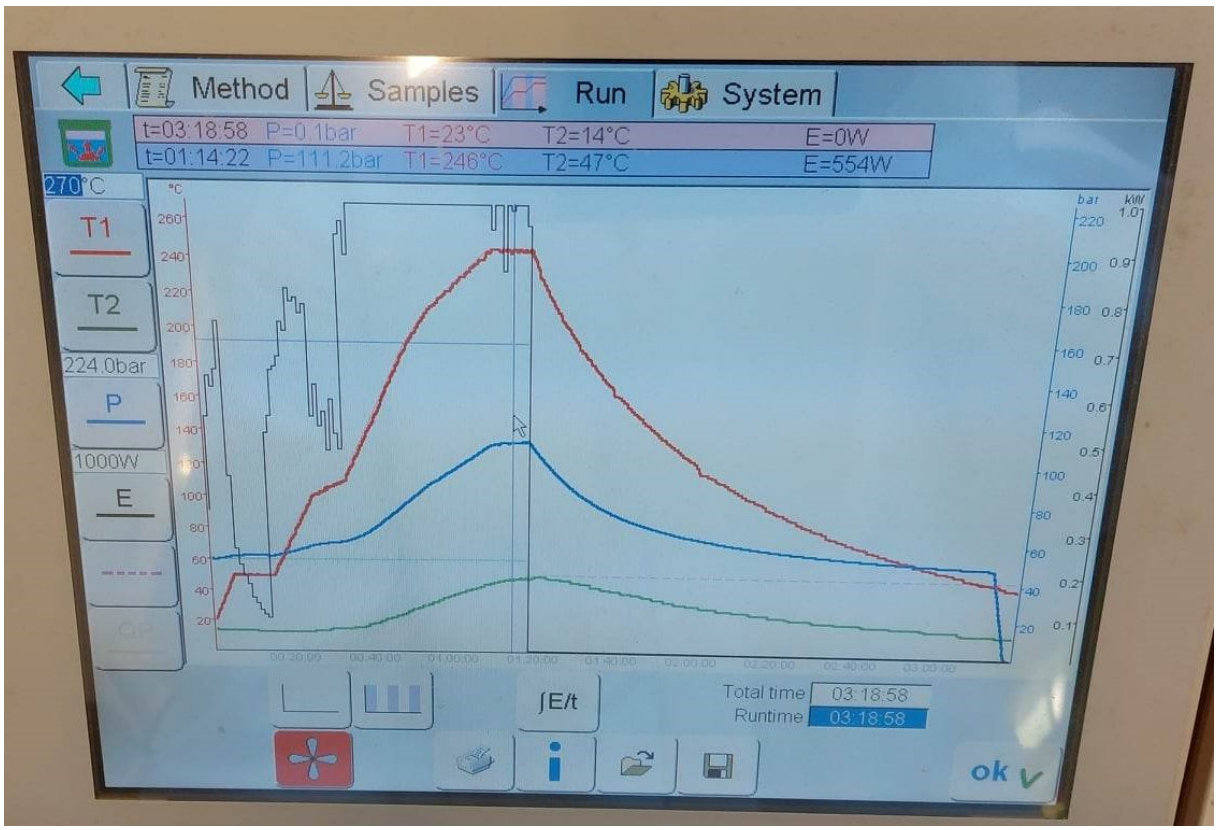

Figure A.2: Temperature profile of the microwave-assisted digestion by using Milestone UltraCLAVE. The y-axis indicates the temperature [°C], while the x-axis indicates the run time.

B Analysis

B.1 Element analysis by Inductively coupled plasma mass spectrometry (ICP-MS)

Elemental composition of the sediment and water samples was analysed using 8800 Triple Quadrupole inductive coupled plasma mass spectrometry (ICP-MS) system (Agilent, USA) equipped with prepFAST M5 autosampler (ESI, USA). The System parameters during analysis for the water and snow samples are listed in table B.1 and for the cryoconite, supraglacial debris, and flow sediment samples are listed in table B.2.

Table B.1: ICP-MS system parameters, element analysis using 8800 Triple Quadrupole inductively coupled plasma mass spectrometry (ICP-MS) system (Agilent, USA), for the water and snow samples.

Tune Mode	Scan Type	Q1	Q2	Name	R	b (blank)	DL	BEC	Units
No Gas	MS/MS	7	7	Li	0.99997	1.96E-03	1.66E-03	2.16E-02	ug/l
No Gas	MS/MS	9	9	Be	1.00000	1.16E-06	2.40E-04	6.17E-05	ug/l
O2	MS/MS	23	23	Na	0.99986	1.47E-01	1.10E-01	2.08E+00	ug/l
O2	MS/MS	24	24	Mg	0.99996	1.34E-02	1.89E-02	8.02E-02	ug/l
H2	MS/MS	27	27	Al	0.99999	2.71E-03	5.71E-03	5.54E-02	ug/l
O2	MS/MS	28	44	Si	1.00000	2.37E-01	5.46E-01	4.04E+00	ug/l
O2	MS/MS	31	47	P	0.99998	1.06E-03	3.45E-02	5.18E-02	ug/l
O2	MS/MS	32	48	S	0.99999	4.42E-02	1.66E-01	1.11E+00	ug/l
O2	MS/MS	39	39	K	0.99998	1.95E-01	5.51E-02	1.73E+00	ug/l
H2	MS/MS	40	40	Ca	1.00000	1.37E-02	1.25E-02	1.38E-01	ug/l
O2	MS/MS	45	61	Sc	0.99973	1.03E-04	1.62E-04	1.09E-04	ug/l
O2	MS/MS	47	63	Ti	0.99934	1.59E-04	8.62E-03	2.45E-03	ug/l
O2	MS/MS	51	67	V	0.99999	6.99E-04	6.16E-04	7.72E-04	ug/l
O2	MS/MS	52	52	Cr	0.99978	1.34E-02	7.59E-03	1.21E-01	ug/l
O2	MS/MS	55	55	Mn	1.00000	2.76E-03	2.80E-03	1.45E-02	ug/l
H2	MS/MS	56	56	Fe	0.99999	9.99E-03	6.01E-03	6.74E-02	ug/l
O2	MS/MS	59	59	Co	0.99999	1.51E-03	1.12E-03	1.17E-02	ug/l
H2	MS/MS	60	60	Ni	0.99996	8.48E-04	7.57E-03	3.69E-02	ug/l
O2	MS/MS	63	63	Cu	0.99861	5.18E-03	2.27E-02	6.65E-02	ug/l
H2	MS/MS	66	66	Zn	0.99997	3.21E-04	8.18E-03	2.00E-02	ug/l
O2	MS/MS	75	91	As	1.00000	1.86E-04	1.27E-03	1.62E-03	ug/l
H2	MS/MS	78	78	Se	0.99998	6.86E-05	2.02E-02	2.21E-02	ug/l
O2	MS/MS	81	81	Br	0.99992	1.93E-04	1.75E-01	2.38E-01	ug/l
O2	MS/MS	85	85	Rb	0.99990	1.95E-03	1.56E-03	7.82E-03	ug/l
H2	MS/MS	88	88	Sr	0.99999	3.83E-04	3.73E-04	1.56E-03	ug/l
O2	MS/MS	89	105	Y	0.99975	6.50E-05	1.16E-04	2.96E-05	ug/l
O2	MS/MS	95	127	Mo	0.99998	1.41E-04	7.84E-04	6.50E-04	ug/l
O2	MS/MS	111	111	Cd	0.99987	9.98E-06	3.94E-04	1.04E-04	ug/l
O2	MS/MS	118	118	Sn	0.99999	4.36E-04	8.78E-04	1.48E-03	ug/l
O2	MS/MS	121	137	Sb	0.99998	2.77E-05	2.75E-04	1.06E-04	ug/l
O2	MS/MS	137	137	Ba	1.00000	1.50E-04	1.30E-03	1.03E-03	ug/l
O2	MS/MS	202	202	Hg	0.99984	4.35E-04	8.58E-03	9.87E-03	ug/l
H2	MS/MS	205	205	Tl	0.99997	1.38E-04	5.87E-04	6.59E-04	ug/l
O2	MS/MS	208	208	Pb	0.99999	4.82E-03	1.08E-03	7.76E-03	ug/l
H2	MS/MS	209	209	Bi	0.99999	1.48E-05	1.82E-04	7.05E-05	ug/l
H2	MS/MS	232	232	Th	0.99999	1.17E-06	3.12E-05	6.01E-06	ug/l
H2	MS/MS	238	238	U	0.99997	5.80E-07	1.87E-05	3.60E-06	ug/l

Table B.2: ICP-MS system parameters, element analysis using 8800 Triple Quadrupole inductively coupled plasma mass spectrometry (ICP-MS) system (Agilent, USA), for the cryoconite, supraglacial debris, and flow sediment samples.

Tune Mode	Scan Type	Q1	Q2	Name	R	b (blank)	DL	BEC	Units
No Gas	MS/MS	7	7	Li	0.99999	2.77E-03	2.80E-04	1.67E-02	ug/l
No Gas	MS/MS	9	9	Be	0.99996	0.00E+00	0.00E+00	0.00E+00	ug/l
O2	MS/MS	23	23	Na	0.99999	1.30E-01	6.07E-02	1.10E+00	ug/l
O2	MS/MS	24	24	Mg	0.99995	1.69E-03	8.03E-03	2.15E-02	ug/l
H2	MS/MS	27	27	Al	0.99995	8.48E-04	1.90E-02	2.39E-02	ug/l
O2	MS/MS	28	44	Si	1.00000	1.90E-01	2.48E-01	2.89E+00	ug/l
O2	MS/MS	31	47	P	0.99997	2.61E-03	1.66E-02	9.29E-02	ug/l
O2	MS/MS	32	48	S	0.99999	4.42E-02	1.03E-01	7.79E-01	ug/l
O2	MS/MS	39	39	K	0.99998	1.39E-01	8.56E-02	1.21E+00	ug/l
H2	MS/MS	40	40	Ca	0.99997	5.22E-03	1.47E-02	4.80E-02	ug/l
O2	MS/MS	45	61	Sc	0.99999	7.98E-05	7.71E-05	7.34E-05	ug/l
O2	MS/MS	47	63	Ti	0.99998	1.59E-05	1.08E-03	2.08E-04	ug/l
O2	MS/MS	51	67	V	0.99993	6.72E-04	1.03E-03	6.37E-04	ug/l
O2	MS/MS	52	52	Cr	0.99999	7.31E-04	1.62E-03	5.23E-03	ug/l
O2	MS/MS	55	55	Mn	0.99999	1.40E-03	2.79E-03	6.13E-03	ug/l
H2	MS/MS	56	56	Fe	0.99994	9.83E-03	1.27E-02	5.53E-02	ug/l
O2	MS/MS	59	59	Co	1.00000	5.49E-04	1.37E-03	2.92E-03	ug/l
O2	MS/MS	60	60	Ni	1.00000	1.10E-04	3.17E-03	3.81E-03	ug/l
O2	MS/MS	63	63	Cu	0.99996	1.01E-03	1.32E-03	1.59E-02	ug/l
H2	MS/MS	66	66	Zn	0.99999	2.71E-04	1.22E-02	1.44E-02	ug/l
O2	MS/MS	75	91	As	0.99995	0.00E+00	0.00E+00	0.00E+00	ug/l
H2	MS/MS	78	78	Se	0.99997	0.00E+00	0.00E+00	0.00E+00	ug/l
O2	MS/MS	79	79	Br	0.99998	2.50E-03	1.13E-01	2.12E-01	ug/l
O2	MS/MS	85	85	Rb	0.99997	5.46E-03	1.46E-03	3.70E-03	ug/l
H2	MS/MS	88	88	Sr	0.99999	2.76E-04	2.40E-03	8.50E-04	ug/l
O2	MS/MS	89	105	Y	0.99999	0.00E+00	0.00E+00	0.00E+00	ug/l
O2	MS/MS	101	101	Ru	0.99993	1.01E-04	4.60E-04	1.86E-03	ug/l
O2	MS/MS	111	111	Cd	0.99993	0.00E+00	0.00E+00	0.00E+00	ug/l
O2	MS/MS	118	118	Sn	0.99999	1.32E-04	7.88E-04	1.79E-03	ug/l
O2	MS/MS	121	121	Sb	0.99995	0.00E+00	0.00E+00	0.00E+00	ug/l
O2	MS/MS	137	137	Ba	1.00000	4.41E-06	2.80E-04	1.08E-04	ug/l
O2	MS/MS	202	202	Hg	0.99998	4.23E-04	6.92E-03	1.83E-02	ug/l
H2	MS/MS	205	205	Tl	0.99902	6.77E-04	4.77E-04	2.66E-03	ug/l
O2	MS/MS	208	208	Pb	1.00000	1.75E-03	1.00E-03	4.60E-03	ug/l
O2	MS/MS	209	209	Bi	0.99999	3.54E-04	3.25E-04	1.13E-03	ug/l
H2	MS/MS	232	232	Th	0.99999	6.72E-06	6.29E-05	1.21E-05	ug/l
H2	MS/MS	238	238	U	0.99999	0.00E+00	0.00E+00	0.00E+00	ug/l

C Results

C.1 ICP-MS

ICP-MS measured concentrations of selected elements in supraglacial debris (sgd), supraglacial debris collected from snow (sgd-s), flow sediment (fs), cryoconite (ch), snow and meltwater (w) samples are presented in tables in this chapter. Table C.1 contains concentrations for meltwater and snoe samples, table C.2 contains concentrations for supraglacial debris samples, and table C.1 contains concentrations for cryoconite, flow sediment and supraglacial debris samples collected from snow. Concentration of cryoconite, supraglacial debris (sgd and sgd-s) and flow sediment samples were measured in µg/g, while snow and meltwater samples were measured µg/L.

Table C.1: ICP-MS measured concentrations of selected elements in snow and meltwater (w) samples. Concentration of snow and meltwater samples were measured in µg/L.

Sample material	Sample ID	Na	Mg	Al	Ca	Fe	Zn	As	Cd	Pb
w	VBW	1689.3532	7349.9165	2.5063	29589.2630	0.3507	0.6312	0.0743	0.0035	0.0004
w	ABW	1585.1823	8734.7251	1.9839	27710.2507	0.3777	0.0634	0.0706	0.0055	0.0005
snow	VBS1	15.6464	11.7348	5.5556	46.0072	13.5847	1.0624	0.0097	0.0001	0.2927
snow	VBS2	206.1962	91.4942	3.3403	259.9035	18.2831	2.8861	0.0089	0.0045	0.0798
snow	VBS3	23.2541	14.0592	4.4992	31.5413	9.0021	0.9669	0.0110	0.0001	0.2224
snow	VBS4	125.6306	33.7601	10.5987	40.6920	50.0082	2.8013	0.0567	0.0013	2.6877
snow	VBS5	29.9279	16.6690	0.9838	35.7273	3.6265	2.2888	0.0061	0.0007	0.1862
snow	VBS6	132.5135	75.3487	7.6564	110.0705	18.4877	2.0054	0.0772	0.0020	0.6660
snow	VBS7	45.8750	29.4831	1.7736	38.9253	2.5389	1.2822	0.0438	0.0007	0.1109
snow	VBS8	38.8881	58.8000	3.7719	93.9705	13.8278	2.6694	0.0558	0.0027	0.5285
snow	VBS9	246.7035	39.3483	4.3999	54.3032	10.9205	2.5940	0.0309	0.0017	0.2144
snow	VBS10	64.5448	60.2999	5.3213	250.4928	8.1572	17.8292	0.0452	0.0028	0.2147
snow	ABS1	97.0320	10.8854	5.3138	38.0426	8.0811	0.8170	0.0338	0.0001	0.0138
snow	ABS2	104.1916	26.7752	11.2965	37.3510	67.9167	3.1675	0.0488	0.0011	0.6597
snow	ABS3	197.4750	30.5579	1.9362	41.0822	5.3680	2.8492	0.0274	0.0013	0.0153
snow	ABS4	123.6521	19.5799	5.3836	25.2471	15.4863	2.4892	0.0374	0.0006	0.0965
snow	ABS5	102.8504	32.3662	1.7876	55.3633	5.7123	4.4821	0.0191	0.0027	0.0126
snow	ABS6	68.9019	91.7871	2.9247	172.1943	4.9007	3.8852	0.0377	0.0058	0.0176
snow	ABS7	38.8559	178.1550	4.0697	355.9719	7.6396	2.7472	0.0829	0.0082	0.0329
snow	ABS8	43.4076	78.5011	5.9803	128.9758	25.8803	3.3709	0.1123	0.0041	0.0470
snow	ABS9	20.7937	91.0072	8.4188	101.7956	62.9548	3.9449	0.0954	0.0047	0.8041
snow	ABS10	109.8772	85.7039	3.3432	192.2545	8.3761	4.8451	0.0533	0.0030	0.0667

Table C.2: ICP-MS measured concentrations of selected elements in supraglacial debris samples (sgds). Concentration of supraglacial debris (sgd) samples were measured in µg/g.

Sample material	Sample ID	Na	Mg	Al	Ca	Fe	Zn	As	Cd	Pb
sgd	VBOM1	658.5351	9145.8312	40067.3558	1584.7502	33673.9994	79.0649	8.4410	0.0681	71.4553
sgd	VBOM2	711.6228	9231.0839	41743.4593	1676.9020	34588.7883	80.7219	9.3741	0.0962	75.1061
sgd	VBOM3	675.0014	9088.1480	41046.8745	1585.5562	33358.1525	76.4255	9.5901	0.0620	71.6459
sgd	VBOM4	560.5329	8240.6110	36644.1324	1394.9412	30537.5032	69.8127	7.1173	0.0642	56.9430
sgd	VBOM5	697.9810	8841.1146	39675.6373	1553.5074	31737.6978	76.1511	8.5756	0.0850	80.0868
sgd	VBOM6	687.4024	8604.5516	39550.8793	1781.3997	32032.3013	73.9587	9.1253	0.0898	67.9509
sgd	VBOM7	656.7346	8841.9423	38167.0730	1954.3414	32380.5643	77.2666	8.4532	0.0742	67.5087
sgd	VBOM8	655.6331	8733.8323	38827.3615	1647.2032	32617.8021	77.8851	8.4488	0.0667	71.0562
sgd	VBOM9	619.5154	8364.3164	37000.8098	1623.5145	31586.6978	73.7285	7.7717	0.0535	65.1786
sgd	VBOM10	655.5966	8872.8486	39838.4334	1523.1547	32288.9880	74.2663	8.3910	0.0649	58.8034
sgd	ABOM 1	889.6714	12792.6216	45975.2874	3592.4891	38787.2375	100.5043	12.0938	0.1489	105.2746
sgd	ABOM 2	917.8011	16411.1565	42946.8661	8181.6850	53547.9983	94.3730	2.5998	0.0798	27.5952
sgd	ABOM 3	676.9213	13474.2463	40786.8737	4334.0700	45868.0796	92.7698	7.2182	0.1490	32.3449
sgd	ABOM 4	461.7830	11988.2799	32527.8451	5155.0264	39190.0746	72.8407	2.0344	0.1142	22.2636
sgd	ABOM 5	790.6647	14111.0874	43421.1059	4250.5322	49688.9189	100.6833	5.4336	0.0846	40.8812
sgd	ABOM 6	788.8300	13959.2852	42869.4298	4431.3184	47839.9687	92.6944	6.0141	0.0938	37.7418
sgd	ABOM 7	685.8971	14328.2020	47541.8963	5652.9350	48932.7171	94.3285	4.0866	0.1039	33.6764
sgd	ABOM 8	750.6162	14982.0181	46716.2803	5936.8327	48234.4340	102.1892	4.5944	0.0810	33.5142
sgd	ABOM 9	752.5990	15645.2791	48110.8750	5908.8901	49353.0339	102.1130	4.5119	0.1049	37.2661
sgd	ABOM 10	772.8694	14715.5535	49012.8913	6195.0294	47644.1593	97.4614	4.1580	0.0519	32.9192

Table C.3: ICP-MS measured concentrations of selected elements in cryoconite (ch), supraglacial debris collected from snow (sgd-s), and flow sediment (fs). Concentration were measured in µg/g.

Sample material	Sample ID	Na	Mg	Al	Ca	Fe	Zn	As	Cd	Pb
ch	VBCH 1	587.7447	8753.7519	37367.1900	1538.7166	32510.4446	73.0140	8.2296	0.0684	61.0169
ch	VBCH 2	604.3620	8909.0492	41040.3555	1575.0909	33591.5891	76.9966	7.9857	0.0434	63.3942
ch	VBCH 3	561.2122	8546.8147	36094.2419	1569.4943	31395.8434	75.2731	8.5166	0.0853	62.8930
ch	VBCH 4	629.7099	8634.2212	38078.4393	1563.4295	31997.9150	75.4560	8.1888	0.0841	72.8341
ch	VBCH5	594.6326	9356.3381	39495.1183	1663.2399	32972.2837	75.2680	8.3746	0.0757	61.0188
ch	ABCH 1	803.3879	14019.5186	40975.9281	5037.1580	46477.3204	97.0410	5.2335	0.0774	35.5770
ch	ABCH 2	581.3085	14959.7203	40111.2452	4152.3245	48777.3710	97.5420	4.4481	0.0719	33.7610
ch	ABCH 3	752.3247	13734.0498	42558.9937	4245.7883	45852.9155	88.8606	4.2547	0.1290	30.5942
ch	ABCH 4	767.7140	14383.4042	42815.5112	3890.9344	48623.2897	100.7238	5.7636	0.0791	37.6488
ch	ABCH 5	618.2394	14405.1018	45162.5965	5657.8333	48656.2514	98.1359	4.3559	0.1120	35.4752
ch	ABCH 6	675.3533	13166.7921	45846.8595	4774.4341	45237.8607	87.7302	38.4445	0.0771	33.2829
fs	VB1	200.5371	40595.1332	9425.7681	133873.4013	8727.3192	33.4133	3.4837	0.2802	4.0582
fs	VB2	209.9142	33276.5346	11953.5370	110413.0547	9563.6460	42.4579	2.6988	0.2525	4.1963
fs	VB3	203.2812	35246.7351	10474.9906	111964.0941	8522.1392	38.1567	2.7125	0.2556	3.9648
fs	VB4	197.8013	46557.3813	9293.1110	127956.9804	9102.9813	35.0928	3.2613	0.2584	4.1106
fs	AB 1	446.9953	6186.2449	31818.8239	7448.3196	26990.8525	47.3525	5.6154	0.0490	14.8559
fs	AB 2	449.2019	6676.7277	33301.8805	8415.1372	29267.4489	52.3633	4.8209	0.0461	18.2125
fs	AB 3	286.1142	5742.7194	23700.1176	7412.6380	25330.7480	48.3391	4.3840	0.0490	11.7263
fs	AB 4	313.5488	5892.9744	25149.8200	8232.1753	27511.9340	44.8592	5.4527	0.0504	15.9594
sgd s	VBSG1	518.1237	8398.6454	35072.6192	1476.3938	29893.5340	70.0267	7.1829	0.0535	50.0289
sgd s	VBSG2	689.9883	8658.3011	38822.6652	1871.1869	32764.9454	79.4782	8.6838	0.0666	68.0664
sgd s	VBSG3	609.4998	8744.9448	36281.8458	2154.9695	31976.6281	74.8942	8.4159	0.0653	61.8914
sgd s	ABSG1	640.6191	15758.6657	45782.0892	3706.5062	53652.8214	99.9992	2.7932	0.0935	34.8079
sgd s	ABSG2	738.0364	16510.5162	49216.8179	3393.1282	56781.4117	105.0138	2.6299	0.0877	40.2062
sgd s	ABSG3	650.9957	14606.9066	43257.2494	4903.1576	46498.5838	93.6897	4.1930	0.1283	31.0367

C.2 TC/TN

Below is table C.4 of the measured samples from batch 1 for TC/TN analysis. Where TC (%) and TN (%) are indicating the persentage concentrations in the sample.

Table C.4: Table of measured samples from batch 1, for TC/TN analysis

Place no.	Sample ID (parallel)	Weight [mg]	TC (%)	TN (%)
1	Standard Glycine	6.39	34.224	17.312
2	Standard Glycine	11.36	33.539	19.004
3	Standard Glycine	20.76	32.439	18.399
4	Standard Glycine	41.02	31.227	18.737
5	Standard Glycine	79.70	31.623	18.774
6	Standard Glycine	122.09	32.036	18.734
7	Standard Glycine	161.70	32.103	18.588
8	VB CH 1 (1)	90.74	2.719	0.228
9	VB CH 2 (1)	91.70	3.517	0.252
10	VB CH 3 (1)	90.84	3.212	0.234
11	VB CH 4 (1)	91.63	3.996	0.298
12	VB CH 5 (1)	90.45	1.523	0.115
13	AB CH 1	91.27	1.340	0.111
14	AB CH 2	91.73	1.165	0.102
15	AB CH 3	91.10	0.959	0.091
16	AB CH 4	91.88	1.839	0.150
17	AB CH 5	100.18	1.352	0.129
18	AB CH 6	94.67	1.643	0.143
19	VB CH 1 (2)	93.06	2.651	0.214
20	VB CH 2 (2)	90.59	3.527	0.276
21	VB CH 3 (2)	92.17	3.099	0.256
22	VB CH 4 (2)	90.83	3.735	0.309
23	VB CH 5 (2)	96.11	2.422	0.205

Below is table C.5 of the measured samples from batch 2 for TC/TN analysis. Where TC (%) and TN (%) are indicating the persentage concentrations in the sample.

Table C.5: Table of measured samples from batch 2, for TC/TN analysis

Place no.	Sample ID (parallel)	Weight [mg]	TC (%)	TN (%)
1	Standard Glycine	6.48	34.692	18.891
2	Standard Glycine	11.83	32.655	18.204
3	Standard Glycine	19.92	32.683	18.551
4	Standard Glycine	42.23	31.376	18.671
5	Standard Glycine	80.59	31.527	18.748
6	Standard Glycine	120.31	32.086	18.708
7	Standard Glycine	160.80	32.095	18.612
8	VBOM1	84.15	4.040	0.299
9	VBOM2	81.24	3.744	0.267
10	VBOM3	88.53	3.636	0.268
11	VBOM4	94.10	2.673	0.202
12	VBOM5	86.03	4.372	0.312
13	VBOM6	92.76	3.037	0.227
14	VBOM7	89.08	2.765	0.214
15	VBOM8	86.87	3.989	0.302
16	VBOM9	90.95	3.241	0.235
17	VBOM10(1)	86.92	2.993	0.224
18	VBOM10(2)	84.93	2.762	0.211
19	VB1	82.95	6.510	0.019
20	ABOM1	82.52	3.314	0.268
21	ABOM2	86.05	0.992	0.074
22	ABOM3	88.59	1.185	0.088
23	ABOM4	84.01	0.622	0.038
24	ABOM5	83.21	2.322	0.141
25	ABOM6	83.51	2.323	0.135
26	ABOM7	81.13	1.394	0.082
27	ABOM8	81.55	1.634	0.094
28	ABOM9	90.73	1.782	0.205
29	ABOM10	97.84	1.232	0.071
30	AB1	80.12	0.496	<LOD

Calibration curves were made out of measured glycine (carbon content 32.00%, nitrogen content 18.66%) as calibration standard material for each TC/TN batch. The standard Calibration curves for determination of TC [mg] and TN [mg] for batch one are plotted in figures C.1 and C.2, respectively. The standard Calibration curves for determination of TC [mg] and TN [mg] for batch two are plotted in figures C.3 and C.4, respectively.

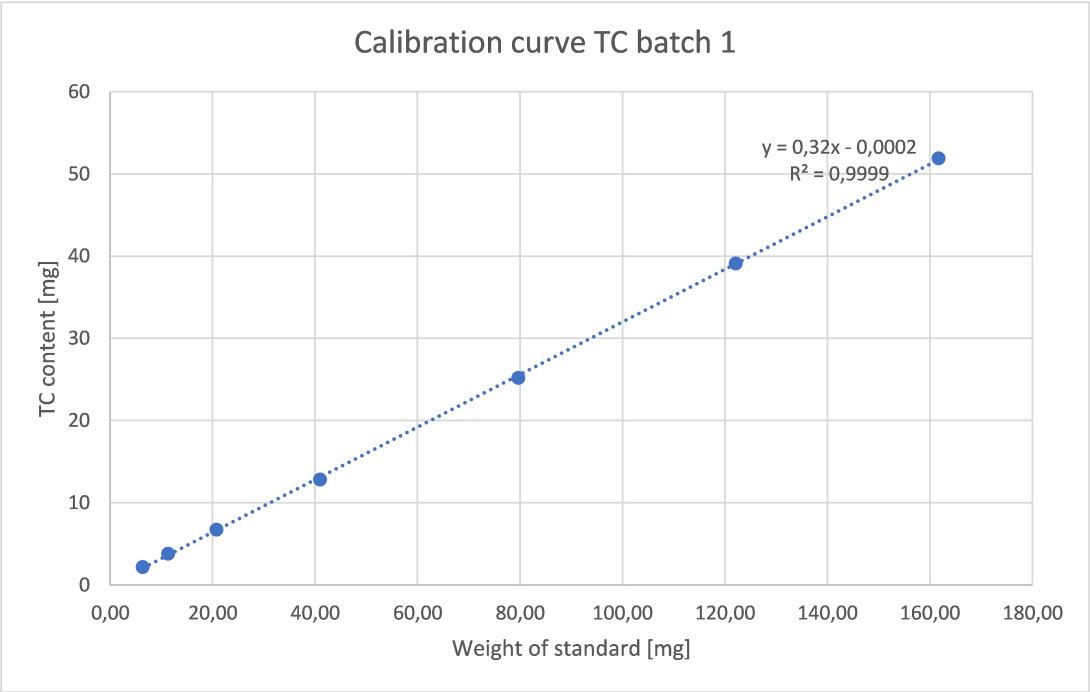

Figure C.1: Standard Calibration curve for determination of TC [mg], batch 1. The measured weight of standard [mg] is plotted as a function of total carbon [mg]. Linear regression line: $y = 0.32x + 0.0002$, and $R^2 = 0.9999$.

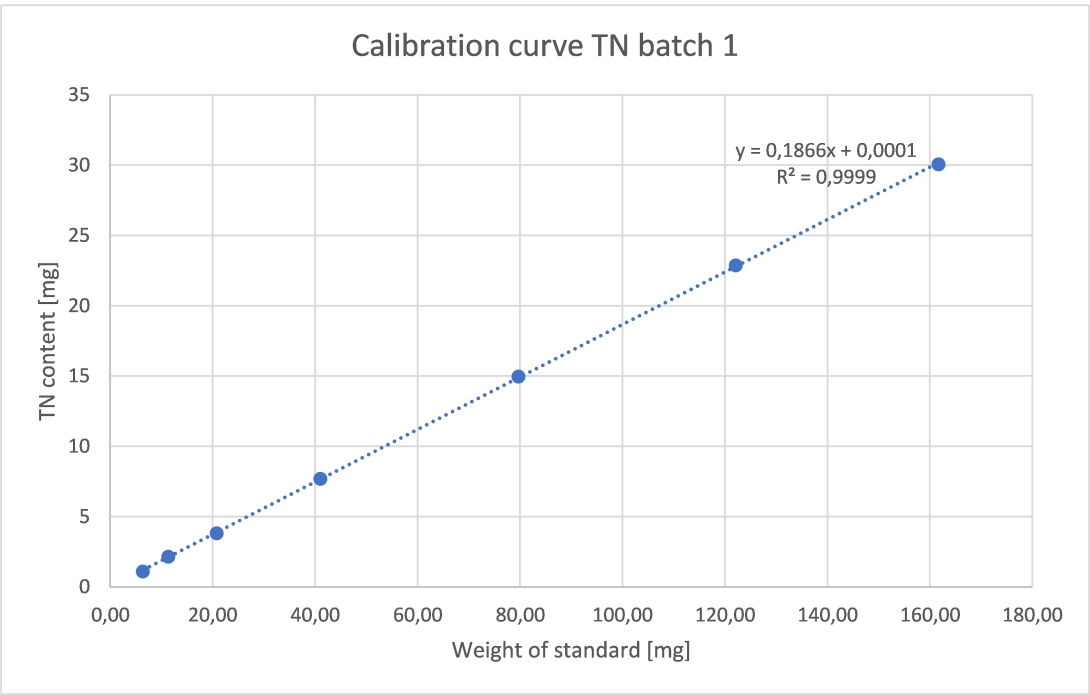

Figure C.2: Standard Calibration curve for determination of TN [mg], batch 1. The measured weight of standard [mg] is plotted as a function of total nitrogen [mg]. Linear regression line: $y = 0.8166x + 0.0001$, and $R^2 = 0.9999$.

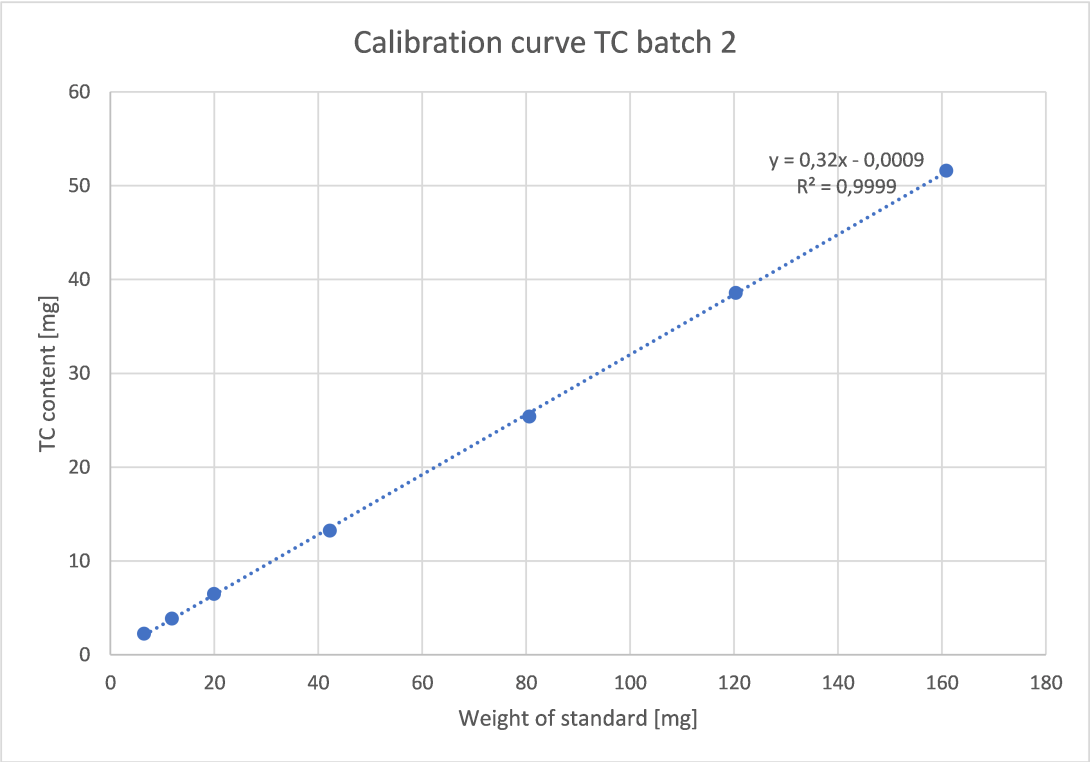

Figure C.3: Standard Calibration curve for determination of TC [mg], batch 2. The measured weight of standard [mg] is plotted as a function of total carbon [mg]. Linear regression line: $y = 0.32x + 0.0009$, and $R^2 = 0.9999$.

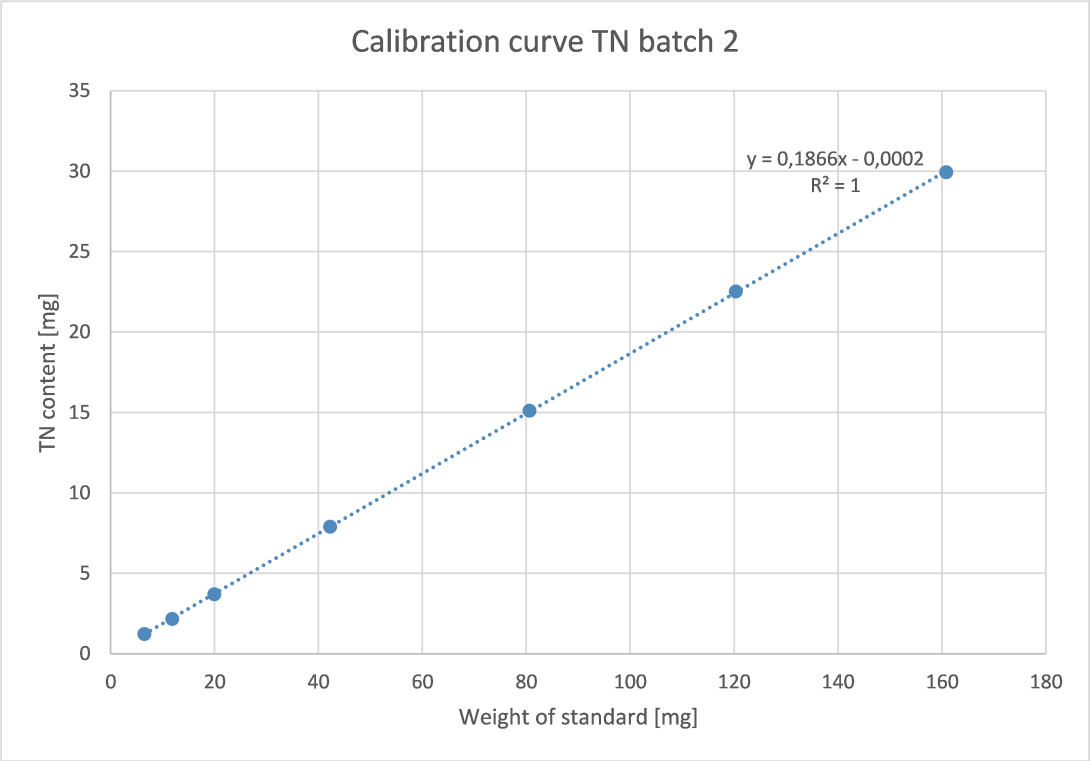

Figure C.4: Standard Calibration curve for determination of TN [mg], batch 2. The measured weight of standard [mg] is plotted as a function of total nitrogen [mg]. Linear regression line: $y = 0.8166x + 0.0001$, and $R^2 = 1$.

D Principal component analysis

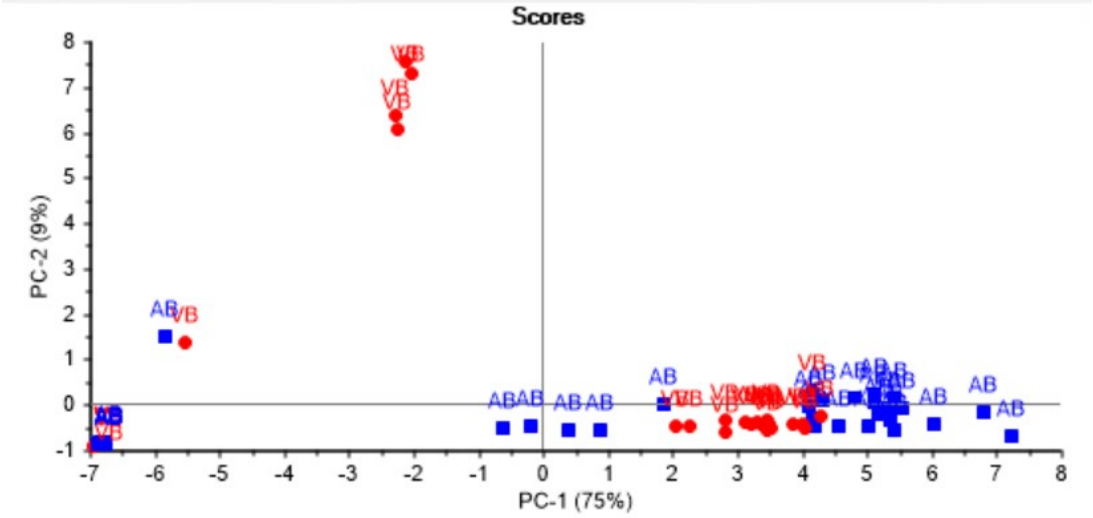

Figure D.1: PC 1 makes up 75 % of the total variance, and PC 2 makes up 9 % of the total variance. Principal component analysis (PCA) scores plot of all samples and components.

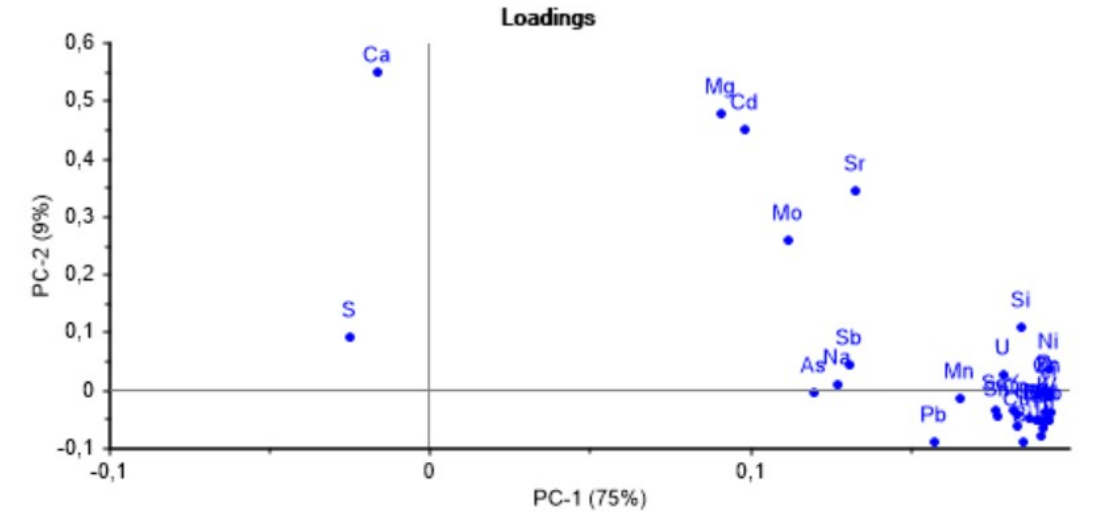

Figure D.2: Principal component analysis (PCA) loadings plot of all samples and components. PC 1 makes up 75 % of the total variance, and PC 2 makes up 9 % of the total variance

E Statistical data

In this chapter results of statistical data from the data sets are listed in tables.

E.1 Testing for normal distribution

The data sets were tested for normal distribution using Shapiro- Wilk test. The significance level was set to $p < 0.05$. Below is table E.1 and E.2 of the mean concentrations of the elements, and total carbon and total nitrogen, from samples collected at Austre Brøggerbreen and Vestre brøggerbreen. The p-values in bold font are not normal distributed.

Table E.1: p- values from testing for normal distribution of mean concentrations of the elements, Na, Mg, Al, Ca, Fe, Zn, As, Cd and Pb in snow, cryoconite, supraglacial debris and flow sediment from Austre Brøggerbreen and Vestre Brøggerbreen, using a Shapiro-Wilk test.

Element	Sample material	Austre Brøggerbreen	Vestre Brøggerbreen
Na	Snow	0.5008	0.06891
	Cryoconite	0.7005	0.9999
	Supraglacial debris	0.2180	0.1831
	Supraglacial debris s	0.3244	1.000
	Flow sediment	0.1766	0.9478
Mg	Snow	0.0772	0.4558
	Cryoconite	0.9980	0.4902
	Supraglacial debris	1.000	0.717
	Supraglacial debris s	1.000	0.8308
	Flow sediment	0.8764	0.8989
Al	Snow	0.2948	0.6546
	Cryoconite	0.7809	0.9998
	Supraglacial debris	1.000	0.9818
	Supraglacial debris s	0.07432	0.8436
	Flow sediment	0.4169	0.4924
Ca	Snow	**0.03134**	**0.003251**
	Cryoconite	0.8339	0.1288
	Supraglacial debris	0.457	0.6053
	Supraglacial debris s	0.6738	1.000
	Flow sediment	0.224	0.3932
Fe	Snow	**0.001789**	**0.05642**
	Cryoconite	0.1173	1.000
	Supraglacial debris	0.08141	0.9908
	Supraglacial debris s	0.9611	0.9021
	Flow sediment	1.000	0.9808

Element	Sample material	Austre Brøggerbreen	Vestre Brøggerbreen
Zn	Snow	0.7116	**0.00005764**
	Cryoconite	0.1563	0.4884
	Supraglacial debris	**0.006208**	0.9641
	Supraglacial debris s	1.000	1.000
	Flow sediment	0.9909	0.9614
As	Snow	0.1768	0.2277
	Cryoconite	**0.001265**	0.9999
	Supraglacial debris	0.0799	0.5389
	Supraglacial debris s	0.319	0.5612
	Flow sediment	0.801	0.3094
Cd	Snow	0.6121	0.4398
	Cryoconite	0.05796	0.2709
	Supraglacial debris	0.5173	0.4115
	Supraglacial debris s	0.4335	0.3055
	Flow sediment	0.5306	0.1593
Pb	Snow	**0.0003348**	**0.0001589**
	Cryoconite	0.986	**0.03713**
	Supraglacial debris	**0.0002317**	0.8617
	Supraglacial debris s	1.000	0.9937
	Flow sediment	1.000	1.000

Table E.2: p- values from testing for normal distribution of mean concentrations of total carbon and total nitrogen in cryoconite and supraglacial debris from Austre Brøggerbreen and Vestre Brøggerbreen, using a Shapiro-Wilk test.

Sample	Sample material	Austre Brøggerbreen	Vestre Brøggerbreen
TC (%)	Cryoconite	0.9864	0.6992
	Supraglacial debris	0.6203	0.3038
TN (%)	Cryoconite	0.8426	0.3996
	Supraglacial debris	0.1328	0.1643

E.2 Testing for statistical significance

Student t -test were used to compare two means which were normal distributed, to test for statistical significance. Where data sets were non-normal distributed, the Mann-Whitney U test was used to compare the mean concentrations. The significance level was set to $p < 0.05$. Below is table E.3 with the p-values from the mean concentrations of the elements in the samples collected at Austre Brøggerbreen and Vestre brøggerbreen. Table E.4 is listing the p-values of TC % and TN % mean concentrations, for statistical significance. Table E.5 is listing the p-values of TC % and TN % mean concentrations, for statistical significance, between the different samples materials, cryoconite and supraglacial debris, collected on the same gracier system, Austre Brøggerbreen or Vestre Brøggerbreen. The p-values in bold font denote a significant difference between the mean concentrations.

Table E.3: p- values from testing for a statistically significant difference between two mean concentrations of the elements, Na, Mg, Al, Ca, Fe, Zn, As, Cd and Pb in samples of snow, cryoconite, supraglacial debris and flow sediment from Austre Brøggerbreen and Vestre Brøggerbreen, using a Student t-test for normal distributed means. When the mean concentrations were non-normal distributed, a Mann-Whitney U test was used.

Element	Sample material	p-value
Na	Snow	0.471401
	Cryoconite	**0.016319**
	Supraglacial debris	**0.02257**
	Supraglacial debris s	0.146653
	Flow sediment	**0.003743**
Mg	Snow	0.12881
	Cryoconite	**<.00001**
	Supraglacial debris	**<.00001**
	Supraglacial debris s	**0.000119**
	Flow sediment	**0.000017**
Al	Snow	0.422688
	Cryoconite	**0.003258**
	Supraglacial debris	**0.004438**
	Supraglacial debris s	**0.00515**
	Flow sediment	**0.000158**
Ca	Snow	0.6579
	Cryoconite	**<.00001**
	Supraglacial debris	**<.00001**
	Supraglacial debris s	**0.006175**
	Flow sediment	<.000001
Fe	Snow	0.4853
	Cryoconite	**<.00001**
	Supraglacial debris	**<.00001**
	Supraglacial debris s	**0.00139**
	Flow sediment	**<.00001**

Element	Sample material	p-value
Zn	Snow	**0.03763**
	Cryoconite	**0.000011**
	Supraglacial debris	**0.000525**
	Supraglacial debris s	**0.002185**
	Flow sediment	**0.002451**
As	Snow	0.063488
	Cryoconite	**0.04113**
	Supraglacial debris	**0.001228**
	Supraglacial debris s	**0.000981**
	Flow sediment	**0.000553**
Cd	Snow	0.061
	Cryoconite	0.07706
	Supraglacial debris	**0.007021**
	Supraglacial debris s	**0.018114**
	Flow sediment	**<.00001**
Pb	Snow	**0.007345**
	Cryoconite	**0.002165**
	Supraglacial debris	**0.0007523**
	Supraglacial debris s	**0.00707**
	Flow sediment	**0.000087**

Table E.4: p- values from testing for a statistically significant difference between two mean concentrations of total carbon and total nitrogen in cryoconite and supraglacial debris from Austre Brøggerbreen and Vestre Brøggerbreen, using a Student t-test for the normal distributed means.

Sample	Sample material	p-value
TC (%)	Cryoconite	**0.000068**
	Supraglacial debris	**0.00001**
TN (%)	Cryoconite	**0.000117**
	Supraglacial debris	**0.000019**

Table E.5: p- values from testing for a statistically significant difference between cryoconite and supraglacial debris mean concentrations of total carbon and total nitrogen from Austre Brøggerbreen and Vestre Brøggerbreen, using a Student t-test for the normal distributed means.

Sample	Sample material	Austre Brøggerbreen p - value	Vestre Brøggerbreen p - value
TC (%)	Cryoconite Supraglacial debris	0.199779	**0.004611**
TN (%)	Cryoconite Supraglacial debris	0.461657	**0.015109**

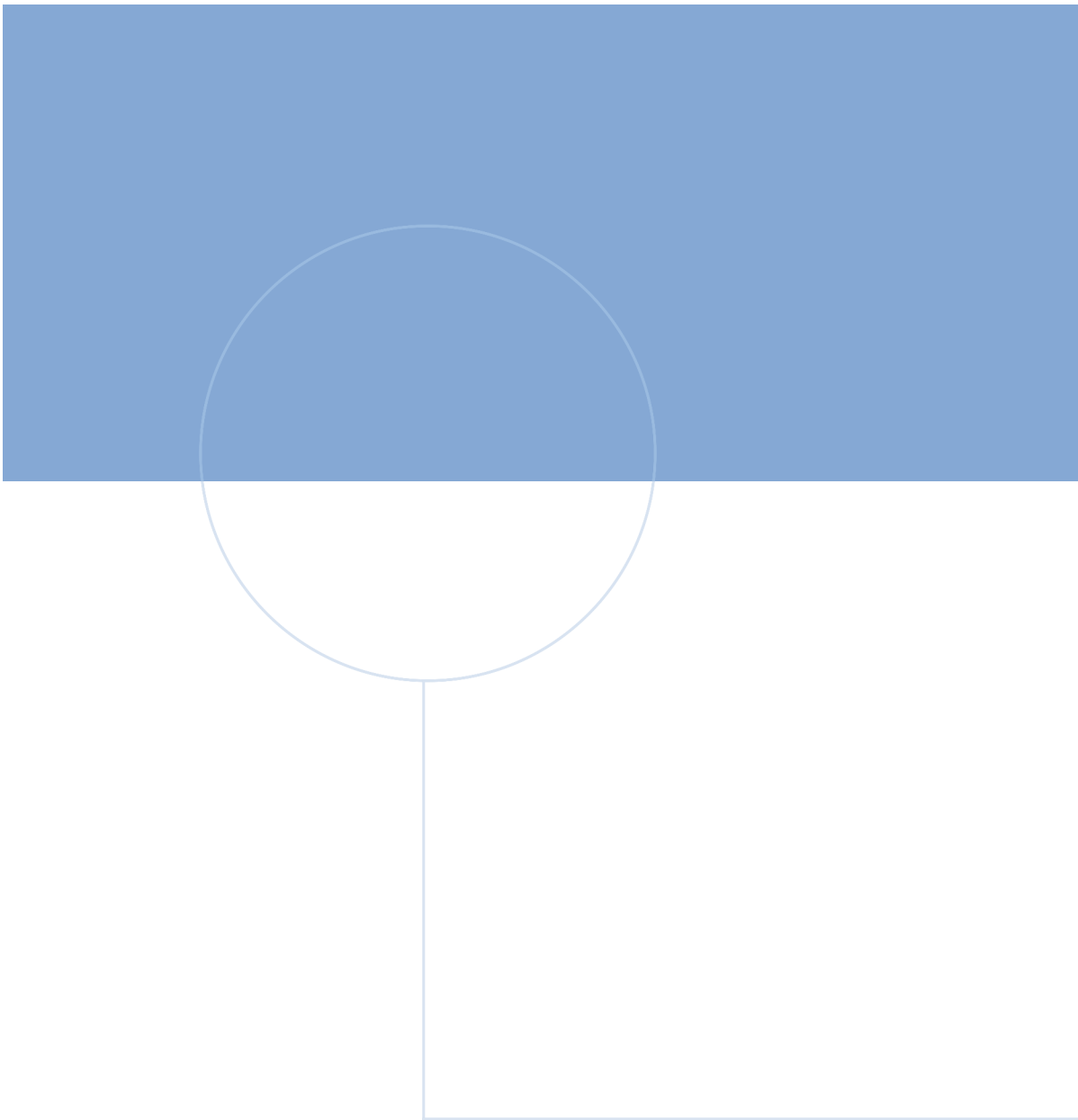

NTNU

Norwegian University of
Science and Technology